

Ice, Cloud, and Land Elevation Satellite 2 (ICESat-2)

Algorithm Theoretical Basis Document (ATBD)

for

Land - Vegetation Along-Track Products (ATL08)

**Contributions by Land/Vegetation SDT Team Members
and ICESat-2 Project Science Office**

**(Amy Neuenschwander, Katherine Pitts, Benjamin Jelley, John Robbins,
Brad Klotz, Sorin Popescu, Ross Nelson, David Harding, Dylan Pederson,
and Ryan Sheridan)**

ATBD prepared by

Amy Neuenschwander and

Katherine Pitts

15 September 2019

**Content reviewed: technical approach, assumptions, scientific soundness,
maturity, scientific utility of the data product**

29 **ATL08 algorithm and product change history**

30

| ATBD Version | Change |
|----------------|--|
| 2016 Nov | Product segment size changed from 250 signal photons to 100 m using five 20m segments from ATL03 (Sec 2) |
| 2016 Nov | Filtered signal classification flag removed from classed_pc_flag (Sec 2.3.2) |
| 2016 Nov | DRAGANN signal flag added (Sec 2.3.4) |
| 2016 Nov | Do not report segment statistics if too few ground photons within segment (Sec 4.15 (3)) |
| 2016 Nov | Product parameters added: h_canopy_uncertainty, landsat_flag, d_flag, delta_time_beg, delta_time_end, night_flag, msw_flag (Sec 2) |
| 2017 May | Revised region boundaries to be separated by continent (Sec 2) |
| 2017 May | Alternative DRAGANN parameter calculation added (Sec 1.1.1) |
| 2017 May | Set canopy flag = 0 when <i>L-km</i> segment is over Antarctica or Greenland regions (Sec 4.4 (1)) |
| 2017 May | Change initial canopy filter search radius from 3 m to 15 m (Sec 4.9 (6)) |
| 2017 May | Product parameters removed: h_rel_ph, terrain_thresh |
| 2017 May | Product parameters added: segment_id, segment_id_beg, segment_id_end, dem_flag, surf_type (Sec 2) |
| 2017 July | Urban flag added (Sec 2.4.17) |
| 2017 July | Dynamic point spread function added (Sec 4.11 (6)) |
| 2017 July | Methodology for processing <i>L-km</i> segments with buffer added (Sec 4.1 (2), Sec 4.17) |
| 2017 July | Revised alternative DRAGANN methodology (see bolded text in Sec 1.1.1) |
| 2017 July | Added post-DRAGANN filtering methodology (Sec 4.7) |
| 2017 July | Updated SNR to be estimated from superset of ATL03 and DRAGANN found signal used for processing ATL08 (Sec 2.5.17) |
| 2017 September | More details added to DRAGANN description (Sec 4.3), and corrections to DRAGANN implementation (Sec 3.1.1, Sec 4.3 (9)) |
| 2017 September | Added Appendix A – very detailed DRAGANN description |
| 2017 September | Revised alternative DRAGANN methodology (see bolded text in Sec 1.1.1) |
| 2017 September | Clarified SNR calculation (Sec 2.5.17, Sec 4.3 (18)) |
| 2017 September | Added cloud flag filtering option (Sec Error! Reference source not found.) |

**ICESat-2 Algorithm Theoretical Basis Document for Land-Vegetation
Along-Track Products (ATL08)
Release 002**

| | |
|----------------|--|
| 2017 September | Added top of canopy median surface filter (Sec 3.5 (a), Sec 4.10 (3), Sec 4.12 (1-3)) |
| 2017 September | Modified 500 canopy photon segment filter (Sec 3.5 (c), Sec 4.12 (6)) |
| 2017 November | Added solar_azimuth, solar_elevation, and n_seg_ph to Reference Data group; parameters were already in product (Sec 2.4) |
| 2017 November | Specified number of ground photons threshold for relative canopy product calculations (Sec 4.16 (2)); no number of ground photons threshold for absolute canopy heights (Sec 4.16.1 (1)) |
| 2017 November | Changed the ATL03 signal used in superset from all ATL03 signal (signal_conf_ph flags 1-4) to the medium-high confidence flags (signal_conf_ph flags 3-4) (Sec 3.1, Sec 4.3 (17)) |
| 2017 November | Removed Date parameter from Table 2.4 since UTC date is in file metadata |
| 2018 March | Clarified that cloud flag filtering option should be turned off by default (Sec Error! Reference source not found.) |
| 2018 March | Changed h_diff_ref QA threshold from 10 m to 25 m (Table 5.2) |
| 2018 March | Added absolute canopy height quartiles, canopy_h_quartile_abs (<i>Later removed</i>) |
| 2018 March | Removed psf_flag from main product; psf_flag will only be a QAQC alert (Sec 5.2) |
| 2018 March | Added an Asmooth filter based on the reference DEM value (Sec 4.6 (4-5)) |
| 2018 March | Changed relief calculation to 95 th – 5 th signal photon heights. (Sec 4.6 (6)) |
| 2018 March | Adjusted the Asmooth smoothing methodology (Sec 4.6 (8)) |
| 2018 March | Recalculate the Asmooth surface after filtering outlying noise from signal, then detrend signal height data (Sec 4.7 (3-4)) |
| 2018 March | Added option to run alternative DRAGANN process again in high noise cases (Sec 4.3.2) |
| 2018 March | Changed global land cover reference to MODIS Global Mosaics product (Sec 2.4.14) |
| 2018 March | Adjusted the top of canopy median filter thresholds based on SNR (Sec 4.12 (1-2)) |
| 2018 March | Added a final photon classification QA check (Sec 4.14, Table 5.2) |
| 2018 March | Added slope adjusted terrain parameters (<i>Later removed</i>) |
| 2018 June | Replaced slope adjusted terrain parameters with terrain best fit parameter (Sec 2.1.14, 4.15 (2.e)) |

**ICESat-2 Algorithm Theoretical Basis Document for Land-Vegetation
Along-Track Products (ATL08)
Release 002**

| | |
|------------------|--|
| 2018 June | Clarified source for water mask (Sec 2.4.15) |
| 2018 June | Clarified source for urban mask (Sec 2.4.17) |
| 2018 June | Added expansion to the terrain_slope calculation (Sec 4.15) |
| 2018 June | Removed canopy_d_quartile |
| 2018 June | Removed canopy_quartile_heights and canopy_quartile_heights_abs, replaced with canopy_h_metrics (Secs 2.2.3, 4.16 (6), 4.16.1 (5)) |
| 2018 *** draft 1 | Delta_time specified as mid-segment time, rather than mean segment time (Sec 2.4.5) |
| 2018 *** draft 1 | QA/QC products to be reported on a per orbit basis, rather than per region (Sec 5.2) |
| 2018 *** draft 1 | Added more detail to landsat_flag description (Sec 2.2.23) |
| 2018 *** draft 1 | Added psf_flag back into ATL08 product, as it is also needed for the QA product (Sec 2.5.12) |
| 2018 *** draft 1 | Specified that the sigma_h value reported here is the mean of the ATL03 reported sigma_h values (Sec 2.5.7) |
| 2018 *** draft 1 | Removed n_photons from all subgroups |
| 2018 *** draft 1 | <p>Better defined the interpolation and smoothing methods used throughout:</p> <ul style="list-style-type: none"> • Error! Reference source not found. (3): Interpolation – nearest • 4.6 (5): Interpolation – PCHIP • 4.6 (8): Smoothing – moving average • 4.7 (3): Interpolation – PCHIP • 4.7 (3): Smoothing – moving average • 4.8 (3): Smoothing – moving average • 4.8 (4): Interpolation – linear • 4.8 (5): Smoothing – moving average • 4.8 (6): Interpolation – linear • 4.8 (7): Smoothing – moving average • 4.8 (8): Smoothing – Savitzky-Golay • 4.8 (9): Interpolation – linear • 4.8 (14): Interpolation – PCHIP • 4.10 (10): Interpolation – linear • 4.11 (all): Smoothing – moving average • 4.10 (6.b): Interpolation – linear • 4.12 (1.a): Interpolation – linear • 4.12 (1.c): Smoothing – lowess • 4.12 (4): Interpolation – PCHIP • 4.12 (7): Interpolation – PCHIP • 4.12 (9): Smoothing – moving average • 4.15 (2.e.i.1): Interpolation – linear |

**ICESat-2 Algorithm Theoretical Basis Document for Land-Vegetation
Along-Track Products (ATL08)
Release 002**

| | |
|------------------|--|
| 2018 *** draft 1 | Added ref_elev and ref_azimuth back in (it was mistakenly removed in a previous version; Secs 2.5.3, 2.5.4) |
| 2018 *** draft 1 | Clarified wording of h_canopy_quad definition (Sec 2.2.17) |
| 2018 *** draft 1 | Updated segment_snowcover description to match the ATL09 snow_ice parameter it references (Sec 2.4.16) and added product reference to Table 4.2 |
| 2018 *** draft 1 | Added ph_ndx_beg (Sec 2.5.21); parameter was already on product |
| 2018 *** draft 1 | Added dem_removal_flag for QA purposes (Sec 2.4.11; Table 5.2) |
| 2018 *** draft 2 | Reformatted QA/QC trending and trigger alert list into a table for better clarification (Table 5.3) |
| 2018 *** draft 2 | Replaced n_photons in Table 5.2 with n_te_photons, n_ca_photons, and n_toc_photons |
| 2018 *** draft 2 | Removed beam_number from Table 2.5. Beam number and weak/strong designation within gtx group attributes. |
| 2018 *** draft 2 | Clarified calculation of h_te_best_fit (Sec 4.15 (2.e)) |
| 2018 *** draft 2 | Changed h_canopy and h_canopy_abs to be 98 th percentile height (Table 2.2, Sec 2.2.5, Sec 2.2.6, Sec 4.16 (4), Sec 4.16.1 (3)) |
| 2018 *** draft 2 | Separated h_canopy_metrics_abs from h_canopy_metrics (Table 2.2, Sec 2.2.3, Sec 4.16.1 (5)) |
| 2018 October | Removed 99 th percentile from h_canopy_metrics and h_canopy_metrics_abs (Table 2.2, Sec 2.2.3, Sec 2.2.4, Sec 4.16 (4), Sec 4.16.1 (5)) |
| 2018 December | Renamed and reworded Section 1.1.1 to better indicate that the DRAGANN preprocessing step is not optional |
| 2018 December | Specified that DRAGANN should use along-track time, and added time rescaling step (Sec 4.3 (1 - 4)) |
| 2018 December | Added DRAGANN changes made to better capture sparse canopy in cases of low noise rates (Sec 4.3, Appendix A) |
| 2018 December | Made corrections to DRAGANN description regarding the determination of the noise Gaussian (Sec 3.1.1, Sec 4.3) |
| 2018 December | Removed h_median_canopy and h_median_canopy_abs, as they are equivalent to canopy_h_metrics(50) and canopy_h_metrics_abs(50) (Table 2.2, Sec 4.16 (5), Sec 4.16.1 (4)) |
| 2018 December | Removed the requirement that > 5% ground photons required to calculate relative canopy height parameters (Table 2.2, Sec 4.16 (2)) |
| 2018 December | Added canopy relative height confidence flag (canopy_rh_conf) based on the percentage of ground and canopy photons in a segment (Table 2.2, Sec 4.16 (2)) |

**ICESat-2 Algorithm Theoretical Basis Document for Land-Vegetation
Along-Track Products (ATL08)
Release 002**

| | |
|--------------------|---|
| 2018 December | Added ATL09 layer_flag to ATL08 output (Table 2.5, Table 4.2) |
| 2019 February | Adjusted cloud filtering to be based on ATL09 backscatter analysis rather than cloud flags (Sec 4.1) |
| 2019 March 5 | Updated ATL09-based product descriptions reported on ATL08 product (Secs 2.5.13, 2.5.14, 2.5.15, 1.1.1) |
| 2019 March 5 | Updated cloud-based low signal filter methodology, and moved to first step of ATL08 processing (Sec 4.1) |
| 2019 March 13 | Replace canopy_closure with new landsat_perc parameter (Table 2.2, Sec 2.2.24) |
| 2019 March 13 | Change ATL08 product output regions to match ATL03 regions (Sec 2), but keep ATL08 regions internally and report in new parameter atl08_regions (Table 2.4, Sec 2.4.19) |
| 2019 March 13 | Add methodology for handling short ATL08 processing segments at the end of an ATL03 granule (Sec 4.2), and output distance the processing segment length is extended into new parameter last_seg_extend (Table 2.4, Sec 2.4.20) |
| 2019 March 13 | Add preprocessing step for removing atmospheric and ocean tide corrections from ATL03 heights (<i>Later removed</i>) |
| 2019 March 27 | Remove preprocessing step for removing atmospheric and ocean tide corrections from ATL03 heights, since those values are now removed from the ATL03 photon heights. |
| 2019 March 27 | Replaced ATL03 region figure with corrected version (Figure 2.2) |
| 2019 March 27 | Specified that at least 50 classed photons are required to create the 100 m land and canopy products (Secs 2, 4.15(1), 4.16(1)) |
| 2019 March 27 | Clarified that any non-extended segments would report a land_seg_extend value of 0 (Sec 4.2, Sec 2.4.20) |
| 2019 April 30 | Fixed the error in Eqn 1.4 for the sigma topo value |
| 2019 May 13 | Specified for cloud flag carry-over from ATL09 that ATL08 will report the highest cloud flag if an 08 segment straddles two 09 segments. (Section 2.5) |
| 2019 May 13 | Changed parameter cloud_flag_asr to cloud_flag_atm since the cloud_flag_asr is likely not to work over land due to varying surface reflectance (Sec, 2.5) |
| 2019 May 13 | Add ATL09 parameter cloud_fold_flag to the ATL08 data product for future qa/qc checks for low clouds. (Secs, 2.5) |
| 2019 May 13 | Clarification on the calculation of gradient for slope that feeds into the calculation of the point spread function (Sec 4.11) |

***ICESat-2 Algorithm Theoretical Basis Document for Land-Vegetation
Along-Track Products (ATL08)
Release 002***

| | |
|--------------------|--|
| 2019 July 1 | Changed Landsat canopy cover percentage to 3 % (from original value of 5%) |
|--------------------|--|

31

32

33 **Contents**

| | | |
|----|---|----|
| 34 | List of Tables..... | 14 |
| 35 | List of Figures..... | 15 |
| 36 | 1 INTRODUCTION | 17 |
| 37 | 1.1. Background..... | 18 |
| 38 | 1.2 Photon Counting Lidar | 20 |
| 39 | 1.3 The ICESat-2 concept..... | 22 |
| 40 | 1.4 Height Retrieval from ATLAS | 25 |
| 41 | 1.5 Accuracy Expected from ATLAS..... | 26 |
| 42 | 1.6 Additional Potential Height Errors from ATLAS..... | 28 |
| 43 | 1.7 Dense Canopy Cases | 29 |
| 44 | 1.8 Sparse Canopy Cases | 29 |
| 45 | 2. ATL08: DATA PRODUCT | 31 |
| 46 | 2.1 Subgroup: Land Parameters | 34 |
| 47 | 2.1.1 Georeferenced_segment_number_beg..... | 35 |
| 48 | 2.1.2 Georeferenced_segment_number_end..... | 35 |
| 49 | 2.1.3 Segment_terrain_height_mean | 36 |
| 50 | 2.1.4 Segment_terrain_height_med..... | 36 |
| 51 | 2.1.5 Segment_terrain_height_min..... | 36 |
| 52 | 2.1.6 Segment_terrain_height_max..... | 37 |
| 53 | 2.1.7 Segment_terrain_height_mode..... | 37 |
| 54 | 2.1.8 Segment_terrain_height_skew..... | 37 |
| 55 | 2.1.9 Segment_number_terrain_photons | 37 |
| 56 | 2.1.10 Segment height_interp | 38 |
| 57 | 2.1.11 Segment h_te_std..... | 38 |

**ICESat-2 Algorithm Theoretical Basis Document for Land-Vegetation
Along-Track Products (ATL08)
Release 002**

| | | | |
|----|--------|--|----|
| 58 | 2.1.12 | Segment_terrain_height_uncertainty | 38 |
| 59 | 2.1.13 | Segment_terrain_slope..... | 38 |
| 60 | 2.1.14 | Segment_terrain_height_best_fit..... | 39 |
| 61 | 2.2 | Subgroup: Vegetation Parameters..... | 39 |
| 62 | 2.2.1 | Georeferenced_segment_number_beg..... | 42 |
| 63 | 2.2.2 | Georeferenced_segment_number_end..... | 42 |
| 64 | 2.2.3 | Canopy_height_metrics_abs..... | 42 |
| 65 | 2.2.4 | Canopy_height_metrics | 43 |
| 66 | 2.2.5 | Absolute_segment_canopy_height..... | 43 |
| 67 | 2.2.6 | Segment_canopy_height | 43 |
| 68 | 2.2.7 | Absolute_segment_mean_canopy..... | 44 |
| 69 | 2.2.8 | Segment_mean_canopy | 44 |
| 70 | 2.2.9 | Segment_dif_canopy | 44 |
| 71 | 2.2.10 | Absolute_segment_min_canopy | 44 |
| 72 | 2.2.11 | Segment_min_canopy..... | 44 |
| 73 | 2.2.12 | Absolute_segment_max_canopy..... | 44 |
| 74 | 2.2.13 | Segment_max_canopy..... | 45 |
| 75 | 2.2.14 | Segment_canopy_height_uncertainty..... | 45 |
| 76 | 2.2.15 | Segment_canopy_openness..... | 46 |
| 77 | 2.2.16 | Segment_top_of_canopy_roughness..... | 46 |
| 78 | 2.2.17 | Segment_canopy_quadratic_height..... | 46 |
| 79 | 2.2.18 | Segment_number_canopy_photons..... | 46 |
| 80 | 2.2.19 | Segment_number_top_canopy_photons..... | 47 |
| 81 | 2.2.20 | Centroid_height..... | 47 |
| 82 | 2.2.21 | Segment_rel_canopy_conf..... | 47 |
| 83 | 2.2.22 | Canopy_flag..... | 47 |

**ICESat-2 Algorithm Theoretical Basis Document for Land-Vegetation
Along-Track Products (ATL08)
Release 002**

| | | | |
|-----|--------|---|----|
| 84 | 2.2.23 | Landsat_flag..... | 47 |
| 85 | 2.2.24 | Landsat_perc..... | 48 |
| 86 | 2.3 | Subgroup: Photons..... | 48 |
| 87 | 2.3.1 | Indices_of_classed_photons | 49 |
| 88 | 2.3.2 | Photon_class..... | 49 |
| 89 | 2.3.3 | Georeferenced_segment_number | 49 |
| 90 | 2.3.4 | DRAGANN_flag | 49 |
| 91 | 2.4 | Subgroup: Reference data..... | 49 |
| 92 | 2.4.1 | Georeferenced_segment_number_beg..... | 51 |
| 93 | 2.4.2 | Georeferenced_segment_number_end..... | 51 |
| 94 | 2.4.3 | Segment_latitude..... | 52 |
| 95 | 2.4.4 | Segment_longitude..... | 52 |
| 96 | 2.4.5 | Delta_time..... | 52 |
| 97 | 2.4.6 | Delta_time_beg | 52 |
| 98 | 2.4.7 | Delta_time_end..... | 52 |
| 99 | 2.4.8 | Night_Flag..... | 52 |
| 100 | 2.4.9 | Segment_reference_DTM..... | 53 |
| 101 | 2.4.10 | Segment_reference_DEM_source..... | 53 |
| 102 | 2.4.11 | Segment_reference_DEM_removal_flag..... | 53 |
| 103 | 2.4.12 | Segment_terrain_difference..... | 53 |
| 104 | 2.4.13 | Segment_terrain flag | 53 |
| 105 | 2.4.14 | Segment_landcover..... | 53 |
| 106 | 2.4.15 | Segment_watermask | 54 |
| 107 | 2.4.16 | Segment_snowcover..... | 54 |
| 108 | 2.4.17 | Urban_flag..... | 54 |
| 109 | 2.4.18 | Surface_type | 55 |

**ICESat-2 Algorithm Theoretical Basis Document for Land-Vegetation
Along-Track Products (ATL08)
Release 002**

| | | | |
|-----|--------|---|----|
| 110 | 2.4.19 | ATL08_region..... | 55 |
| 111 | 2.4.20 | Last_segment_extend | 55 |
| 112 | 2.5 | Subgroup: Beam data..... | 56 |
| 113 | 2.5.1 | Georeferenced_segment_number_beg..... | 58 |
| 114 | 2.5.2 | Georeferenced_segment_number_end..... | 58 |
| 115 | 2.5.3 | Beam_coelevation..... | 59 |
| 116 | 2.5.4 | Beam_azimuth..... | 59 |
| 117 | 2.5.5 | ATLAS_Pointing_Angle | 59 |
| 118 | 2.5.6 | Reference_ground_track..... | 59 |
| 119 | 2.5.7 | Sigma_h..... | 59 |
| 120 | 2.5.8 | Sigma_along..... | 60 |
| 121 | 2.5.9 | Sigma_across..... | 60 |
| 122 | 2.5.10 | Sigma_topo..... | 60 |
| 123 | 2.5.11 | Sigma_ATLAS_LAND..... | 60 |
| 124 | 2.5.12 | PSF_flag..... | 60 |
| 125 | 2.5.13 | Layer_flag..... | 61 |
| 126 | 2.5.14 | Cloud_flag_atm | 61 |
| 127 | 2.5.15 | MSW | 61 |
| 128 | 2.5.16 | Cloud Fold Flag..... | 62 |
| 129 | 2.5.17 | Computed_Apparent_Surface_Reflectance | 62 |
| 130 | 2.5.18 | Signal_to_Noise_Ratio | 62 |
| 131 | 2.5.19 | Solar_Azimuth..... | 62 |
| 132 | 2.5.20 | Solar_Elevation..... | 62 |
| 133 | 2.5.21 | Number_of_segment_photons..... | 62 |
| 134 | 2.5.22 | Photon_Index_Begin | 62 |
| 135 | 3 | ALGORITHM METHODOLOGY..... | 64 |

**ICESat-2 Algorithm Theoretical Basis Document for Land-Vegetation
Along-Track Products (ATL08)
Release 002**

| | | | |
|-----|-------|---|-----|
| 136 | 3.1 | Noise Filtering | 64 |
| 137 | 3.1.1 | DRAGANN | 65 |
| 138 | 3.2 | Surface Finding | 69 |
| 139 | 3.2.1 | De-trending the Signal Photons..... | 71 |
| 140 | 3.2.2 | Canopy Determination | 71 |
| 141 | 3.2.3 | Variable Window Determination | 73 |
| 142 | 3.2.4 | Compute descriptive statistics | 74 |
| 143 | 3.2.5 | Ground Finding Filter (Iterative median filtering)..... | 76 |
| 144 | 3.3 | Top of Canopy Finding Filter..... | 78 |
| 145 | 3.4 | Classifying the Photons | 78 |
| 146 | 3.5 | Refining the Photon Labels | 79 |
| 147 | 3.6 | Canopy Height Determination | 83 |
| 148 | 3.7 | Link Scale for Data products..... | 83 |
| 149 | 4. | ALGORITHM IMPLEMENTATION..... | 85 |
| 150 | 4.1 | Cloud based filtering..... | 88 |
| 151 | 4.2 | Preparing ATL03 data for input to ATL08 algorithm..... | 90 |
| 152 | 4.3 | Noise filtering via DRAGANN | 91 |
| 153 | 4.3.1 | DRAGANN Quality Assurance | 94 |
| 154 | 4.3.2 | Preprocessing to dynamically determine a DRAGANN parameter..... | 94 |
| 155 | 4.3.3 | Iterative DRAGANN processing | 97 |
| 156 | 4.4 | Is Canopy Present | 98 |
| 157 | 4.5 | Compute Filtering Window..... | 98 |
| 158 | 4.6 | De-trend Data..... | 99 |
| 159 | 4.7 | Filter outlier noise from signal..... | 100 |
| 160 | 4.8 | Finding the initial ground estimate..... | 100 |
| 161 | 4.9 | Find the top of the canopy (if canopy_flag = 1) | 102 |

**ICESat-2 Algorithm Theoretical Basis Document for Land-Vegetation
Along-Track Products (ATL08)
Release 002**

| | | | |
|-----|--------|---|-----|
| 162 | 4.10 | Compute statistics on de-trended data | 103 |
| 163 | 4.11 | Refine Ground Estimates..... | 104 |
| 164 | 4.12 | Canopy Photon Filtering..... | 106 |
| 165 | 4.13 | Compute individual Canopy Heights | 108 |
| 166 | 4.14 | Final photon classification QA check..... | 109 |
| 167 | 4.15 | Compute segment parameters for the Land Products | 109 |
| 168 | 4.16 | Compute segment parameters for the Canopy Products..... | 112 |
| 169 | 4.16.1 | Canopy Products calculated with absolute heights..... | 114 |
| 170 | 4.17 | Record final product without buffer..... | 114 |
| 171 | 5 | DATA PRODUCT VALIDATION STRATEGY | 115 |
| 172 | 5.1 | Validation Data..... | 115 |
| 173 | 5.2 | Internal QC Monitoring | 118 |
| 174 | 6 | REFERENCES..... | 125 |
| 175 | | | |

176 **List of Tables**

| | | |
|-----|---|-----|
| 177 | Table 2.1. Summary table of land parameters on ATL08..... | 34 |
| 178 | Table 2.2. Summary table of canopy parameters on ATL08. | 40 |
| 179 | Table 2.3. Summary table for photon parameters for the ATL08 product..... | 48 |
| 180 | Table 2.4. Summary table for reference parameters for the ATL08 product..... | 50 |
| 181 | Table 2.5. Summary table for beam parameters for the ATL08 product..... | 56 |
| 182 | Table 3.1. Standard deviation ranges utilized to qualify the spread of photons within | |
| 183 | moving window..... | 75 |
| 184 | Table 4.1. Input parameters to ATL08 classification algorithm..... | 85 |
| 185 | Table 4.2. Additional external parameters referenced in ATL08 product. | 86 |
| 186 | Table 5.1. Airborne lidar data vertical height (Z accuracy) requirements for | |
| 187 | validation data. | 115 |
| 188 | Table 5.2. ATL08 parameter monitoring. | 118 |
| 189 | Table 5.3. QA/QC trending and triggers..... | 123 |
| 190 | | |

191 List of Figures

| | | |
|-----|--|----|
| 192 | Figure 1.1. Various modalities of lidar detection. Adapted from Harding, 2009..... | 21 |
| 193 | Figure 1.2. Schematic of 6-beam configuration for ICESat-2 mission. The laser | |
| 194 | energy will be split into 3 laser beam pairs – each pair having a weak spot (1X) and a | |
| 195 | strong spot (4X). | 23 |
| 196 | Figure 1.3. Illustration of off-nadir pointing scenarios. Over land (green regions) in | |
| 197 | the mid-latitudes, ICESat-2 will be pointed away from the repeat ground tracks to | |
| 198 | increase the density of measurements over terrestrial surfaces..... | 24 |
| 199 | Figure 1.4. Illustration of the point spread function, also referred to as Znoise, for a | |
| 200 | series of photons about a surface. | 27 |
| 201 | Figure 2.1. HDF5 data structure for ATL08 products..... | 32 |
| 202 | Figure 2.2. ATL03 granule regions; graphic from ATL03 ATBD (Neumann et al.)..... | 33 |
| 203 | Figure 2.3. ATL08 product regions..... | 34 |
| 204 | Figure 2.4. Illustration of canopy photons (red dots) interaction in a vegetated area. | |
| 205 | Relative canopy heights, H_i , are computed by differencing the canopy photon height | |
| 206 | from an interpolated terrain surface. | 40 |
| 207 | Figure 3.1. Combination of noise filtering algorithms to create a superset of input | |
| 208 | data for surface finding algorithms. | 65 |
| 209 | Figure 3.2. Histogram of the number of photons within a search radius. This | |
| 210 | histogram is used to determine the threshold for the DRAGANN approach..... | 67 |
| 211 | Figure 3.3. Output from DRAGANN filtering. Signal photons are shown as blue..... | 69 |
| 212 | Figure 3.4. Flowchart of overall surface finding method..... | 70 |
| 213 | Figure 3.5. Plot of Signal Photons (black) from 2014 MABEL flight over Alaska and | |
| 214 | de-trended photons (red). | 71 |
| 215 | Figure 3.6. Shape Parameter for variable window size. | 74 |
| 216 | Figure 3.7. Illustration of the standard deviations calculated for each moving | |
| 217 | window to identify the amount of spread of signal photons within a given window. | |
| 218 | | 76 |
| 219 | Figure 3.8. Three iterations of the ground finding concept for L -km segments with | |
| 220 | canopy..... | 77 |

**ICESat-2 Algorithm Theoretical Basis Document for Land-Vegetation
Along-Track Products (ATL08)
Release 002**

| | | |
|-----|--|-----|
| 221 | Figure 3.9. Example of the intermediate ground and top of canopy surfaces | |
| 222 | calculated from MABEL flight data over Alaska during July 2014. | 80 |
| 223 | Figure 3.10. Example of classified photons from MABEL data collected in Alaska | |
| 224 | 2014. Red photons are photons classified as terrain. Green photons are classified as | |
| 225 | top of canopy. Canopy photons (shown as blue) are considered as photons lying | |
| 226 | between the terrain surface and top of canopy..... | 81 |
| 227 | Figure 3.11. Example of classified photons from MABEL data collected in Alaska | |
| 228 | 2014. Red photons are photons classified as terrain. Green photons are classified as | |
| 229 | top of canopy. Canopy photons (shown as blue) are considered as photons lying | |
| 230 | between the terrain surface and top of canopy..... | 82 |
| 231 | Figure 3.12. Example of classified photons from MABEL data collected in Alaska | |
| 232 | 2014. Red photons are photons classified as terrain. Green photons are classified as | |
| 233 | top of canopy. Canopy photons (shown as blue) are considered as photons lying | |
| 234 | between the terrain surface and top of canopy..... | 83 |
| 235 | Figure 5.1. Example of <i>L-km</i> segment classifications and interpolated ground | |
| 236 | surface. | 122 |
| 237 | | |

1 INTRODUCTION

This document describes the theoretical basis and implementation of the processing algorithms and data parameters for Level 3 land and vegetation heights for the non-polar regions of the Earth. The ATL08 product contains heights for both terrain and canopy in the along-track direction as well as other descriptive parameters derived from the measurements. At the most basic level, a derived surface height from the ATLAS instrument at a given time is provided relative to the WGS-84 ellipsoid. Height estimates from ATL08 can be compared with other geodetic data and used as input to higher-level ICESat-2 products, namely ATL13 and ATL18. ATL13 will provide estimates of inland water-related heights and associated descriptive parameters. ATL18 will consist of gridded maps for terrain and canopy features.

The ATL08 product will provide estimates of terrain heights, canopy heights, and canopy cover at fine spatial scales in the along-track direction. Along-track is defined as the direction of travel of the ICESat-2 satellite in the velocity vector. Parameters for the terrain and canopy will be provided at a fixed step-size of 100 m along the ground track referred to as a segment. A fixed segment size of 100 m was chosen to provide continuity of data parameters on the ATL08 data product. From an analysis perspective, it is difficult and cumbersome to attempt to relate canopy cover over variable lengths. Furthermore, a segment size of 100 m will facilitate a simpler combination of along-track data to create the gridded products.

We anticipate that the signal returned from the weak beam will be sufficiently weak and may prohibit the determination of both a terrain and canopy segment height, particularly over areas of dense vegetation. However, in more arid regions we anticipate producing a terrain height for both the weak and strong beams.

In this document, section 1 provides a background of lidar in the ecosystem community as well as describing photon counting systems and how they differ from discrete return lidar systems. Section 2 provides an overview of the Land and

Vegetation parameters and how they are defined on the data product. Section 3 describes the basic methodology that will be used to derive the parameters for ATL08. Section 4 describes the processing steps, input data, and procedure to derive the data parameters. Section 5 will describe the test data and specific tests that NASA's implementation of the algorithm should pass in order to determine a successful implementation of the algorithm.

1.1. Background

The Earth's land surface is a complex mosaic of geomorphic units and land cover types resulting in large variations in terrain height, slope, roughness, vegetation height and reflectance, often with the variations occurring over very small spatial scales. Documentation of these landscape properties is a first step in understanding the interplay between the formative processes and response to changing conditions. Characterization of the landscape is also necessary to establish boundary conditions for models which are sensitive to these properties, such as predictive models of atmospheric change that depend on land-atmosphere interactions. Topography, or land surface height, is an important component for many height applications, both to the scientific and commercial sectors. The most accurate global terrain product was produced by the Shuttle Radar Topography Mission (SRTM) launched in 2000; however, elevation data are limited to non-polar regions. The accuracy of SRTM derived elevations range from 5 – 10 m, depending upon the amount of topography and vegetation cover over a particular area. ICESat-2 will provide a global distribution of geodetic measurements (of both the terrain surface and relative canopy heights) which will provide a significant benefit to society through a variety of applications including sea level change monitoring, forest structural mapping and biomass estimation, and improved global digital terrain models.

In addition to producing a global terrain product, monitoring the amount and

distribution of above ground vegetation and carbon pools enables improved characterization of the global carbon budget. Forests play a significant role in the terrestrial carbon cycle as carbon pools. Events, such as management activities (Krankina et al. 2012) and disturbances can release carbon stored in forest above ground biomass (AGB) into the atmosphere as carbon dioxide, a greenhouse gas that contributes to climate change (Ahmed et al. 2013). While carbon stocks in nations with continuous national forest inventories (NFIs) are known, complications with NFI carbon stock estimates exist, including: (1) ground-based inventory measurements are time consuming, expensive, and difficult to collect at large-scales (Houghton 2005; Ahmed et al. 2013); (2) asynchronously collected data; (3) extended time between repeat measurements (Houghton 2005); and (4) the lack of information on the spatial distribution of forest AGB, required for monitoring sources and sinks of carbon (Houghton 2005). Airborne lidar has been used for small studies to capture canopy height and in those studies canopy height variation for multiple forest types is measured to approximately 7 m standard deviation (Hall et al., 2011).

Although the spatial extent and changes to forests can be mapped with existing satellite remote sensing data, the lack of information on forest vertical structure and biomass limits the knowledge of biomass/biomass change within the global carbon budget. Based on the global carbon budget for 2015 (Quere et al., 2015), the largest remaining uncertainties about the Earth's carbon budget are in its terrestrial components, the global residual terrestrial carbon sink, estimated at 3.0 ± 0.8 GtC/year for the last decade (2005-2014). Similarly, carbon emissions from land-use changes, including deforestation, afforestation, logging, forest degradation and shifting cultivation are estimated at 0.9 ± 0.5 GtC /year. By providing information on vegetation canopy height globally with a higher spatial resolution than previously afforded by other spaceborne sensors, the ICESat-2 mission can contribute significantly to reducing uncertainties associated with forest vegetation carbon.

Although ICESat-2 is not positioned to provide global biomass estimates due to its profiling configuration and somewhat limited detection capabilities, it is anticipated that the data products for vegetation will be complementary to ongoing biomass and vegetation mapping efforts. Synergistic use of ICESat-2 data with other space-based mapping systems is one solution for extended use of ICESat-2 data. Possibilities include NASA's Global Ecosystems Dynamics Investigation (GEDI) lidar planned to fly onboard the International Space Station (ISS) or imaging sensors, such as Landsat 8, or NASA/ISRO -NISAR radar mission.

1.2 Photon Counting Lidar

Rather than using an analog, full waveform system similar to what was utilized on the ICESat/GLAS mission, ICESat-2 will employ a photon counting lidar. Photon counting lidar has been used successfully for ranging for several decades in both the science and defense communities. Photon counting lidar systems operate on the concept that a low power laser pulse is transmitted and the detectors used are sensitive at the single photon level. Due to this type of detector, any returned photon whether from the reflected signal or solar background can trigger an event within the detector. A discussion regarding discriminating between signal and background noise photons is discussed later in this document. A question of interest to the ecosystem community is to understand where within the canopy is the photon likely to be reflected. Figure 1.1 is an example of three different laser detector modalities: full waveform, discrete return, and photon counting. Full waveform sensors record the entire temporal profile of the reflected laser energy through the canopy. In contrast, discrete return systems have timing hardware that record the time when the amplitude of the reflected signal energy exceeds a certain threshold amount. A photon counting system, however, will record the arrival time associated with a single photon detection that can occur anywhere within the vertical distribution of the reflected signal. If a photon counting lidar system were to dwell over a surface for a

significant number of shots (i.e. hundreds or more), the vertical distribution of the reflected photons will resemble a full waveform. Thus, while an individual photon could be reflected from anywhere within the vertical canopy, the probability distribution function (PDF) of that reflected photon would be the full waveform. Furthermore, the probability of detecting the top of the tree is not as great as detecting reflective surfaces positioned deeper into the canopy where the bulk of leaves and branches are located. As one might imagine, the PDF will differ according to canopy structure and vegetation physiology. For example, the PDF of a conifer tree will look different than broadleaf trees.

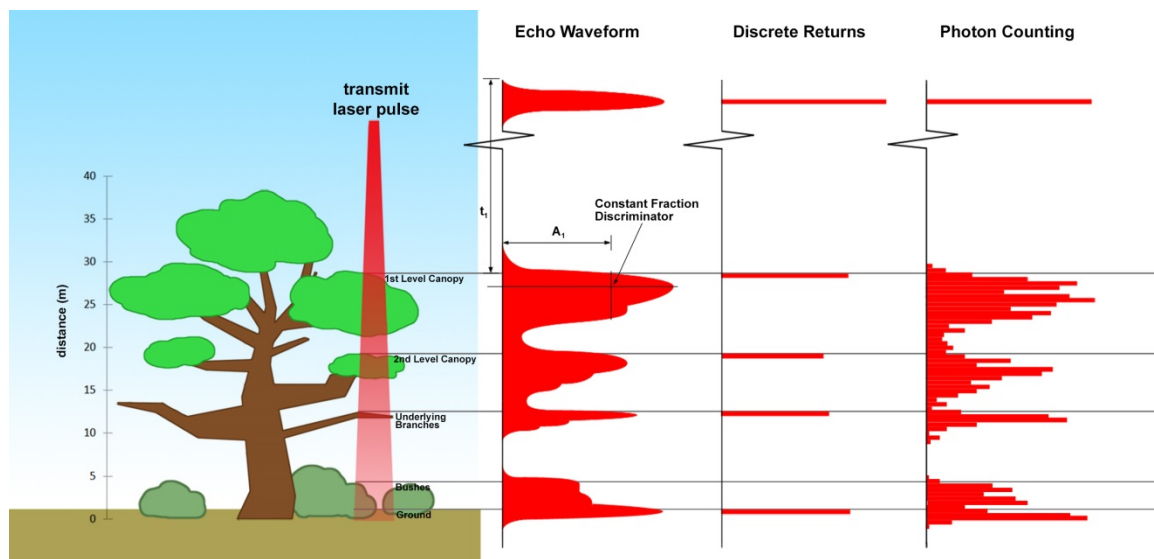


Figure 1.1. Various modalities of lidar detection. Adapted from Harding, 2009.

A cautionary note, the photon counting PDF that is illustrated in Figure 1.1 is merely an illustration if enough photons (i.e. hundreds of photons or more) were to be reflected from a target. In reality, due to the spacecraft speed, ATLAS will record 0 – 4 photons per transmit laser pulse over vegetation.

1.3 The ICESat-2 concept

The Advanced Topographic Laser Altimeter System (ATLAS) instrument designed for ICESat-2 will utilize a different technology than the GLAS instrument used for ICESat. Instead of using a high-energy, single-beam laser and digitizing the entire temporal profile of returned laser energy, ATLAS will use a multi-beam, micropulse laser (sometimes referred to as photon-counting). The travel time of each detected photon is used to determine a range to the surface which, when combined with satellite attitude and pointing information, can be geolocated into a unique XYZ location on or near the Earth's surface. For more information on how the photons from ICESat-2 are geolocated, refer to ATL03 ATBD. The XYZ positions from ATLAS are subsequently used to derive surface and vegetation properties. The ATLAS instrument will operate at 532 nm in the green range of the electromagnetic (EM) spectrum and will have a laser repetition rate of 10 kHz. The combination of the laser repetition rate and satellite velocity will result in one outgoing laser pulse approximately every 70 cm on the Earth's surface and each spot on the surface is ~13 m in diameter. Each transmitted laser pulse is split by a diffractive optical element in ATLAS to generate six individual beams, arranged in three pairs (Figure 1.2). The beams within each pair have different transmit energies ('weak' and 'strong', with an energy ratio of approximately 1:4) to compensate for varying surface reflectance. The beam pairs are separated by ~3.3 km in the across-track direction and the strong and weak beams are separated by ~2.5 km in the along-track direction. As ICESat-2 moves along its orbit, the ATLAS beams describe six tracks on the Earth's surface; the array is rotated slightly with respect to the satellite's flight direction so that tracks for the fore and aft beams in each column produce pairs of tracks – each separated by approximately 90 m.

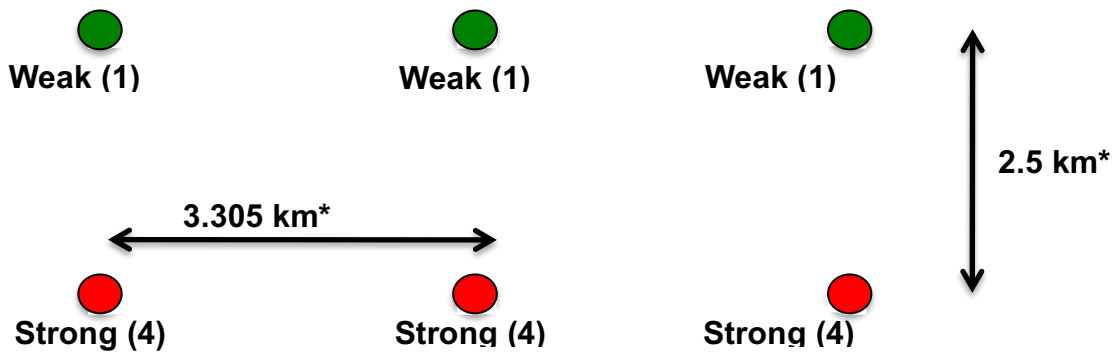
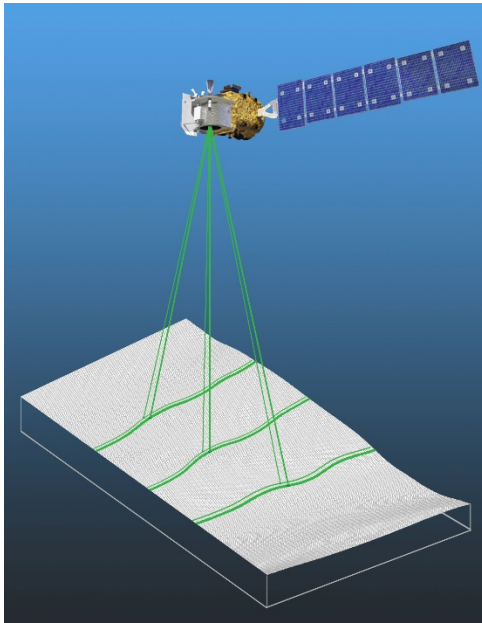


Figure 1.2. Schematic of 6-beam configuration for ICESat-2 mission. The laser energy will be split into 3 laser beam pairs – each pair having a weak spot (1X) and a strong spot (4X).

The motivation behind this multi-beam design is its capability to compute cross-track slopes on a per-orbit basis, which contributes to an improved understanding of ice dynamics. Previously, slope measurements of the terrain were determined via repeat-track and crossover analysis. The laser beam configuration as proposed for ICESat-2 is also beneficial for terrestrial ecosystems compared to GLAS as it enables a denser spatial sampling in the non-polar regions. To achieve a spatial sampling goal of no more than 2 km between equatorial ground tracks, ICESat-2 will

be off-nadir pointed a maximum of 1.8 degrees from the reference ground track during the entire mission.

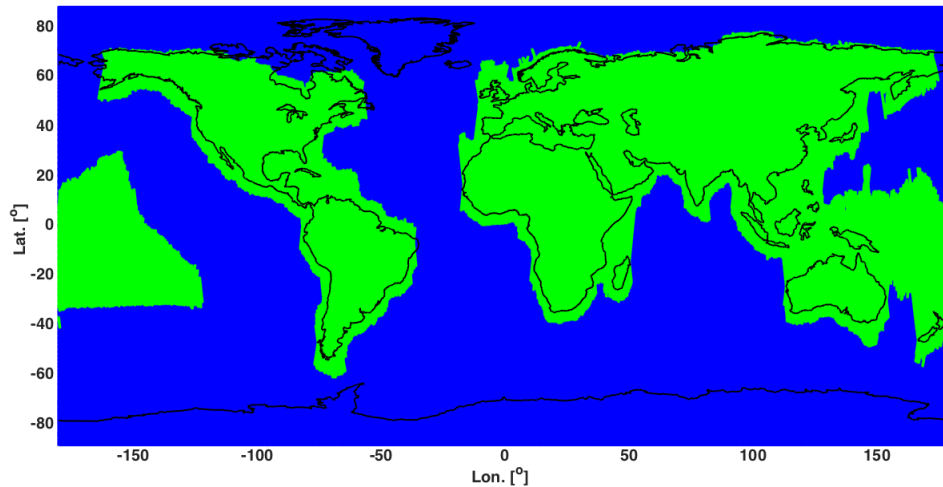


Figure 1.3. Illustration of off-nadir pointing scenarios. Over land (green regions) in the mid-latitudes, ICESat-2 will be pointed away from the repeat ground tracks to increase the density of measurements over terrestrial surfaces.

ICESat-2 is designed to densely sample the Earth's surface, permitting scientists to measure and quantitatively characterize vegetation across vast expanses, e.g., nations, continents, globally. ICESat-2 will acquire synoptic measurements of vegetation canopy height, density, the vertical distribution of photosynthetically active material, leading to improved estimates of forest biomass, carbon, and volume. In addition, the orbital density, i.e., the number of orbits per unit area, at the end of the three year mission will facilitate the production of gridded global products. ICESat-2 will provide the means by which an accurate "snapshot" of global biomass and carbon may be constructed for the mission period.

1.4 Height Retrieval from ATLAS

Light from the ATLAS lasers reaches the earth's surface as flat disks of down-traveling photons approximately 50 cm in vertical extent and spread over approximately 14 m horizontally. Upon hitting the earth's surface, the photons are reflected and scattered in every direction and a handful of photons return to the ATLAS telescope's focal plane. The number of photon events per laser pulse is a function of outgoing laser energy, surface reflectance, solar conditions, and scattering and attenuation in the atmosphere. For highly reflective surfaces (such as land ice) and clear skies, approximately 10 signal photons from a single strong beam are expected to be recorded by the ATLAS instrument for a given transmit laser pulse. Over vegetated land where the surface reflectance is considerably less than snow or ice surfaces, we expect to see fewer returned photons from the surface. Whereas snow and ice surfaces have high reflectance at 532 nm (typical Lambertian reflectance between 0.8 and 0.98 (Martino, GSFC internal report, 2010)), canopy and terrain surfaces have much lower reflectance (typically around 0.3 for soil and 0.1 for vegetation) at 532 nm. As a consequence we expect to see 1/3 to 1/9 as many photons returned from terrestrial surfaces as from ice and snow surfaces. For vegetated surfaces, the number of reflected signal photon events per transmitted laser pulse is estimated to range between 0 to 4 photons.

The time measured from the detected photon events are used to compute a range, or distance, from the satellite. Combined with the precise pointing and attitude information about the satellite, the range can be geolocated into a XYZ point (known as a geolocated photon) above the WGS-84 reference ellipsoid. In addition to recording photons from the reflected signal, the ATLAS instrument will detect background photons from sunlight which are continually entering the telescope. A primary objective of the ICESat-2 data processing software is to correctly discriminate between signal photons and background photons. Some of this processing occurs at the ATL03 level and some of it also occurs within the software

for ATL08. At ATL03, this discrimination is done through a series of three steps of progressively finer resolution with some processing occurring onboard the satellite prior to downlink of the raw data. The ATL03 data product produces a classification between signal and background (i.e. noise) photons, and further discussion on that classification process can be read in the ATL03 ATBD. In addition, all geophysical corrections (e.g. ocean tide, solid earth tide models, etc.) are not applied to the position of the individual geolocated photons at the ATL03 level, but they are provided on the data product if there exists a need to apply them. Thus, all of the heights processed in the ATL08 algorithm consists of the ATL03 heights with respect to the WGS-84 ellipsoid.

1.5 Accuracy Expected from ATLAS

There are a variety of elements that contribute to the elevation accuracy that are expected from ATLAS and the derived data products. Elevation accuracy is a composite of ranging precision of the instrument, radial orbital uncertainty, geolocation knowledge, forward scattering in the atmosphere, and tropospheric path delay uncertainty. The ranging precision seen by ATLAS will be a function of the laser pulse width, the surface area potentially illuminated by the laser, and uncertainty in the timing electronics. The requirement on radial orbital uncertainty is specified to be less than 4 cm and tropospheric path delay uncertainty is estimated to be 3 cm. In the case of ATLAS, the ranging precision for flat surfaces, is expected to have a standard deviation of approximately 25 cm. The composite of each of the errors can also be thought of as the spread of photons about a surface (see Figure 1.4) and is referred to as the point spread function or Znoise.

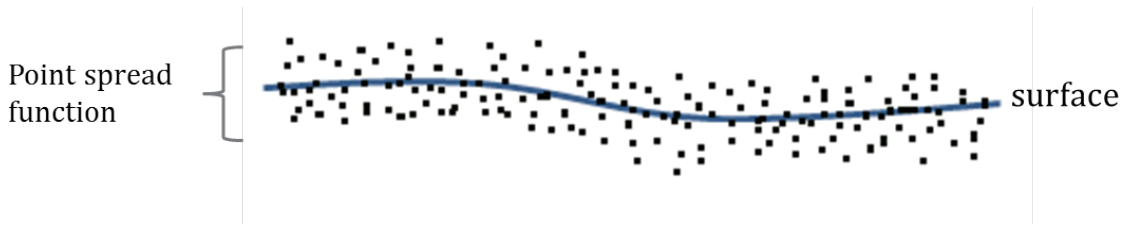


Figure 1.4. Illustration of the point spread function, also referred to as Znoise, for a series of photons about a surface.

The estimates of σ_{Orbit} , $\sigma_{troposphere}$, $\sigma_{forwardscattering}$, $\sigma_{pointing}$, and σ_{timing} for a photon will be represented on the ATL03 data product as the final geolocated accuracy in the X, Y, and Z (or height) direction. In reality, these parameters have different temporal and spatial scales, however until ICESat-2 is on orbit, it is uncertain how these parameters will vary over time. As such, Equation 1.1 may change once the temporal aspects of these parameters are better understood. For a preliminary quantification of the uncertainties, Equation 1.1 is valid to incorporate the instrument related factors.

$$\sigma_Z = \sqrt{\sigma_{Orbit}^2 + \sigma_{trop}^2 + \sigma_{forwardscattering}^2 + \sigma_{pointing}^2 + \sigma_{timing}^2} \quad \text{Eqn. 1.1}$$

Although σ_Z on the ATL03 product represents the best understanding of the uncertainty for each geolocated photon, it does not incorporate the uncertainty associated with local slope of the topography. The slope component to the geolocation uncertainty is a function of both the geolocation knowledge of the pointing (which is required to be less than 6.5 m) multiplied by the tangent of the surface slope. In a case of flat topography (≤ 1 degree slope), $\sigma_Z \leq 25$ cm, whereas in the case of a 10 degree surface slope, $\sigma_Z = 119$ cm. The uncertainty associated with the local slope will be combined with σ_Z to produce the term $\sigma_{Atlas_{Land}}$.

$$\sigma_{Atlas_{Land}} = \sqrt{\sigma_Z^2 + \sigma_{topo}^2} \quad \text{Eqn. 1.2}$$

489 $\sigma_{topo} =$ Eqn. 1.3

490 Ultimately, the uncertainty that will be reported on the data product ATL08
491 will include the $\sigma_{Atlas_{Land}}$ term and the local rms values of heights computed within
492 each data parameter segment. For example, calculations of terrain height will be
493 made on photons classified as terrain photons (this process is described in the
494 following sections). The uncertainty of the terrain height for a segment is described
495 in Equation 1.4, where the root mean square term of $\sigma_{Atlas_{Land}}$ and rms of terrain
496 heights are normalized by the number of terrain photons for that given segment.

497 $\sigma_{ATL08_{segment}} = \sqrt{\sigma_{Atlas_{Land}}^2 + \sigma_{Zrms_{segment_class}}^2}$ Eqn. 1.4

498

499 **1.6 Additional Potential Height Errors from ATLAS**

500 Some additional potential height errors in the ATL08 terrain and vegetation
501 product can come from a variety of sources including:

- 502 a. Vertical sampling error. ATLAS height estimates are based on a
503 random sampling of the surface height distribution. Photons may
504 be reflected from anywhere within the PDF of the reflecting surface;
505 more specifically, anywhere from within the canopy. A detailed
506 look at the potential effect of vertical sampling error is provided in
507 Neuenschwander and Magruder (2016).
- 508 b. Background noise. Random noise photons are mixed with the
509 signal photons so classified photons will include random outliers.
- 510 c. Complex topography. The along-track product may not always
511 represent complex surfaces, particularly if the density of ground
512 photons does not support an accurate representation.

- d. Vegetation. Dense vegetation may preclude reflected photon events from reaching the underlying ground surface. An incorrect estimation of the underlying ground surface will subsequently lead to an incorrect canopy height determination.
- e. Misidentified photons. The product from ATL03 combined with additional noise filtering may not identify the correct photons as signal photons.

1.7 Dense Canopy Cases

Although the height accuracy produced from ICESat-2 is anticipated to be superior to other global height products (e.g. SRTM), for certain biomes photon counting lidar data as it will be collected by the ATLAS instrument present a challenge for extracting both the terrain and canopy heights, particularly for areas of dense vegetation. Due to the relatively low laser power, we anticipate that the along-track signal from ATLAS may lose ground signal under dense forest (e.g. >96% canopy closure) and in situations where cloud cover obscures the terrestrial signal. In areas having dense vegetation, it is likely that only a handful of photons will be returned from the ground surface with the majority of reflections occurring from the canopy. A possible source of error can occur with both the canopy height estimates and the terrain heights if the vegetation is particularly dense and the ground photons were not correctly identified.

1.8 Sparse Canopy Cases

Conversely, sparse canopy cases also pose a challenge to vegetation height retrievals. In these cases, expected reflected photon events from sparse trees or shrubs may be difficult to discriminate between solar background noise photons. The

***ICESat-2 Algorithm Theoretical Basis Document for Land-Vegetation
Along-Track Products (ATL08)
Release 002***

539 algorithms being developed for ATL08 operate under the assumption that signal
540 photons are close together and noise photons will be more isolated in nature. Thus,
541 signal (in this case canopy) photons may be incorrectly identified as solar background
542 noise on the data product. Due to the nature of the photon counting processing,
543 canopy photons identified in areas that have extremely low canopy cover <15% will
544 be filtered out and reassigned as noise photons.

545

2. ATL08: DATA PRODUCT

The ATL08 product will provide estimates of terrain height, canopy height, and canopy cover at fine spatial scales in the along-track direction. In accordance with the HDF-driven structure of the ICESat-2 products, the ATL08 product will characterize each of the six Ground Tracks (GT) associated with each Reference Ground Track (RGT) for each cycle and orbit number. Each ground track group has a distinct beam number, distance from the reference track, and transmit energy strength, and all beams will be processed independently using the same sequence of steps described within ATL08. Each ground track group (GT) on the ATL08 product contains subgroups for land and canopy heights segments as well as beam and reference parameters useful in the ATL08 processing. In addition, the labeled photons that are used to determine the data parameters will be indexed back to the ATL03 products such that they are available for further, independent analysis. A layout of the ATL08 HDF product is shown in Figure 2.1. The six GTs are numbered from left to right, regardless of satellite orientation.

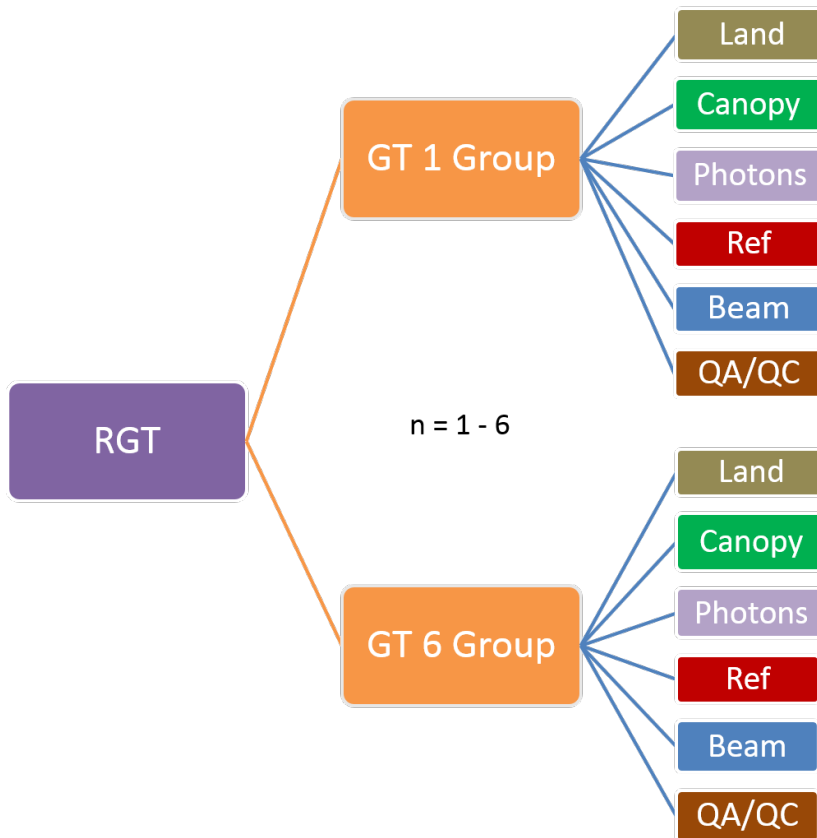
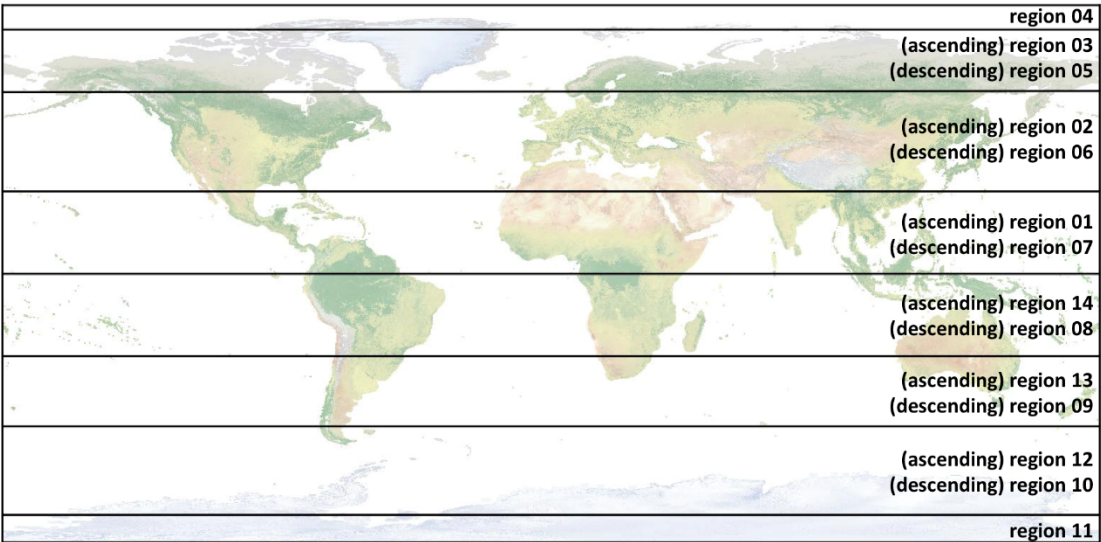


Figure 2.1. HDF5 data structure for ATL08 products

For each data parameter, terrain surface elevation and canopy heights will be provided at a fixed segment size of 100 meters along the ground track. Based on the satellite velocity and the expected number of reflected photons for land surfaces, each segment should have more than 100 signal photons, but in some instances there may be less than 100 signal photons per segment. If a segment has less than 50 classed (i.e., labeled by ATL08 as ground, canopy, or top of canopy) photons we feel this would not accurately represent the surface. Thus, an invalid value will be reported in all height fields. In the event that there are more than 50 classed photons, but a terrain height cannot be determined due to an insufficient number of ground photons, (e.g.

573 lack of photons penetrating through dense canopy), the only reported terrain height
574 will be the interpolated surface height.

575 The ATL08 product will be produced per granule based on the ATL03 defined
576 regions (see Figure 2.2). Thus, the ATL08 file/name convention scheme will match
577 the file/naming convention for ATL03 –in attempt for reducing complexity to allow
578 users to examine both data products.



579
580 Figure 2.2. ATL03 granule regions; graphic from ATL03 ATBD (Neumann et al.).

581 The ATL08 product additionally has its own internal regions, which are
582 roughly assigned by continent, as shown by Figure 2.3. For the regions covering
583 Antarctica (regions 7, 8, 9, 10) and Greenland (region 11), the ATL08 algorithm will
584 assume that no canopy is present. These internal ATL08 regions will be noted in the
585 ATL08 product (see parameter atl08_region in Section 2.4.19). Note that the regions
586 for each ICESat-2 product are not the same.

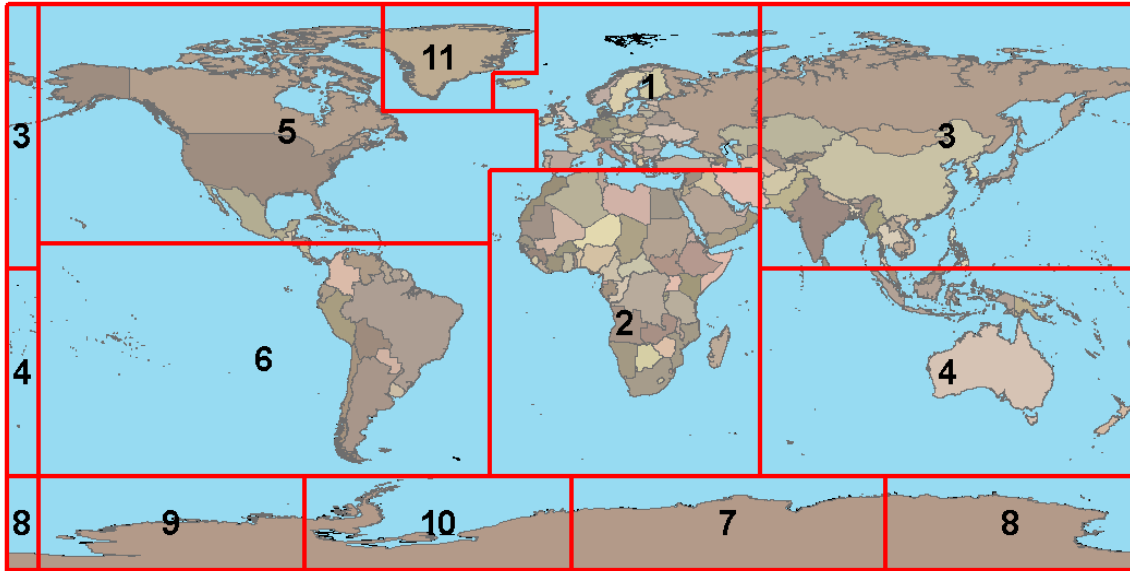


Figure 2.3. ATL08 product regions.

2.1 Subgroup: Land Parameters

ATL08 terrain height parameters are defined in terms of the absolute height above the reference ellipsoid.

Table 2.1. Summary table of land parameters on ATL08.

| Group | Data type | Description | Source |
|-----------------------|-----------|--|----------|
| segment_id_beg | Integer | First along-track segment_id number in 100-m segment | ATL03 |
| segment_id_end | Integer | Last along-track segment_id number in 100-m segment | ATL03 |
| h_te_mean | Float | Mean terrain height for segment | computed |
| h_te_median | Float | Median terrain height for segment | computed |
| h_te_min | Float | Minimum terrain height for segment | computed |
| h_te_max | Float | Maximum terrain height for segment | computed |
| h_te_mode | Float | Mode of terrain height for segment | computed |

**ICESat-2 Algorithm Theoretical Basis Document for Land-Vegetation
Along-Track Products (ATL08)
Release 002**

| | | | |
|-------------------------|---------|---|----------------------------|
| h_te_skew | Float | Skew of terrain height for segment | computed |
| n_te_photons | Integer | Number of ground photons in segment | computed |
| h_te_interp | Float | Interpolated terrain surface height at mid-point of segment | computed |
| h_te_std | Float | Standard deviation of ground heights about the interpolated ground surface | computed |
| h_te_uncertainty | Float | Uncertainty of ground height estimates. Includes all known uncertainties such as geolocation, pointing angle, timing, radial orbit errors, etc. | computed from Equation 1.4 |
| terrain_slope | Float | Slope of terrain within segment | computed |
| h_te_best_fit | Float | Best fit terrain elevation at the 100 m segment mid-point location | computed |

594

595 **2.1.1 Georeferenced_segment_number_beg**

596 (parameter = segment_id_beg). The first along-track segment_id in each 100-m
597 segment. Each 100-m segment consists of five sequential 20-m segments provided
598 from the ATL03 product, which are labeled as segment_id. The segment_id is a seven
599 digit number that uniquely identifies each along track segment, and is written at the
600 along-track geolocation segment rate (i.e. ~20m along track). The four digit RGT
601 number can be combined with the seven digit segment_id number to uniquely define
602 any along-track segment number. Values are sequential, with 0000001 referring to
603 the first segment after the equatorial crossing of the ascending node.

604 **2.1.2 Georeferenced_segment_number_end**

605 (parameter = segment_id_end). The last along-track segment_id in each 100-m
606 segment. Each 100-m segment consists of five sequential 20-m segments provided
607 from the ATL03 product, which are labeled as segment_id. The segment_id is a seven
608 digit number that uniquely identifies each along track segment, and is written at the

along-track geolocation segment rate (i.e. ~20m along track). The four digit RGT number can be combined with the seven digit segment_id number to uniquely define any along-track segment number. Values are sequential, with 0000001 referring to the first segment after the equatorial crossing of the ascending node.

2.1.3 Segment_terrain_height_mean

(parameter = h_te_mean). Estimated mean of the terrain height above the reference ellipsoid derived from classified ground photons within the 100 m segment. If a terrain height cannot be directly determined within the segment (i.e. there are not a sufficient number of ground photons), only the interpolated terrain height will be reported. Required input data is classified point cloud (i.e. photons labeled as either canopy or ground in the ATL08 processing). This parameter will be derived from only classified ground photons.

2.1.4 Segment_terrain_height_med

(parameter = h_te_median). Median terrain height above the reference ellipsoid derived from the classified ground photons within the 100 m segment. If there are not a sufficient number of ground photons, an invalid value will be reported –no interpolation will be done. Required input data is classified point cloud (i.e. photons labeled as either canopy or ground in the ATL08 processing). This parameter will be derived from only classified ground photons.

2.1.5 Segment_terrain_height_min

(parameter = h_te_min). Minimum terrain height above the reference ellipsoid derived from the classified ground photons within the 100 m segment. If there are not a sufficient number of ground photons, an invalid value will be reported –no interpolation will be done. Required input data is classified point cloud (i.e. photons labeled as either canopy or ground in the ATL08 processing). This parameter will be derived from only classified ground photons.

2.1.6 Segment_terrain_height_max

(parameter = h_te_max). Maximum terrain height above the reference ellipsoid derived from the classified ground photons within the 100 m segment. If there are not a sufficient number of ground photons, an invalid value will be reported –no interpolation will be done. Required input data is classified point cloud (i.e. photons labeled as either canopy or ground in the ATL08 processing). This parameter will be derived from only classified ground photons.

2.1.7 Segment_terrain_height_mode

(parameter = h_te_mode). Mode of the classified ground photon heights above the reference ellipsoid within the 100 m segment. If there are not a sufficient number of ground photons, an invalid value will be reported –no interpolation will be done. Required input data is classified point cloud (i.e. photons labeled as either canopy or ground in the ATL08 processing). This parameter will be derived from only classified ground photons.

2.1.8 Segment_terrain_height_skew

(parameter = h_te_skew). The skew of the classified ground photons within the 100 m segment. If there are not a sufficient number of ground photons, an invalid value will be reported –no interpolation will be done. Required input data is classified point cloud (i.e. photons labeled as either canopy or ground in the ATL08 processing). This parameter will be derived from only classified ground photons.

2.1.9 Segment_number_terrain_photons

(parameter = n_te_photons). Number of terrain photons identified in segment.

2.1.10 Segment height_interp

(parameter = h_te_interp). Interpolated terrain surface height above the reference ellipsoid from ATL08 processing at the mid-point of each segment. This interpolated surface is the FINALGROUND estimate (described in section 4.9).

2.1.11 Segment h_te_std

(parameter = h_te_std). Standard deviations of terrain points about the interpolated ground surface within the segment. Provides an indication of surface roughness.

2.1.12 Segment_terrain_height_uncertainty

(parameter = h_te_uncertainty). Uncertainty of the mean terrain height for the segment. This uncertainty incorporates all systematic uncertainties (e.g. timing, orbits, geolocation, etc.) as well as uncertainty from errors of identified photons. This parameter is described in Section 1, Equation 1.4. If there are not a sufficient number of ground photons, an invalid value will be reported –no interpolation will be done. Required input data is classified point cloud (i.e. photons labeled as either canopy or ground in the ATL08 processing). This parameter will be derived from only classified ground photons. The $\sigma_{segmentclass}$ term in Equation 1.4 represents the standard deviation of the terrain height residuals about the FINALGROUND estimate.

2.1.13 Segment_terrain_slope

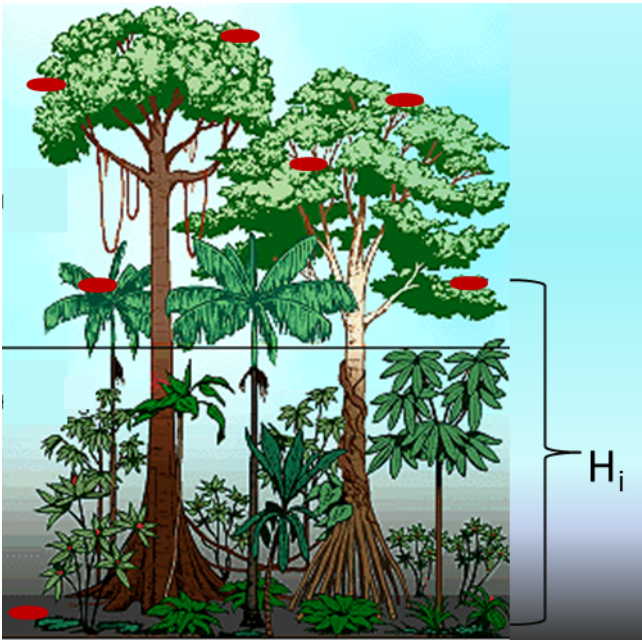
(parameter = terrain_slope). Slope of terrain within each segment. Slope is computed from a linear fit of the terrain photons. It estimates the rise [m] in relief over each segment [100 m]; e.g., if the slope value is 0.04, there is a 4 m rise over the 100 m segment. Required input data are the classified terrain photons.

2.1.14 Segment_terrain_height_best_fit

(parameter = h_te_best_fit). The best fit terrain elevation at the mid-point location of each 100 m segment. The mid-segment terrain elevation is determined by selecting the best of three fits – linear, 3rd order and 4th order polynomials – to the terrain photons and interpolating the elevation at the mid-point location of the 100 m segment. For the linear fit, a slope correction and weighting is applied to each ground photon based on the distance to the slope height at the center of the segment.

2.2 Subgroup: Vegetation Parameters

Canopy parameters will be reported on the ATL08 data product in terms of both the absolute height above the reference ellipsoid as well as the relative height above an estimated ground. The relative canopy height, H_i , is computed as the height from an identified canopy photon minus the interpolated ground surface for the same horizontal geolocation (see Figure 2.3). Thus, each identified signal photon above an interpolated surface (including a buffer distance based on the instrument point spread function) is by default considered a canopy photon. Canopy parameters will only be computed for segments where more than 5% of the classed photons are classified as canopy photons.



699

700 Figure 2.4. Illustration of canopy photons (red dots) interaction in a vegetated area.
701 Relative canopy heights, H_i , are computed by differencing the canopy photon height from
702 an interpolated terrain surface.

703 Table 2.2. Summary table of canopy parameters on ATL08.

| Group | Data type | Description | Source |
|-----------------------------|-----------|--|----------|
| segment_id_beg | Integer | First along-track segment_id number in 100-m segment | ATL03 |
| segment_id_end | Integer | Last along-track segment_id number in 100-m segment | ATL03 |
| canopy_h_metrics_abs | Float | Absolute (H##) canopy height metrics calculated at the following percentiles: 25, 50, 60, 70, 75, 80, 85, 90, 95. | computed |
| canopy_h_metrics | Float | Relative (RH##) canopy height metrics calculated at the following percentiles: 25, 50, 60, 70, 75, 80, 85, 90, 95. | computed |
| h_canopy_abs | Float | 98% height of all the individual absolute canopy heights for segment. | computed |
| h_canopy | Float | 98% height of all the individual relative canopy heights for segment. | computed |
| h_mean_canopy_abs | Float | Mean of individual absolute canopy heights within segment | computed |

**ICESat-2 Algorithm Theoretical Basis Document for Land-Vegetation
Along-Track Products (ATL08)
Release 002**

| | | | |
|-----------------------------|----------|--|----------|
| h_mean_canopy | Float | Mean of individual relative canopy heights within segment | computed |
| h_dif_canopy | Float | Difference between h_canopy and canopy_h_metrics(50) | computed |
| h_min_canopy_abs | Float | Minimum of individual absolute canopy heights within segment | computed |
| h_min_canopy | Float | Minimum of individual relative canopy heights within segment | computed |
| h_max_canopy_abs | Float | Maximum of individual absolute canopy heights within segment. Should be equivalent to H100 | computed |
| h_max_canopy | Float | Maximum of individual relative canopy heights within segment. Should be equivalent to RH100 | computed |
| h_canopy_uncertainty | Float | Uncertainty of the relative canopy height (h_canopy) | computed |
| canopy_openness | Float | STD of relative heights for all photons classified as canopy photons within the segment to provide inference of canopy openness | computed |
| toc_roughness | Float | STD of relative heights of all photons classified as top of canopy within the segment | computed |
| h_canopy_quad | Float | Quadratic mean canopy height | computed |
| n_ca_photons | Integer4 | Number of canopy photons within 100 m segment | computed |
| n_toc_photons | Integer4 | Number of top of canopy photons within 100 m segment | computed |
| centroid_height | Float | Absolute height above reference ellipsoid associated with the centroid of all signal photons | computed |
| canopy_rh_conf | Integer | Canopy relative height confidence flag based on percentage of ground and canopy photons within a segment: 0 (<5% canopy), 1 (>5% canopy, <5% ground), 2 (>5% canopy, >5% ground) | computed |
| canopy_flag | Integer | Flag indicating that canopy was detected using the Landsat Tree Cover Continuous Fields data product | computed |
| landsat_flag | Integer | Flag indicating that Landsat Tree Cover Continuous Fields data product had more than 50% values >100 for L-km segment | computed |
| landsat_perc | Float | Average percentage value of the valid (value <= 100) Landsat Tree Cover | |

Continuous Fields product for each 100
m segment

704

705 **2.2.1** Georeferenced_segment_number_beg

706 (parameter = segment_id_beg). The first along-track segment_id in each 100-m
707 segment. Each 100-m segment consists of five sequential 20-m segments provided
708 from the ATL03 product, which are labeled as segment_id. The segment_id is a seven
709 digit number that uniquely identifies each along track segment, and is written at the
710 along-track geolocation segment rate (i.e. ~20m along track). The four digit RGT
711 number can be combined with the seven digit segment_id number to uniquely define
712 any along-track segment number. Values are sequential, with 0000001 referring to
713 the first segment after the equatorial crossing of the ascending node.

714 **2.2.2** Georeferenced_segment_number_end

715 (parameter = segment_id_end). The last along-track segment_id in each 100-m
716 segment. Each 100-m segment consists of five sequential 20-m segments provided
717 from the ATL03 product, which are labeled as segment_id. The segment_id is a seven
718 digit number that uniquely identifies each along track segment, and is written at the
719 along-track geolocation segment rate (i.e. ~20m along track). The four digit RGT
720 number can be combined with the seven digit segment_id number to uniquely define
721 any along-track segment number. Values are sequential, with 0000001 referring to
722 the first segment after the equatorial crossing of the ascending node.

723 **2.2.3** Canopy_height_metrics_abs

724 (parameter = canopy_h_metrics_abs). The absolute height metrics (H##) of
725 classified canopy photons above the ellipsoid. The height metrics are sorted based on
726 a cumulative distribution and calculated at the following percentiles: 25, 50, 60, 70,
727 75, 80, 85, 90, 95. These height metrics are often used in the literature to characterize
728 vertical structure of vegetation. One important distinction of these canopy height

metrics compared to those derived from other lidar systems (e.g., LVIS or GEDI) is that the ICESat-2 canopy height metrics are heights above the ground surface. These metrics do not include the ground photons. Required input data are the absolute canopy heights of all canopy photons.

2.2.4 Canopy_height_metrics

(parameter = canopy_h_metrics). Relative height metrics above the estimated terrain surface (RH##) of classified canopy photons. The height metrics are sorted based on a cumulative distribution and calculated at the following percentiles: 25, 50, 60, 70, 75, 80, 85, 90, 95. These height metrics are often used in the literature to characterize vertical structure of vegetation. One important distinction of these canopy height metrics compared to those derived from other lidar systems (e.g., LVIS or GEDI) is that the ICESat-2 canopy height metrics are heights above the ground surface. These metrics do not include the ground photons. Required input data are relative canopy heights above the estimated terrain surface for all canopy photons.

2.2.5 Absolute_segment_canopy_height

(parameter = h_canopy_abs). The absolute 98% height of classified canopy photon heights above the ellipsoid. The absolute height from classified canopy photons are sorted into a cumulative distribution, and the height associated with the 98% height is reported.

2.2.6 Segment_canopy_height

(parameter = h_canopy). The relative 98% height of classified canopy photon heights above the estimated terrain surface. Relative canopy heights have been computed by differencing the canopy photon height from the estimated terrain surface in the ATL08 processing. The relative canopy heights are sorted into a cumulative distribution, and the height associated with the 98% height is reported.

2.2.7 Absolute_segment_mean_canopy

(parameter = h_mean_canopy_abs). The absolute mean canopy height for the segment. Absolute canopy heights are the photons heights above the reference ellipsoid. These heights are averaged.

2.2.8 Segment_mean_canopy

(parameter = h_mean_canopy). The mean canopy height for the segment. Relative canopy heights have been computed by differencing the canopy photon height from the estimated terrain surface in the ATL08 processing. These heights are averaged.

2.2.9 Segment_dif_canopy

(parameter = h_dif_canopy). Difference between h_canopy and canopy_h_metrics(50). This parameter is one metric used to describe the vertical distribution of the canopy within the segment.

2.2.10 Absolute_segment_min_canopy

(parameter = h_min_canopy_abs). The minimum absolute canopy height for the segment. Required input data is classified point cloud (i.e. photons labeled as either canopy or ground in the ATL08 processing).

2.2.11 Segment_min_canopy

(parameter = h_min_canopy). The minimum relative canopy height for the segment. Required input data is classified point cloud (i.e. photons labeled as either canopy or ground in the ATL08 processing).

2.2.12 Absolute_segment_max_canopy

(parameter = h_max_canopy_abs). The maximum absolute canopy height for the segment. This product is equivalent to H100 metric reported in the literature. This parameter, however, has the potential for error as random solar background noise

may not have been fully rejected. It is recommended that h_{canopy} or $h_{\text{canopy_abs}}$ (i.e., the 98% canopy height) be considered as the top of canopy measurement. Required input data is classified point cloud (i.e. photons labeled as either canopy or ground in the ATL08 processing).

2.2.13 Segment_max_canopy

(parameter = $h_{\text{max_canopy}}$). The maximum relative canopy height for the segment. This product is equivalent to RH100 metric reported in the literature. This parameter, however, has the potential for error as random solar background noise may not have been fully rejected. It is recommended that h_{canopy} or $h_{\text{canopy_abs}}$ (i.e., the 98% canopy height) be considered as the top of canopy measurement. Required input data is classified point cloud (i.e. photons labeled as either canopy or ground in the ATL08 processing).

2.2.14 Segment_canopy_height_uncertainty

(parameter = $h_{\text{canopy_uncertainty}}$). Uncertainty of the relative canopy height for the segment. This uncertainty incorporates all systematic uncertainties (e.g. timing, orbits, geolocation, etc.) as well as uncertainty from errors of identified photons. This parameter is described in Section 1, Equation 1.4. If there are not a sufficient number of ground photons, an invalid value will be reported –no interpolation will be done. In the case for canopy height uncertainty, the parameter $\sigma_{\text{segmentclass}}$ is comprised of both the terrain uncertainty within the segment but also the top of canopy residuals. Required input data is classified point cloud (i.e. photons labeled as either top of canopy or ground in the ATL08 processing). This parameter will be derived from only classified top of canopy photons. The canopy height uncertainty is derived from Equation 1.4, shown below as Equation 1.5, represents the standard deviation of the terrain points and the standard deviation of the top of canopy height photons.

$$\sigma_{\text{ATL08}_{\text{segment_ch}}} = \text{Eqn 1.5}$$

806

807 **2.2.15** Segment_canopy_openness

(parameter = canopy_openness). Standard deviation of relative canopy heights within each segment. This parameter will potentially provide an indicator of canopy openness as a greater standard deviation of heights indicates greater penetration of the laser energy into the canopy. Required input data is classified point cloud (i.e. photons labeled as either canopy or ground in the ATL08 processing).

813 **2.2.16** Segment_top_of_canopy_roughness

(parameter = toc_roughness). Standard deviation of relative top of canopy heights within each segment. This parameter will potentially provide an indicator of canopy variability. Required input data is classified point cloud (i.e. photons labeled as the top of the canopy in the ATL08 processing).

818 **2.2.17** Segment_canopy_quadratic_height

(parameter = h_canopy_quad). The quadratic mean relative height of classified canopy photons. The quadratic mean height is computed as:

$$qm h = \sqrt{\sum_{i=1}^{n_ca_photons} \frac{h_i^2}{n_ca_photons}}$$

822 **2.2.18** Segment_number_canopy_photons

(parameter = n_ca_photons). Number of canopy photons within each segment.
 Required input data is classified point cloud (i.e. photons labeled as either canopy or
 ground in the ATL08 processing).

2.2.19 Segment_number_top_canopy_photons

(parameter = n_toc_photons). Number of top of canopy photons within each segment. Required input data is classified point cloud (i.e. photons labeled as top of canopy in the ATL08 processing).

2.2.20 Centroid_height

(parameter = centroid_height). Optical centroid of all photons classified as either canopy or ground points within a segment. The heights used in this calculation are absolute heights above the reference ellipsoid. This parameter is equivalent to the centroid height produced on ICESat GLA14.

2.2.21 Segment_rel_canopy_conf

(parameter = canopy_rh_conf). Canopy relative height confidence flag based on percentage of ground photons and percentage of canopy photons, relative to the total classified (ground and canopy) photons within a segment: 0 (<5% canopy), 1 (>5% canopy and <5% ground), 2 (>5% canopy and >5% ground). This is a measure based on the quantity, not the quality, of the classified photons in each segment.

2.2.22 Canopy_flag

(parameter = canopy_flag). Flag indicating that canopy was detected using the Landsat Continuous Cover product for the *L-km* segment. Currently, if more than 5% of the Landsat CC pixels along the profile have canopy in them, we make the assumption canopy is present along the entire *L-km* segment.

2.2.23 Landsat_flag

(parameter = landsat_flag). Flag indicating that more than 50% of the Landsat Tree Cover Continuous Fields product have values >100 (indicating water, cloud, shadow, or filled values) for the *L-km* segment. Canopy is assumed present along the *L-km* segment if landsat_flag is 1.

2.2.24 Landsat_perc

(parameter = landsat_perc). Average percentage value of the valid (value <= 100) Landsat Tree Cover Continuous Fields product pixels that overlap within each 100 m segment.

2.3 Subgroup: Photons

The subgroup for photons contains the classified photons that were used to generate the parameters within the land or canopy subgroups. Each photon that is identified as being likely signal will be classified as: 0 = noise, 1 = ground, 2 = canopy, or 3 = top of canopy. The index values for each classified photon will be provided such that they can be extracted from the ATL03 data product for independent evaluation.

Table 2.3. Summary table for photon parameters for the ATL08 product.

| Group | Data Type | Description | Source |
|------------------------|-----------|---|----------|
| classed_PC_indx | Float | Indices of photons tracking back to ATL03 that surface finding software identified and used within the creation of the data products. | ATL03 |
| classed_PC_flag | Integer | Classification flag for each photon as either noise, ground, canopy, or top of canopy. | computed |
| ph_segment_id | Integer | Georeferenced bin number (20-m) associated with each photon | ATL03 |
| d_flag | Integer | Flag indicating whether DRAGANN labeled the photon as noise or signal | computed |

2.3.1 Indices_of_classed_photons

(parameter = `classed_PC_indx`). Indices of photons tracking back to ATL03 that surface finding software identified and used within the creation of the data products for a given segment.

2.3.2 Photon_class

(parameter = `classed_PC_flag`). Classification flags for a given segment. 0 = noise, 1 = ground, 2 = canopy, 3 = top of canopy. The final ground and canopy classification are flags 1-3. The full canopy is the combination of flags 2 and 3.

2.3.3 Georeferenced_segment_number

(parameter = `ph_segment_id`). The `segment_id` associated with every photon in each 100-m segment. Each 100-m segment consists of five sequential 20-m segments provided from the ATL03 product, which are labeled as `segment_id`. The `segment_id` is a seven digit number that uniquely identifies each along track segment, and is written at the along-track geolocation segment rate (i.e. ~20m along track). The four digit RGT number can be combined with the seven digit `segment_id` number to uniquely define any along-track segment number. Values are sequential, with 0000001 referring to the first segment after the equatorial crossing of the ascending node.

2.3.4 DRAGANN_flag

(parameter = `d_flag`). Flag indicating the labeling of DRAGANN noise filtering for a given photon. 0 = noise, 1=signal.

2.4 Subgroup: Reference data

The reference data subgroup contains parameters and information that are useful for determining the terrain and canopy heights that are reported on the

**ICESat-2 Algorithm Theoretical Basis Document for Land-Vegetation
Along-Track Products (ATL08)
Release 002**

product. In addition to position and timing information, these parameters include the reference DEM height, reference landcover type, and flags indicating water or snow.

Table 2.4. Summary table for reference parameters for the ATL08 product.

| Group | Data Type | Description | Source |
|--------------------------|-----------|--|----------|
| segment_id_beg | Integer | First along-track segment_id number in 100-m segment | ATL03 |
| segment_id_end | Integer | Last along-track segment_id number in 100-m segment | ATL03 |
| latitude | Float | Center latitude of signal photons within each segment | ATL03 |
| longitude | Float | Center longitude of signal photons within each segment | ATL03 |
| delta_time | Float | Mid-segment GPS time in seconds past an epoch. The epoch is provided in the metadata at the file level | ATL03 |
| delta_time_beg | Float | Delta time of the first photon in the segment | ATL03 |
| delta_time_end | Float | Delta time of the last photon in the segment | ATL03 |
| night_flag | Integer | Flag indicating whether the measurements were acquired during night time conditions | computed |
| dem_h | Float4 | Reference DEM elevation | external |
| dem_flag | | Source of reference DEM | external |
| dem_removal_flag | Integer | Quality check flag to indicate > 20% photons removed due to large distance from dem_h | computed |
| h_dif_ref | Float4 | Difference between h_te_median and dem_h | computed |
| terrain_flg | Integer | Terrain flag quality check to indicate a deviation from the reference DTM | computed |
| segment_landcover | Integer4 | Reference landcover for segment derived from best global landcover product available | external |
| segment_watermask | Integer4 | Water mask indicating inland water produced from best sources available | external |

**ICESat-2 Algorithm Theoretical Basis Document for Land-Vegetation
Along-Track Products (ATL08)
Release 002**

| | | | |
|--------------------------|----------|---|----------|
| segment_snowcover | Integer4 | Daily snow cover mask derived from best sources | external |
| urban_flag | Integer | Flag indicating segment is located in an urban area | external |
| surf_type | Integer1 | Flags describing surface types: 0=not type, 1=is type. Order of array is land, ocean, sea ice, land ice, inland water. | ATL03 |
| atl08_region | Integer | ATL08 region(s) encompassed by ATL03 granule being processed | computed |
| last_seg_extend | Float | The distance (km) that the last ATL08 processing segment in a file is either extended or overlapped with the previous ATL08 processing segment | computed |

893

894 **2.4.1 Georeferenced_segment_number_beg**

895 (parameter = segment_id_beg). The first along-track segment_id in each 100-m
896 segment. Each 100-m segment consists of five sequential 20-m segments provided
897 from the ATL03 product, which are labeled as segment_id. The segment_id is a seven
898 digit number that uniquely identifies each along track segment, and is written at the
899 along-track geolocation segment rate (i.e. ~20m along track). The four digit RGT
900 number can be combined with the seven digit segment_id number to uniquely define
901 any along-track segment number. Values are sequential, with 0000001 referring to
902 the first segment after the equatorial crossing of the ascending node.

903 **2.4.2 Georeferenced_segment_number_end**

904 (parameter = segment_id_end). The last along-track segment_id in each 100-m
905 segment. Each 100-m segment consists of five sequential 20-m segments provided
906 from the ATL03 product, which are labeled as segment_id. The segment_id is a seven
907 digit number that uniquely identifies each along track segment, and is written at the
908 along-track geolocation segment rate (i.e. ~20m along track). The four digit RGT

number can be combined with the seven digit segment_id number to uniquely define any along-track segment number. Values are sequential, with 0000001 referring to the first segment after the equatorial crossing of the ascending node.

2.4.3 Segment_latitude

(parameter = latitude). Center latitude of signal photons within each segment

2.4.4 Segment_longitude

(parameter = longitude). Center longitude of signal photons within each segment

2.4.5 Delta_time

(parameter = delta_time). Mid-segment GPS time for the segment in seconds past an epoch. The epoch is listed in the metadata at the file level.

2.4.6 Delta_time_beg

(parameter = delta_time_beg). Delta time for the first photon in the segment in seconds past an epoch. The epoch is listed in the metadata at the file level.

2.4.7 Delta_time_end

(parameter = delta_time_end). Delta time for the last photon in the segment in seconds past an epoch. The epoch is listed in the metadata at the file level.

2.4.8 Night_Flag

(parameter = night_flag). Flag indicating the data were acquired in night conditions: 0 = day, 1 = night. Night flag is set when solar elevation is below 0.0 degrees.

2.4.9 Segment_reference_DTM

(parameter = dem_h). Reference terrain height value for segment determined by the “best” DEM available based on data location. All heights in ICESat-2 are referenced to the WGS 84 ellipsoid unless clearly noted otherwise. DEM is taken from a variety of ancillary data sources: GIMP, GMTED, MSS. The DEM source flag indicates which source was used.

2.4.10 Segment_reference_DEM_source

(parameter = dem_flag). Indicates source of the reference DEM height. Values: 0=None, 1=GIMP, 2=GMTED, 3=MSS.

2.4.11 Segment_reference_DEM_removal_flag

(parameter = dem_removal_flag). Quality check flag to indicate > 20% classified photons removed from land segment due to large distance from dem_h.

2.4.12 Segment_terrain_difference

(parameter = h_dif_ref). Difference between h_te_median and dem_h. Since the mean terrain height is more sensitive to outliers, the median terrain height will be evaluated against the reference DEM. This parameter will be used as an internal data quality check with the notion being that if the difference exceeds a threshold (TBD) a terrain quality flag (terrain_flg) will be triggered.

2.4.13 Segment_terrain flag

(parameter = terrain_flg). Terrain flag to indicate confidence in the derived terrain height estimate. If h_dif_ref exceeds a threshold (TBD) the terrain_flg parameter will be set to 1. Otherwise, it is 0.

2.4.14 Segment_landcover

(parameter = segment_landcover). Segment landcover will be based on best available global landcover product used for reference. One potential source is the 0.5

km global mosaics of the standard MODIS land cover product (Channan et al, 2015; Friedl et al, 2010; available online at <http://glcf.umd.edu/data/lc/index.shtml>). Here, 17 classes are defined ranging from evergreen (needle and broadleaf forest), deciduous (needle and broadleaf forest), shrublands, woodlands, savanna and grasslands, agriculture, to urban. The most current year processed for this product is based on MODIS measurements from 2012.

2.4.15 Segment_watermask

(parameter = segment_watermask). Water mask (i.e., flag) indicating inland water as referenced from the Global Raster Water Mask at 250 m spatial resolution (Carroll et al, 2009; available online at <http://glcf.umd.edu/data/watermask/>). 0 = no water; 1 = water.

2.4.16 Segment_snowcover

(parameter = segment_snowcover). Daily snowcover mask (i.e., flag) indicating a likely presence of snow or ice within each segment produced from best available source used for reference. The snow mask will be the same snow mask as used for ATL09 Atmospheric Products: NOAA snow-ice flag. 0=ice free water; 1=snow free land; 2=snow; 3=ice.

2.4.17 Urban_flag

(parameter = urban_flag). The urban flag indicates that a segment is likely located over an urban area. In these areas, buildings may be misclassified as canopy, and thus the canopy products may be incorrect. The urban flag is sourced from the “urban and built up” classification on the MODIS land cover product (Channan et al, 2015; Friedl et al, 2010; available online at <http://glcf.umd.edu/data/lc/index.shtml>). 0 = not urban; 1 = urban.

2.4.18 Surface_type

(parameter = surf_type). The surface type for a given segment is determined at the major frame rate (every 200 shots, or ~140 meters along-track) and is a two-dimensional array surf_type(n, nsurf), where n is the major frame number, and nsurf is the number of possible surface types such that surf_type(n, isurf) is set to 0 or 1 indicating if surface type isurf is present (1) or not (0), where isurf = 1 to 5 (land, ocean, sea ice, land ice, and inland water) respectively.

2.4.19 ATL08_region

(parameter = atl08_region). The ATL08 regions that encompass the ATL03 granule being processed through the ATL08 algorithm. The ATL08 regions are shown by Figure 2.3. In ATL08 regions 11 (Greenland) and 7 – 10 (Antarctica), the canopy_flag is automatically set to false for ATL08 processing.

2.4.20 Last_segment_extend

(parameter = last_seg_extend). The distance (km) that the last ATL08 10 km processing segment is either extended beyond 10 km or uses data from the previous 10 km processing segment to allow for enough data for processing the ATL03 photons through the ATL08 algorithm. If the last portion of an ATL03 granule being processed would result in a segment with less than 3.4 km (170 geosegments) worth of data, that last portion is added to the previous 10 km processing window to be processed together as one extended ATL08 processing segment. The resulting last_seg_extend value would be a positive value of distance beyond 10 km that the ATL08 processing segment was extended by. If the last ATL08 processing segment would be less than 10 km but greater than 3.4 km, a portion extending from the start of current ATL08 processing segment backwards into the previous ATL08 processing segment would be added to the current ATL08 processing segment to make it 10 km in length. The distance of this backward data gathering would be reported in last_seg_extend as a negative distance value. Only new 100 m ATL08 segment products generated from

1006 this backward extension would be reported. All other segments that are not extended
1007 will report a last_seg_extend value of 0.

1008

1009 **2.5 Subgroup: Beam data**

1010 The subgroup for beam data contains basic information on the geometry and
1011 pointing accuracy for each beam.

1012 Table 2.5. Summary table for beam parameters for the ATL08 product.

| Group | Data Type | Units | Description | Source |
|----------------|-----------|-------|---|--------|
| segment_id_beg | Integer | | First along-track segment_id number in 100-m segment | ATL03 |
| segment_id_end | Integer | | Last along-track segment_id number in 100-m segment | ATL03 |
| ref_elev | Float | | Elevation of the unit pointing vector for the reference photon in the local ENU frame in radians. The angle is measured from East-North plane and positive towards up | ATL03 |
| ref_azimuth | Float | | Azimuth of the unit pointing vector for the reference photon in the ENU frame in radians. The angle is measured from North and positive toward East. | ATL03 |
| atlas_pa | Float | | Off nadir pointing angle of the spacecraft | ATL03 |
| rgt | Integer | | The reference ground track (RGT) is the track on the earth at which the vector bisecting laser beams 3 and 4 is | ATL03 |

**ICESat-2 Algorithm Theoretical Basis Document for Land-Vegetation
Along-Track Products (ATL08)
Release 002**

| | | | |
|-------------------------|---------|--|----------|
| | | pointed during repeat operations | |
| sigma_h | Float | Total vertical uncertainty due to PPD and POD | ATL03 |
| sigma_along | Float | Total along-track uncertainty due to PPD and POD knowledge | ATL03 |
| sigma_across | Float | Total cross-track uncertainty due to PPD and POD knowledge | ATL03 |
| sigma_topo | Float | Uncertainty of the geolocation knowledge due to local topography (Equation 1.3) | computed |
| sigma_atlas_land | Float | Total uncertainty that includes sigma_h plus the geolocation uncertainty due to local slope Equation 1.2 | computed |
| psf_flag | integer | Flag indicating sigma_atlas_land (aka PSF) as computed in Equation 1.2 exceeds a value of 1m. | computed |
| layer_flag | Integer | Cloud flag indicating presence of clouds or blowing snow | ATL09 |
| cloud_flag_asr | Integer | Cloud confidence flag from ATL09 indicating clear skies | ATL09 |
| msw_flag | Integer | Multiple scattering warning product produced on ATL09 | ATL09 |
| asr | Float | Apparent surface reflectance | ATL09 |
| snr | Float | Background signal to noise level | Computed |
| solar_azimuth | Float | The azimuth (in degrees) of the sun position vector from the reference photon bounce point position in the local ENU frame. The angle is measured from | ATL03g |

| | | | |
|------------------------|---------|---|----------|
| solar_elevation | Float | North and is positive towards East. The elevation of the sun position vector from the reference photon bounce point position in the local ENU frame. The angle is measured from the East-North plane and is positive Up. | ATL03g |
| n_seg_ph | Integer | Number of photons within each land segment | computed |
| ph_ndx_beg | Integer | Photon index begin | computed |

1013

1014 **2.5.1 Georeferenced_segment_number_beg**

1015 (parameter = segment_id_beg). The first along-track segment_id in each 100-m
 1016 segment. Each 100-m segment consists of five sequential 20-m segments provided
 1017 from the ATL03 product, which are labeled as segment_id. The segment_id is a seven
 1018 digit number that uniquely identifies each along track segment, and is written at the
 1019 along-track geolocation segment rate (i.e. ~20m along track). The four digit RGT
 1020 number can be combined with the seven digit segment_id number to uniquely define
 1021 any along-track segment number. Values are sequential, with 0000001 referring to
 1022 the first segment after the equatorial crossing of the ascending node.

1023 **2.5.2 Georeferenced_segment_number_end**

1024 (parameter = segment_id_end). The last along-track segment_id in each 100-m
 1025 segment. Each 100-m segment consists of five sequential 20-m segments provided
 1026 from the ATL03 product, which are labeled as segment_id. The segment_id is a seven
 1027 digit number that uniquely identifies each along track segment, and is written at the
 1028 along-track geolocation segment rate (i.e. ~20m along track). The four digit RGT
 1029 number can be combined with the seven digit segment_id number to uniquely define

1030 any along-track segment number. Values are sequential, with 0000001 referring to
1031 the first segment after the equatorial crossing of the ascending node.

1032 **2.5.3 Beam_coelevation**

1033 (parameter = ref_elev). Elevation of the unit pointing vector for the reference
1034 photon in the local ENU frame in radians. The angle is measured from East-North
1035 plane and positive towards up.

1036 **2.5.4 Beam_azimuth**

1037 (parameter = ref_azimuth). Azimuth of the unit pointing vector for the
1038 reference photon in the ENU frame in radians. The angle is measured from North and
1039 positive toward East.

1040 **2.5.5 ATLAS_Pointing_Angle**

1041 (parameter = atlas_pa). Off nadir pointing angle (in radians) of the satellite to
1042 increase spatial sampling in the non-polar regions.

1043 **2.5.6 Reference_ground_track**

1044 (parameter = rgt). The reference ground track (RGT) is the track on the earth
1045 at which the vector bisecting laser beams 3 and 4 (or GT2L and GT2R) is pointed
1046 during repeat operations. Each RGT spans the part of an orbit between two ascending
1047 equator crossings and are numbered sequentially. The ICESat-2 mission has 1387
1048 RGTs, numbered from 0001xx to 1387xx. The last two digits refer to the cycle number.

1049 **2.5.7 Sigma_h**

1050 (parameter = sigma_h). Total vertical uncertainty due to PPD (Precise Pointing
1051 Determination), POD (Precise Orbit Determination), and geolocation errors.
1052 Specifically, this parameter includes radial orbit error, σ_{orbit} , tropospheric errors,
1053 σ_{trop} , forward scattering errors, $\sigma_{forwardscattering}$, instrument timing errors, σ_{timing} ,
1054 and off-nadir pointing geolocation errors. The component parameters are pulled

from ATL03 and ATL09. Sigma_h is the root sum of squares of these terms as detailed in Equation 1.1. The sigma_h reported here is the mean of the sigma_h values reported within the five ATL03 geosegments that are used to create the 100 m ATL08 segment.

2.5.8 Sigma_along

(parameter = sigma_along). Total along-track uncertainty due to PPD and POD knowledge. This parameter is pulled from ATL03.

2.5.9 Sigma_across

(parameter = sigma_across). Total cross-track uncertainty due to PPD and POD knowledge. This parameter is pulled from ATL03.

2.5.10 Sigma_topo

(parameter = sigma_topo). Uncertainty in the geolocation due to local surface slope as described in Equation 1.3. The local slope is multiplied by the 6.5 m geolocation uncertainty factor that will be used to determine the geolocation uncertainty. The geolocation error will be computed from a 100 m sample due to the local slope calculation at that scale.

2.5.11 Sigma_ATLAS_LAND

(parameter = sigma_atlas_land). Total vertical geolocation error due to ranging, and local surface slope. The parameter is computed for ATL08 as described in Equation 1.2. The geolocation error will be computed from a 100 m sample due to the local slope calculation at that scale.

2.5.12 PSF_flag

(parameter = psf_flag). Flag indicating that the point spread function (computed as sigma_atlas_land) has exceeded 1m.

2.5.13 Layer_flag

(parameter = layer_flag). Flag is a combination of multiple ATL09 flags and takes daytime/nighttime into consideration. A value of 1 means clouds or blowing snow is likely present. A value of 0 indicates the likely absence of clouds or blowing snow. If no ATL09 product is available for an ATL08 segment, an invalid value will be reported.

2.5.14 Cloud_flag

(parameter = cloud_flag_asr). Cloud confidence flag from ATL09. Flag indicates potential clear skies from ATL09. If no ATL09 product is available for an ATL08 segment, an invalid value will be reported. Cloud flags:

- 0 = High confidence clear skies
- 1 = Medium confidence clear skies
- 2 = Low confidence clear skies
- 3 = Low confidence cloudy skies
- 4 = Medium confidence cloudy skies
- 5 = High confidence cloudy skies

2.5.15 MSW

(parameter = msw_flag). Multiple scattering warning flag with values from -1 to 5 as computed in the ATL09 atmospheric processing and delivered on the ATL09 data product. If no ATL09 product is available for an ATL08 segment, an invalid value will be reported. MSW flags:

- 1 = signal to noise ratio too low to determine presence of cloud or blowing snow
- 0 = no_scattering
- 1 = clouds at > 3 km
- 2 = clouds at 1-3 km
- 3 = clouds at < 1 km

1105 4 = blowing snow at < 0.5 optical depth

1106 5 = blowing snow at >= 0.5 optical depth

1107 **2.5.16** Computed_Apparent_Surface_Reflectance

1108 (parameter = asr). Apparent surface reflectance computed in the ATL09
1109 atmospheric processing and delivered on the ATL09 data product. If no ATL09
1110 product is available for an ATL08 segment, an invalid value will be reported.

1111 **2.5.17** Signal_to_Noise_Ratio

1112 (parameter = snr). The Signal to Noise Ratio of geolocated photons as
1113 determined by the ratio of the superset of ATL03 signal and DRAGANN found signal
1114 photons used for processing the ATL08 segments to the background photons (i.e.,
1115 noise) within the same ATL08 segments.

1116 **2.5.18** Solar_Azimuth

1117 (parameter = solar_azimuth). The azimuth (in degrees) of the sun position
1118 vector from the reference photon bounce point position in the local ENU frame. The
1119 angle is measured from North and is positive towards East.

1120 **2.5.19** Solar_Elevation

1121 (parameter = solar_elevation). The elevation of the sun position vector from
1122 the reference photon bounce point position in the local ENU frame. The angle is
1123 measured from the East-North plane and is positive up.

1124 **2.5.20** Number_of_segment_photons

1125 (parameter = n_seg_ph). Number of photons in each land segment.

1126 **2.5.21** Photon_Index_Begin

1127 (parameter = ph_ndx_beg). Index (1-based) within the photon-rate data of
1128 the first photon within this each land segment.

1129

1130

3 ALGORITHM METHODOLOGY

For the ecosystem community, identification of the ground and canopy surface is by far the most critical task, as meeting the science objective of determining global canopy heights hinges upon the ability to detect both the canopy surface and the underlying topography. Since a space-based photon counting laser mapping system is a relatively new instrument technology for mapping the Earth's surface, the software to accurately identify and extract both the canopy surface and ground surface is described here. The methodology adopted for ATL08 establishes a framework to potentially accept multiple approaches for capturing both the upper and lower surface of signal photons. One method used is an iterative filtering of photons in the along-track direction. This method has been found to preserve the topography and capture canopy photons, while rejecting noise photons. An advantage of this methodology is that it is self-parameterizing, robust, and works in all ecosystems if sufficient photons from both the canopy and ground are available. For processing purposes, along-track data signal photons are parsed into L -km segment of the orbit which is recommended to be 10 km in length.

3.1 Noise Filtering

Solar background noise is a significant challenge in the analysis of photon counting laser data. Range measurement data created from photon counting lidar detectors typically contain far higher noise levels than the more common photon integrating detectors available commercially in the presence of passive, solar background photons. Given the higher detection sensitivity for photon counting devices, a background photon has a greater probability of triggering a detection event over traditional integral measurements and may sometimes dominate the dataset. Solar background noise is a function of the surface reflectance, topography, solar elevation, and atmospheric conditions. Prior to running the surface finding

algorithms used for ATL08 data products, the superset of output from the GSFC medium-high confidence classed photons (ATL03 signal_conf_ph: flags 3-4) and the output from DRAGANN will be considered as the input data set. ATL03 input data requirements include the latitude, longitude, height, segment delta time, segment ID, and a preliminary signal classification for each photon. The motivation behind combining the results from two different noise filtering methods is to ensure that all of the potential signal photons for land surfaces will be provided as input to the surface finding software. The description of the methodology for the ATL03 classification is described separately in the ATL03 ATBD. The methodology behind DRAGANN is described in the following section.

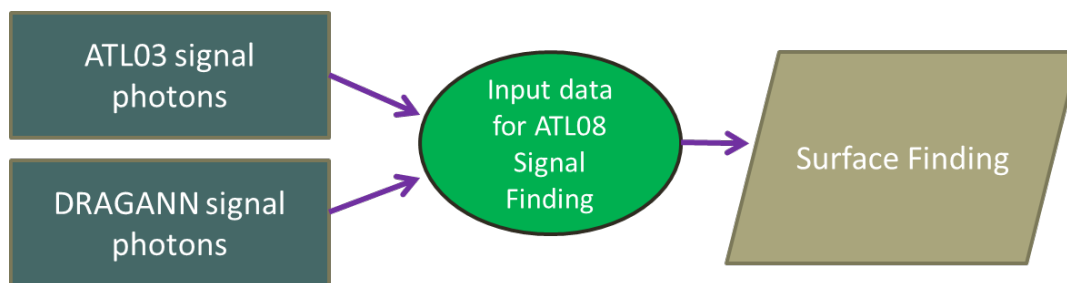


Figure 3.1. Combination of noise filtering algorithms to create a superset of input data for surface finding algorithms.

3.1.1 DRAGANN

The Differential, Regressive, and Gaussian Adaptive Nearest Neighbor (DRAGANN) filtering technique was developed to identify and remove noise photons from the photon counting data point cloud. DRAGANN utilizes the basic premise that signal photons will be closer in space than random noise photons. The first step of the filtering is to implement an adaptive nearest neighbor search. By using an adaptive method, different thresholds can be applied to account for variable amounts of

background noise and changing surface reflectance along the data profile. This search finds an effective radius by computing the probability of finding P number of points within a search area. For MABEL and mATLAS, P=20 points within the search area was empirically derived but found to be an effective and efficient number of neighbors.

There may be cases, however, where the value of P needs to be changed. For example, during night acquisitions it is anticipated that the background noise rate will be considerably low. Since DRAGANN is searching for two distributions in neighborhood searching space, the software could incorrectly identify signal photons as noise photons. The parameter P, however, can be determined dynamically from estimations of the signal and noise rates from the photon cloud. In cases of low background noise (night), P would likely be changed to a value lower than 20. Similarly, in cases of high amounts of solar background, P may need to be increased to better capture the signal and avoid classifying small, dense clusters of noise as signal. In this case, however, it is likely that noise photons near signal photons will also be misclassified as signal. The method for dynamically determining a P value is explained further in section 1.1.1.

After P is defined, a histogram of the number of neighbors within a search radius for each point is generated. The distribution of neighbor radius occurrences is analyzed to determine the noise threshold.

$$\frac{P}{N_{total}} = \frac{V}{V_{total}} \quad \text{Eqn. 3.1}$$

where N_{total} is the total number of photons in the point cloud, V is the volume of the nearest neighborhood search, and V_{total} is the bounding volume of the enclosed point cloud. For a 2-dimensional data set, V becomes

$$V = \pi r^2 \quad \text{Eqn. 3.2}$$

where r is the radius. A good practice is to first normalize the data set along each dimension before running the DRAGANN filter. Normalization prevents the algorithm from favoring one dimension over the others in the radius search (e.g., when the latitude and longitude are in degrees and height is in meters).

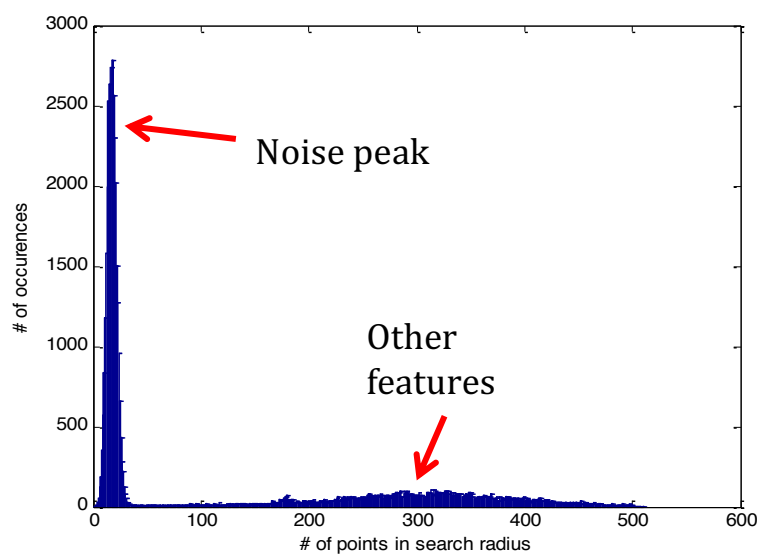


Figure 3.2. Histogram of the number of photons within a search radius. This histogram is used to determine the threshold for the DRAGANN approach.

Once the radius has been computed, DRAGANN counts the number of points within the radius for each point and histograms that set of values. The distribution of the number of points, Figure 3.2, reveals two distinct peaks; a noise peak and a signal peak. The motivation of DRAGANN is to isolate the signal photons by determining a threshold based on the number of photons within the search radius. The noise peak is characterized as having a large number of occurrences of photons with just a few neighboring photons within the search radius. The signal photons comprise the broad second peak. The first step in determining the threshold between the noise and signal

is to implement Gaussian fitting to the number of photons distribution (i.e., the distribution shown in Figure 3.2). The Gaussian function has the form

$$g(x) = ae^{\frac{-(x-b)^2}{2c^2}} \quad \text{Eqn. 3.3}$$

where a is the amplitude of the peak, b is the center of the peak, and c is the standard deviation of the curve. A first derivative sign crossing method is one option to identify peaks within the distribution.

To determine the noise and signal Gaussians, up to ten Gaussian curves are fit to the histogram using an iterative process of fitting and subtracting the maximum amplitude peak component from the histogram until all peaks have been extracted. Then, the potential Gaussians pass through a rejection process to eliminate those with poor statistical fits or other apparent errors (Goshtasby and O'Neill, 1994; Chauve et al. 2008). A Gaussian with an amplitude less than 1/5 of the previous Gaussian and within two standard deviations of the previous Gaussian should be rejected. Once the errant Gaussians are rejected, the final two remaining are assumed to represent the noise and signal. These are separated based on the remaining two Gaussian components within the histogram using the logic that the leftmost Gaussian is noise (low neighbor counts) and the other is signal (high neighbor counts).

The intersection of these two Gaussians (noise and signal) determines a data threshold value. The threshold value is the parameter used to distinguish between noise points and signal points when the point cloud is re-evaluated for surface finding. In the event that only one curve passes the rejection process, the threshold is set at 1 σ above the center of the noise peak.

An example of the noise filtered product from DRAGANN is shown in Figure 3.3. The signal photons identified in this process will be combined with the coarse signal finding output available on the ATL03 data product.

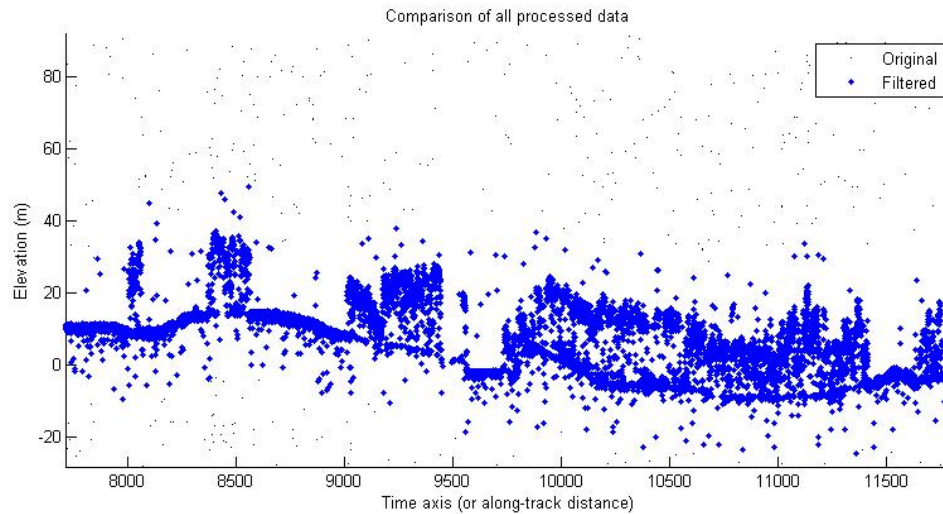


Figure 3.3. Output from DRAGANN filtering. Signal photons are shown as blue.

Figure 3.3 provides an example of along-track (profiling) height data collected in September 2012 from the MABEL (ICESat-2 simulator) over vegetation in North Carolina. The photons have been filtered such that the signal photons returned from vegetation and the ground surface are remaining. Noise photons that are adjacent to the signal photons are also retained in the input dataset; however, these should be classified as noise photons during the surface finding process. It is possible that some additional outlying noise may be retained during the DRAGANN process when noise photons are densely grouped, and these photons should be filtered out before the surface finding process. Estimates of the ground surface and canopy height can then be derived from the signal photons.

3.2 Surface Finding

Once the signal photons have been determined, the objective is to find the ground and canopy photons from within the point cloud. With the expectation that one algorithm may not work everywhere for all biomes, we are employing a framework that will allow us to combine the solutions of multiple algorithms into one

final composite solution for the ground surface. The composite ground surface solution will then be utilized to classify the individual photons as ground, canopy, top of canopy, or noise. Currently, the framework described here utilizes one algorithm for finding the ground surface and canopy surface. Additional methods, however, could be integrated into the framework at a later time. Figure 3.4 below describes the framework.

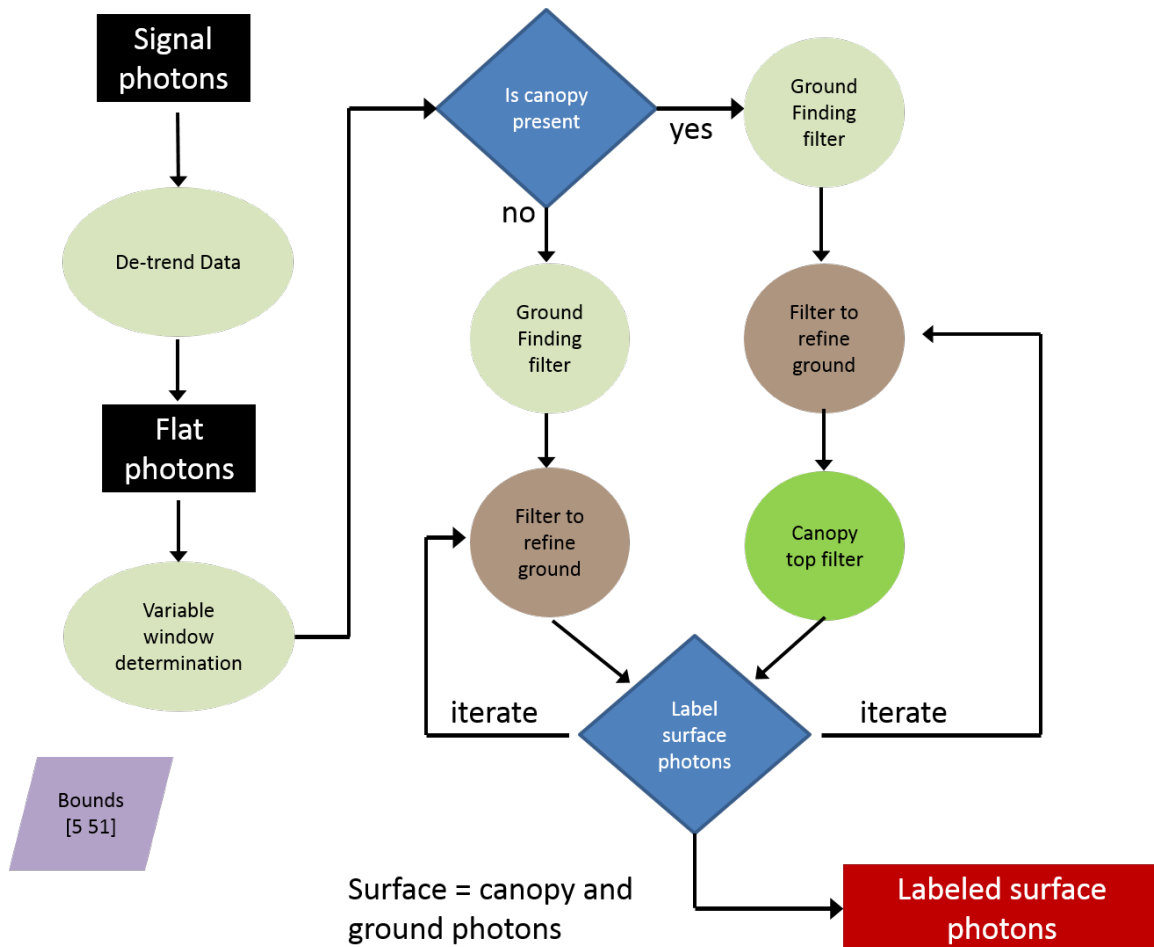


Figure 3.4. Flowchart of overall surface finding method.

3.2.1 De-trending the Signal Photons

An important step in the success of the surface finding algorithm is to remove the effect of topography on the input data, thus improving the performance of the algorithm. This is done by de-trending the input signal photons by subtracting a heavily smoothed “surface” that is derived from the input data. Essentially, this is a low pass filter of the original data and most of the analysis to detect the canopy and ground will subsequently be implemented on the high pass data. The amount of smoothing that is implemented in order to derive this first surface is dependent upon the relief. For segments where the relief is high, the smoothing window size is decreased so topography isn’t over-filtered.

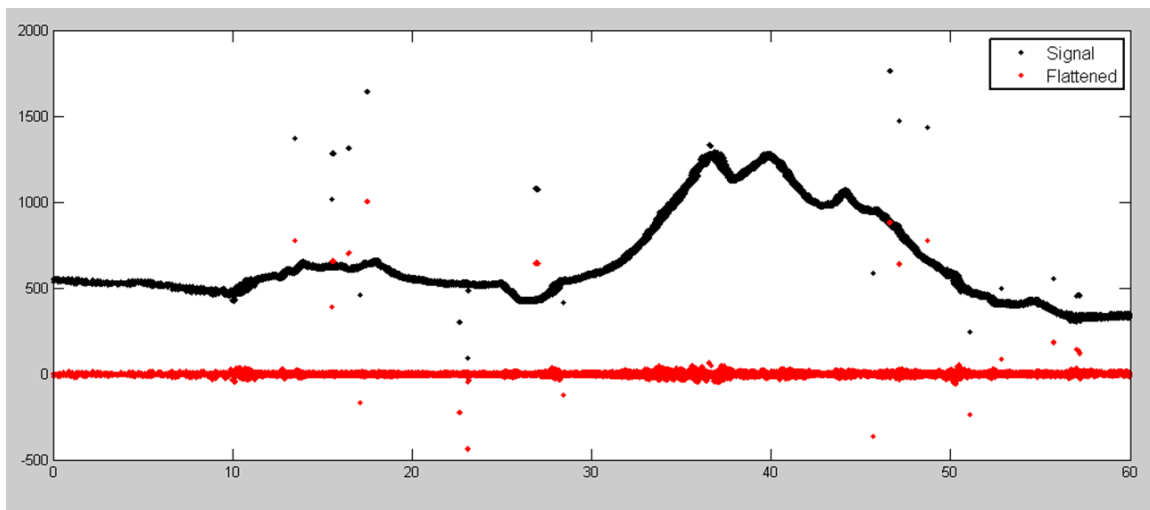


Figure 3.5. Plot of Signal Photons (black) from 2014 MABEL flight over Alaska and de-trended photons (red).

3.2.2 Canopy Determination

A key factor in the success of the surface finding algorithm is for the software to automatically **account for the presence of canopy** along a given L -km segment.

Due to the large volume of data, this process has to occur in an automated fashion, allowing the correct methodology for extracting the surface to be applied to the data. In the absence of canopy, the iterative filtering approach to finding ground works extremely well, but if canopy does exist, we need to accommodate for that fact when we are trying to recover the ground surface.

Currently, the Landsat Tree Cover Continuous Fields dataset from the 2000 epoch is used to set a canopy flag within the ATL08 algorithm. Each of these Landsat Tree Cover tiles contain 30 m pixels indicating the percentage canopy cover for vegetation over 5 m high in that pixel area. The 2000 epoch is used over the newer 2005 epoch due to “striping” in the 2005 tiles, caused by the failure of the scan line corrector (SLC) in 2003. The striping artifacts result in inconsistent pixel values across a landscape which in turn can result in a tenfold difference in the average canopy cover percentage calculated between the epochs for a flight segment. There is currently available a 2015 Tree Cover Beta Release that utilizes Landsat 8 data. This new release of the 2015 Tree Cover product will replace the 2000 epoch for setting the canopy flag in the ATL08 algorithm. The Tree Cover data are available via ftp at <http://glcf.umd.edu/data/landsatTreecover/>.

For each L -km segment of ATLAS data, a comparison is made between the midpoint location of the segment and the midpoint locations of the WRS Landsat tiles to find the closest tile that encompasses the L -km segment. Using the closest found tile, each signal photon’s X-Y location is used to identify the corresponding Landsat pixel. Multiple instances of the same pixels found for the L -km segment are discarded, and the percentage canopy values of the unique pixels determined to be under the L -km segment are averaged to produce an average canopy cover percentage for that segment. If the average canopy cover percentage for a segment is over 5% (threshold subject to change under further testing), then the ATL08 algorithm will assume the presence of canopy and identify both ground and vegetation photons in that

segment's output. Else, the ATL08 algorithm uses a simplified calculation to identify only ground photons in that segment.

The canopy flag determines if the algorithm will calculate only ground photons (canopy flag = 0) or both ground and vegetation photons (canopy flag = 1) for each *L-km* segment.

For ATL08 product regions over Antarctica (regions 7, 8, 9, 10) and Greenland (region 11), the algorithm will assume only ground photons (canopy flag = 0) (see Figure 2.2).

3.2.3 Variable Window Determination

The method for generating a best estimated terrain surface will vary depending upon whether canopy is present. *L-km segments* without canopy are much easier to analyze because the ground photons are usually continuous. *L-km segments* with canopy, however, require more scrutiny as the number of signal photons from ground are fewer due to occlusion by the vegetation.

There are some common elements for finding the terrain surface for both cases (canopy/no canopy) and with both methods. In both cases, we will use a variable windowing span to compute statistics as well as filter and smooth the data. For clarification, the window size is variable for each *L-km segment*, but it is constant within the *L-km segment*. For the surface finding algorithm, we will employ a Savitzky-Golay smoothing/median filtering method. Using this filter, we compute a variable smoothing parameter (or window size). It is important to bound the filter appropriately as the output from the median filter can lose fidelity if the scan is over-filtered.

We have developed an empirically-determined shape function, bound between [5 51], that sets the window size (Sspan) based on the number of photons within each L -km segment.

$$Sspan = \text{ceil}[5 + 46 * (1 - e^{-a*length})] \quad \text{Eqn. 3.4}$$

$$a = \frac{\log\left(1 - \frac{21}{51-5}\right)}{-28114} \approx 21 \times 10^{-6} \quad \text{Eqn. 3.5}$$

where a is the shape parameter and length is the total number of photons in the L -km segment. The shape parameter, a , was determined using data collected by MABEL and is shown in Figure 3.6. It is possible that the model of the shape function, or the filtering bounds, will need to be adjusted once ICESat-2/ATLAS is on orbit and collecting data.

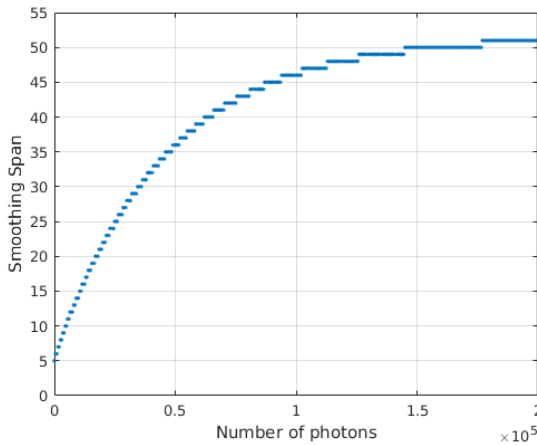


Figure 3.6. Shape Parameter for variable window size.

3.2.4 Compute descriptive statistics

To help characterize the input data and initialize some of the parameters used in the algorithm, we employ a moving window to compute descriptive statistics on the de-trended data. The moving window's width is the smoothing span function

computed in Equation 5 and the window slides $\frac{1}{4}$ of its size to allow of overlap between windows. By moving the window with a large overlap helps to ensure that the approximate ground location is returned. The statistics computed for each window step include:

- Mean height
- Min height
- Max height
- Standard deviation of heights

Dependent upon the amount of vegetation within each window, the estimated ground height is estimated using different statistics. A standard deviation of the photon elevations computed within each moving window are used to classify the vertical spread of photons as belonging to one of four classes with increasing amounts of variation: open, canopy level 1, canopy level 2, canopy level 3. The canopy indices are defined in Table 3.1.

Table 3.1. Standard deviation ranges utilized to qualify the spread of photons within moving window.

| Name | Definition | Lower Limit | Upper Limit |
|----------------|---|--------------------------|---|
| Open | Areas with little or no spread in signal photons determined due to low standard deviation | N/A | Photons falling within 1 st quartile of Standard deviation |
| Canopy Level 1 | Areas with small spread in signal photons | 1 st quartile | Median |

| | | | |
|----------------|--|--------------------------|--------------------------|
| Canopy Level 2 | Areas with a medium amount of spread | Median | 3 rd quartile |
| Canopy Level 3 | Areas with high amount of spread in signal photons | 3 rd quartile | N/A |

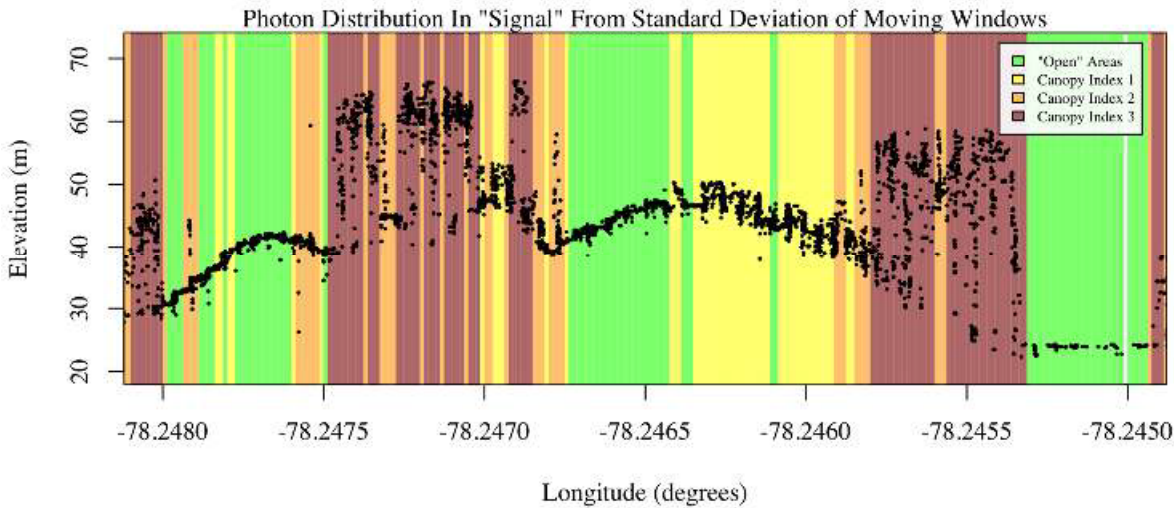


Figure 3.7. Illustration of the standard deviations calculated for each moving window to identify the amount of spread of signal photons within a given window.

3.2.5 Ground Finding Filter (Iterative median filtering)

A combination of an iterative median filtering and smoothing filter approach will be employed to derive the output solution of both the ground and canopy surfaces. The input to this process is the set of de-trended photons. Finding the ground in the presence of canopy often poses a challenge because often there are fewer ground photons underneath the canopy. The algorithm adopted here uses an iterative median filtering approach to retain/eliminate photons for ground finding in

the presence of canopy. When canopy exists, a smoothed line will lay somewhere between the canopy top and the ground. This fact is used to iteratively label points above the smoothed line as canopy. The process is repeated five times to eliminate canopy points that fall above the estimated surface as well as noise points that fall below the ground surface. An example of iterative median filtering is shown in Figure 3.8. The final median filtered line is the preliminary surface estimate. A limitation of this approach, however, is in cases of dense vegetation and few photons reaching the ground surface. In these instances, the output of the median filter may lie within the canopy.

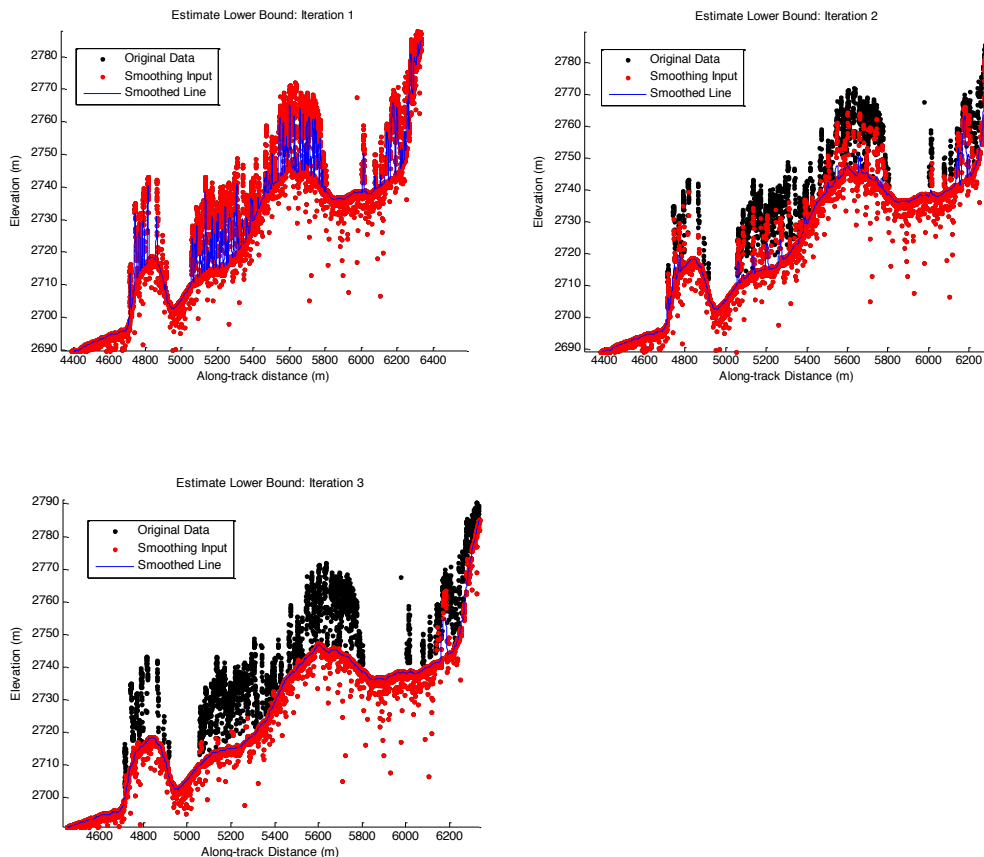


Figure 3.8. Three iterations of the ground finding concept for L -km segments with canopy.

3.3 Top of Canopy Finding Filter

Finding the top of the canopy surface uses the same methodology as finding the ground surface, except now the de-trended data are “flipped” over. The “flip” occurs by multiplying the photons heights by -1 and adding the mean of all the heights back to the data. The same procedure used to find the ground surface can be used to find the indices of the top of canopy points.

3.4 Classifying the Photons

Once a composite ground surface is determined, photons falling within the point spread function of the surface are labeled as ground photons. Based on the expected performance of ATLAS, the point spread function should be approximately 35 cm rms. Signal photons that are not labeled as ground and are below the ground surface (buffered with the point spread function) are considered noise, but keep the signal label.

The top of canopy photons that are identified can be used to generate an upper canopy surface through a shape-preserving surface fitting method. All signal photons that are not labeled ground and lie above the ground surface (buffered with the point spread function) and below the upper canopy surface are considered to be canopy photons (and thus labeled accordingly). Signal photons that lie above the top of canopy surface are considered noise, but keep the signal label.

| | |
|--------|-------------------------|
| FLAGS, | 0 = noise |
| | 1 = ground |
| | 2 = canopy |
| | 3 = TOC (top of canopy) |

The final ground and canopy classifications are flags 1 – 3. The full canopy is the combination of flags 2 and 3.

1440

1441 **3.5 Refining the Photon Labels**

1442 During the first iteration of the algorithm, it is possible that some photons are
1443 mislabeled; most likely this would be noise photons mislabeled as canopy. To reject
1444 these mislabeled photons, we apply three criteria:

- 1445 a) If top of canopy photons are 2 standard deviations above a
- 1446 smoothed median top of canopy surface
- 1447 b) If there are less than 3 canopy indices within a 15m radius
- 1448 c) If, for 500 signal photon segments, the number of canopy photons
- 1449 is < 5% of the total (when SNR > 1), or < 10% of the total (when SNR
- 1450 <= 1). This minimum number of canopy indices criterion implies a
- 1451 minimum amount of canopy cover within a region.

1452 There are also instances where the ground points will be redefined. This
1453 reassigning of ground points is based on how the final ground surface is determined.
1454 Following the “iterate” steps in the flowchart shown in Figure 3.4, if there are no
1455 canopy indices identified for the *L-km* segment, the final ground surface is
1456 interpolated from the identified ground photons and then will undergo a final round
1457 of median filtering and smoothing.

1458 If canopy photons are identified, the final ground surface is interpolated based
1459 upon the level/amount of canopy at that location along the segment. The final ground
1460 surface is a composite of various intermediate ground surfaces, defined thusly:

ASmooth heavily smoothed surface used to de-trend the signal data

Interp_Aground interpolated ground surface based upon the identified ground
photons

AgroundSmooth median filtered and smoothed version of Interp_Aground

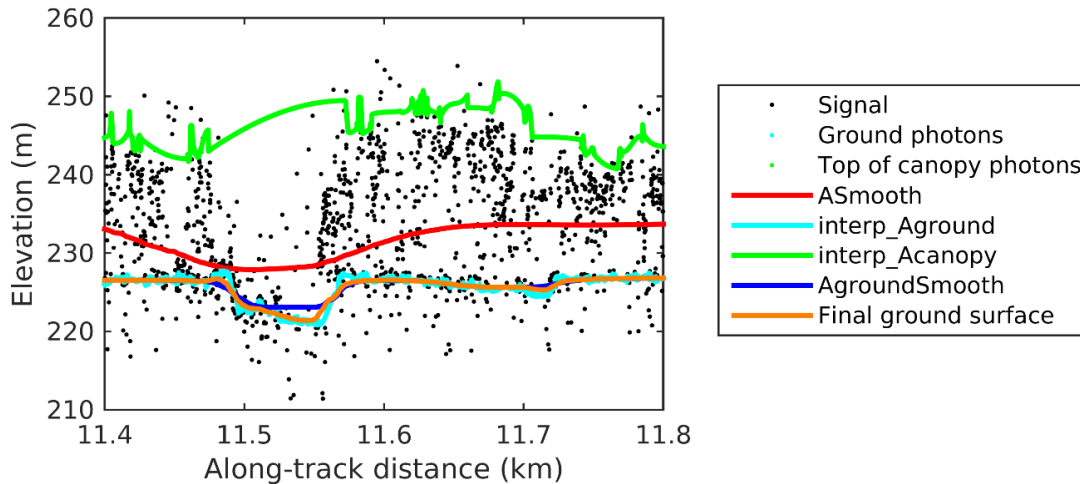


Figure 3.9. Example of the intermediate ground and top of canopy surfaces calculated from MABEL flight data over Alaska during July 2014.

During the first round of ground surface refinement, where there are canopy photons identified in the segment, the ground surface at that location is defined by the smoothed ground surface (AgroundSmooth) value. Else, if there is a location along-track where the standard deviation of the ground-only photons is greater than the 75% quartile for all signal photon standard deviations (i.e., canopy level 3), then the ground surface at that location is a weighted average between the interpolated ground surface (Interp_Aground*1/3) and the smoothed interpolated ground surface (AgroundSmooth*2/3). For all remaining locations long the segment, the ground surface is the average of the interpolated ground surface (Interp_Aground) and the heavily smoothed surface (ASmooth).

The second round of ground surface refinement is simpler than the first. Where there are canopy photons identified in the segment, the ground surface at that location is defined by the smoothed ground surface (AgroundSmooth) value again.

For all other locations, the ground surface is defined by the interpolated ground surface (Interp_Aground). This composite ground surface is run through the median and smoothing filters again.

The pseudocode for this surface refining process can be found in section 4.11.

Examples of the ground and canopy photons for several MABEL lines are shown in Figures 3.10 – 3.12.

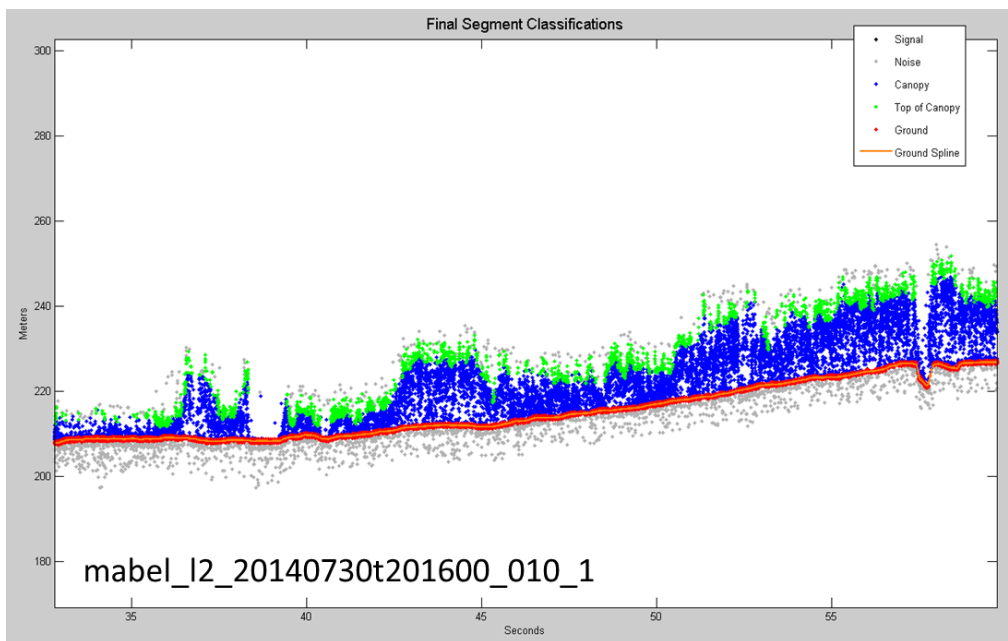
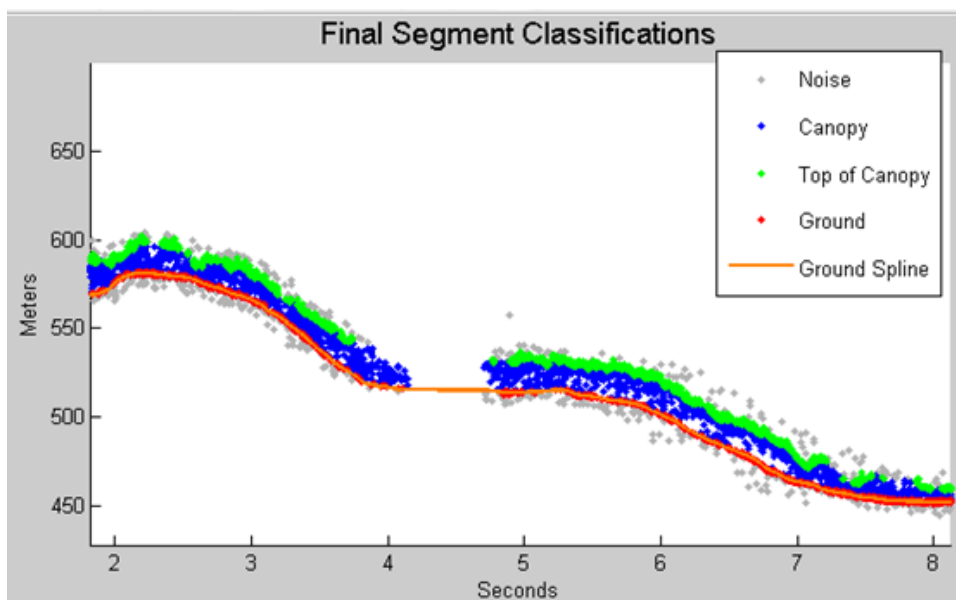


Figure 3.10. Example of classified photons from MABEL data collected in Alaska 2014. Red photons are photons classified as terrain. Green photons are classified as top of canopy. Canopy photons (shown as blue) are considered as photons lying between the terrain surface and top of canopy.



1490

1491 Figure 3.11. Example of classified photons from MABEL data collected in Alaska 2014.

1492 Red photons are photons classified as terrain. Green photons are classified as top of canopy.

1493 Canopy photons (shown as blue) are considered as photons lying between the terrain

1494 surface and top of canopy.

1495

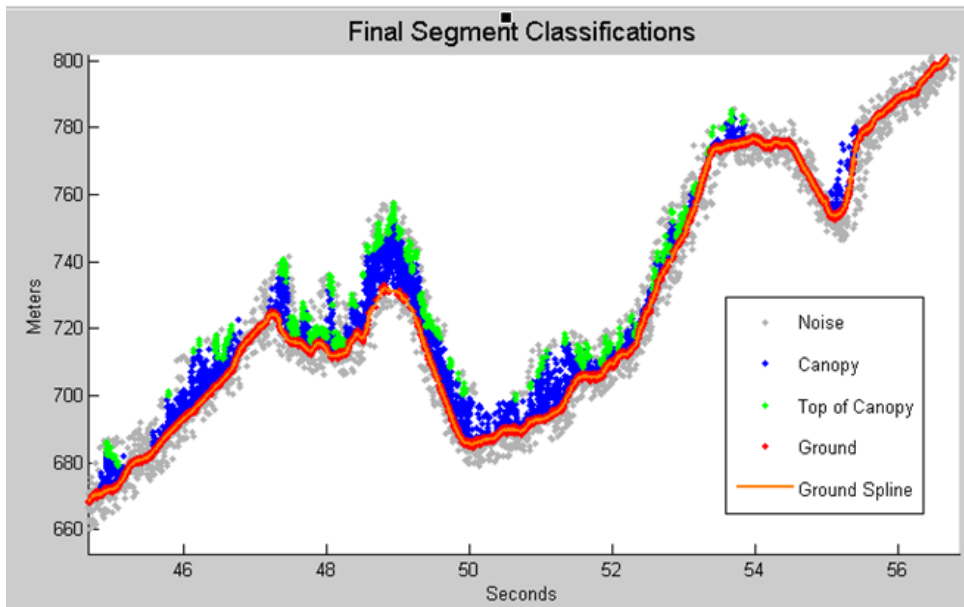


Figure 3.12. Example of classified photons from MABEL data collected in Alaska 2014. Red photons are photons classified as terrain. Green photons are classified as top of canopy. Canopy photons (shown as blue) are considered as photons lying between the terrain surface and top of canopy.

3.6 Canopy Height Determination

Once a final ground surface is determined, canopy heights for individual photons are computed by removing the ground surface height for that photon's latitude/longitude. These relative canopy height values will be used to compute the canopy statistics on the ATL08 data product.

3.7 Link Scale for Data products

The link scale for each segment within which values for vegetation parameters will be derived will be defined over a fixed distance of 100 m. A fixed segment length ensures that canopy and terrain metrics are consistent between segments, in addition

***ICESat-2 Algorithm Theoretical Basis Document for Land-Vegetation
Along-Track Products (ATL08)
Release 002***

1512 to increased ease of use of the final products. A size of 100 m was selected as it should
1513 provide approximately 140 photons (a statistically sufficient number) from which to
1514 make the calculations for terrain and canopy height.

1515

4. ALGORITHM IMPLEMENTATION

Prior to running the surface finding algorithms used for ATL08 data products, the superset of output from the GSFC medium-high confidence classed photons (ATL03 signal_conf_ph: flags 3-4) and the output from DRAGANN will be considered as the input data set. ATL03 input data requirements include the along-track time, latitude, longitude, height, and classification for each photon. The motivation behind combining the results from two different noise filtering methods is to ensure that all of the potential signal photons for land surfaces will be provided as input to the surface finding software.

Table 4.1. Input parameters to ATL08 classification algorithm.

| Name | Data Type | Long Name | Units | Description | Source |
|-----------------------|-----------|--------------------------|---------|---|--------|
| delta_time | DOUBLE | GPS elapsed time | seconds | Elapsed GPS seconds since start of the granule for a given photon. Use the metadata attribute granule_start_seconds to compute full gps time. | ATL03 |
| lat_ph | FLOAT | latitude of photon | degrees | Latitude of each received photon. Computed from the ECEF Cartesian coordinates of the bounce point. | ATL03 |
| lon_ph | FLOAT | longitude of photon | degrees | Longitude of each received photon. Computed from the ECEF Cartesian coordinates of the bounce point. | ATL03 |
| h_ph | FLOAT | height of photon | meters | Height of each received photon, relative to the WGS-84 ellipsoid. | ATL03 |
| sigma_h | FLOAT | height uncertainty | m | Estimated height uncertainty (1-sigma) for the reference photon. | ATL03 |
| signal_conf_ph | UINT_1_LE | photon signal confidence | counts | Confidence level associated with each photon event selected as signal (0-noise, 1- added to allow for buffer but algorithm classifies as background, 2-low, 3-med, 4-high). | ATL03 |

**ICESat-2 Algorithm Theoretical Basis Document for Land-Vegetation
Along-Track Products (ATL08)
Release 002**

| | | | | | |
|---------------------------|---------|--------------------------------------|------------|--|---|
| segment_id | UNIT_32 | along-track segment ID number | unitless | A seven-digit number uniquely identifying each along-track segment. These are sequential, starting with one for the first segment after an ascending equatorial crossing node. | ATL03 |
| cab_prof | FLOAT | Calibrated Attenuated Backscatter | unitless | Calibrated Attenuated Backscatter from 20 to -1 km with vertical resolution of 30m | ATL09 |
| dem_h | FLOAT | DEM Height | meters | Best available DEM (in priority of GIMP/ANTARCTIC/GMTED/MS S) value at the geolocation point. Height is in meters above the WGS84 Ellipsoid. | ATL09 |
| Landsat tree cover | UINT_8 | Landsat Tree Cover Continuous Fields | percentage | Percentage of woody vegetation greater than 5 meters in height across a 30 meter pixel | Global Land Cover Facility (Sexton, 2013) |

1525

1526 Table 4.2. Additional external parameters referenced in ATL08 product.

| Name | Data Type | Long Name | Units | Description | Source |
|---------------------|-----------|-----------|---------|---|--------|
| atlas_pa | | | | Off nadir pointing angle of the spacecraft | |
| ground_track | | | | Ground track, as numbered from left to right: 1 = 1L, 2 = 1R, 3 = 2L, 4 = 2R, 5 = 3L, 6 = 3R | |
| dem_h | | | | Reference DEM height | ANC06 |
| ref_azimuth | FLOAT | azimuth | radians | Azimuth of the unit pointing vector for the reference photon in the local ENU frame in radians. The angle is measured from north and positive towards east. | ATL03 |
| ref_elev | FLOAT | elevation | radians | Elevation of the unit pointing vector for the reference photon in the local ENU frame in radians. The angle is measured from east- | ATL03 |

**ICESat-2 Algorithm Theoretical Basis Document for Land-Vegetation
Along-Track Products (ATL08)
Release 002**

| | | | | | |
|-----------------------|------------|--------------------------------------|----------|---|-------------------------|
| | | | | north plane and positive towards up. | |
| rgt | INTEGER_2 | reference ground track | unitless | The reference ground track (RGT) is the track on the Earth at which a specified unit vector within the observatory is pointed. Under nominal operating conditions, there will be no data collected along the RGT, as the RGT is spanned by GT2L and GT2R. During slews or off-pointing, it is possible that ground tracks may intersect the RGT. The ICESat-2 mission has 1,387 RGTs. | ATL03 |
| sigma_along | DOUBLE | along-track geolocation uncertainty | meters | Estimated Cartesian along-track uncertainty (1-sigma) for the reference photon. | ATL03 |
| sigma_across | DOUBLE | across-track geolocation uncertainty | meters | Estimated Cartesian across-track uncertainty (1-sigma) for the reference photon. | ATL03 |
| surf_type | INTEGER_1 | surface type | unitless | Flags describing which surface types this interval is associated with. 0=not type, 1=is type. Order of array is land, ocean, sea ice, land ice, inland water. | ATL03 , Section 4 |
| layer_flag | Integer | Consolidated cloud flag | unitless | Flag indicating the presence of clouds or blowing snow with good confidence | ATL09 |
| cloud_flag_asr | Integer(3) | Cloud probability from ASR | unitless | Cloud confidence flag, from 0 to 5, indicating low, med, or high confidence of clear or cloudy sky | ATL09 |
| msw_flag | Byte(3) | Multiple scattering warning flag | unitless | Flag with values from 0 to 5 indicating presence of multiple scattering, which may be due to blowing snow or cloud/aerosol layers. | ATL09 |
| asr | Float(3) | Apparent surface reflectance | unitless | Surface reflectance as modified by atmospheric transmission | ATL09 |

**ICESat-2 Algorithm Theoretical Basis Document for Land-Vegetation
Along-Track Products (ATL08)
Release 002**

| | | | | | |
|-----------------|---------------|------------------|----------|---|-------|
| snow_ice | INTEGER_ 1 | Snow Ice Flag | unitless | NOAA snow-ice flag. 0=ice free water; 1=snow free land; 2=snow; 3=ice | ATL09 |
|-----------------|---------------|------------------|----------|---|-------|

1527

1528 **4.1 Cloud based filtering**

1529 It is possible for the presence of clouds to affect the number of surface photon
1530 returns through signal attenuation, or to cause false positive classifications of
1531 ground or canopy photons on low cloud returns. Either of these cases would reduce
1532 the accuracy of the ATL08 product. To improve the performance of the ATL08
1533 algorithm, ideally all clouds would be identified prior to processing through the
1534 ATL08 algorithm. There will be instances, however, where low lying clouds (e.g.
1535 <800 m above the ground surface) may be difficult to identify. Currently, ATL08
1536 provides an ATL09 derived cloud flag (layer_flag) on its 100 m product and
1537 encourages the user to make note of the presence of clouds when using ATL08
1538 output. Unfortunately at present, a review of on-orbit data from ATL03 and ATL09
1539 indicate that the cloud layer flag is not being set correctly in the ATL09 algorithm.
1540 Ultimately, the final cloud based filtering process used in the ATL08 algorithm will
1541 most likely be derived from parameters/flag on the ATL09 data product. Until the
1542 ATL09 cloud flags are proven reliable, however, a preliminary cloud screening
1543 method is presented below. This methodology utilizes the calibrated attenuated
1544 backscatter on the ATL09 data product to identify (and subsequently remove for
1545 processing) clouds or other problematic issues (i.e. incorrectly telemetered
1546 windows). Using this new method, telemetered windows identified as having either
1547 low or no surface signal due to the presence of clouds (likely above the telemetered
1548 band), as well as photon returns suspected to be clouds instead of surface returns,
1549 will be omitted from the ATL08 processing. This process, however, will not identify
1550 the extremely low clouds (i.e. <800 m). The steps are as follows:

- 1551 1. Match up the ATL09 calibrated attenuated backscatter (cab_prof) columns to
- 1552 the ATL03 granule being processed using segment ID.

- 1553 2. Flip the matching cab_prof vertical columns so that the elevation bins go
1554 from low to high.
- 1555 3. For each of the matching ATL09 cab_prof vertical columns, perform a cubic
1556 Savitsky-Golay smoothing filter with a span size of 15 vertical bins. Call this
1557 cab_smooth.
- 1558 4. Perform the same smoothing filter on each horizontal row of the cab_smooth
1559 output, this time using a span size of 7 horizontal bins. Call this
1560 cab_smoother.
- 1561 5. Create a low_signal logical array the length of the number of matching ATL09
1562 columns and set to false.
- 1563 6. For each column of cab_smoother:
- 1564 a. Set any values below 0 to 0.
- 1565 b. Set a logical array of cab_smoother bins that are below 15 km in
1566 elevation to true. Call this cab15.
- 1567 c. Using the ATL09 dem_h value for that column, find the ATL09
1568 cab_smoother bins that are 240 m above and 240 m below (~8 ATL09
1569 vertical bins each direction) the dem_h value. The bins found here that
1570 are also within cab15 are designated as sfc_bins.
- 1571 d. Find the maximum peak value of cab_smoother within the sfc_bins, if
1572 any. This will represent the surface peak.
- 1573 e. Find the maximum value of cab_smoother that is higher in elevation
1574 than the sfc_bins and within cab15, if any. This will represent the
1575 cloud peak.
- 1576 f. If there is no surface peak, set the low_signal flag to true.
- 1577 g. If there are both surface and cloud peak values returned, determine a
1578 surface peak / cloud peak ratio. If that ratio is less than or equal to 0.4,
1579 set low_signal flag for that column to true.
- 1580 7. After each matching ATL09 column of cab_smoother has been analyzed for
1581 low signal, assign the low_signal flag to an ATL03 photon resolution logical

array by matching up the ATL03 photon segment_id values to the ATL09 range of segment IDs for each ATL09 cab_prof column.

8. For each ATL09 cab_prof column where the low_signal flag was not set, check for any ATL03 photons greater than 800 meters (TBD) in elevation away (higher or lower) from the ATL09 dem_h value. Assign an ATL03 photon resolution too_far_signal flag to true when this conditional is met.
9. A logical array mask is created for any ATL03 photons that have either the low_signal flag or the too_far_signal flag set to true such that those photons will not be further processed by the ATL08 function.

4.2 Preparing ATL03 data for input to ATL08 algorithm

1. Break up data into *L-km* segments. Segments equivalent of 10 km in along-track distance of an orbit would be appropriate.
 - a. If the last portion of an ATL03 granule being processed would result in an *L-km* segment with less than 3.4 km (170 geosegments) worth of data, that last portion is added to the previous *L-km* processing window to be processed together as one extended *L-km* processing segment.
 - i. The resulting **last_seg_extend** value would be reported as a positive value of distance beyond 10 km that the ATL08 processing segment was extended by.
 - b. If the last *L-km* segment would be less than 10 km but greater than 3.4 km, a portion extending from the start of current *L-km* processing segment backwards into the previous *L-km* processing segment would be added to the current ATL08 processing segment to make it 10 km in length. Only new 100 m ATL08 segment products generated from this backward extension would be reported.

- 1609 i. The distance of this backward data gathering would be
1610 reported in **last_seg_extend** as a negative distance value.
- 1611 c. All other segments that are not extended will report a last_seg_extend
1612 value of 0.
- 1613 2. Add a buffer of 200 m (or 10 segment_id's) to both ends of each *L-km*
1614 segment. The total processing segment length is $(L-km + 2*buffer)$, but will
1615 be referred to as *L-km* segments for simplicity.
- 1616 a. The first *L-km* segment from an ATL03 granule would only have a
1617 buffer at the end, and the last *L-km* segment from an ATL03 granule
1618 would only have a buffer at the beginning.
- 1619 3. The input data for ATL08 algorithm is X, Y, Z, T (where T is time).

1620

1621 **4.3 Noise filtering via DRAGANN**

1622 DRAGANN will use ATL03 photons with all signal classification flags (0-4). These
1623 will include both signal and noise photons. This section give a broad overview of the
1624 DRAGANN function. See Appendix A for more details.

- 1625 1. Determine the relative along-track time, ATT, of each geolocated photon
1626 from the beginning of each *L-km* segment.
- 1627 2. Rescale the ATT with equal-time spacing between each data photon, keeping
1628 the relative beginning and end time values the same.
- 1629 3. Normalize the height and rescaled ATT data from 0 – 1 for each *L-km*
1630 segment based on the min/max of each field. So, $normtime = (time -$
1631 $mintime)/(maxtime - mintime)$.
- 1632 4. Build a kd-tree based on normalized Z and normalized and rescaled ATT.
- 1633 5. Determine the search radius starting with Equation 3.1. $P=[$ determined by
1634 preprocessor; see Sec 1.1.1], and $V_{total}=1$. N_{total} is the number of photons
1635 within the data *L-km* segment. Solve for V.
- 1636 6. Now that you know V, determine the radius using Equation 3.2.

- 1637 7. Compute the number of neighbors for each photon using this search radius.
- 1638 8. Generate a histogram of the neighbor count distribution. As illustrated in
- 1639 Figure 3.2, the noise peak is the first peak (usually with the highest
- 1640 amplitude).
- 1641 9. Determine the 10 highest peaks of the histogram.
- 1642 10. Fit Gaussians to the 10 highest peaks. For each peak,
- 1643 a. Compute the amplitude, a , which is located at peak position b .
- 1644 b. Determine the width, c , by stepping one bin at a time away from b and
- 1645 finding the last histogram value that is $> \frac{1}{2}$ the amplitude, a .
- 1646 c. Use the amplitude and width to fit a Gaussian to the peak of the
- 1647 histogram, as described in Equation 3.3.
- 1648 d. Subtract the Gaussian from the histogram, and move on to calculate
- 1649 the next highest peak's Gaussian.
- 1650 e. Reject Gaussians that are too near (< 2 standard deviations) and
- 1651 amplitude too low ($< 1/5$ previous amplitude) from the previous
- 1652 signal Gaussian.
- 1653 11. Reject any of the returned Gaussians with imaginary components.
- 1654 12. Determine if there is a narrow noise Gaussian at the beginning of the
- 1655 histogram. These typically occur when there is little noise, such as during
- 1656 nighttime passes.
- 1657 a. Search for the Gaussian with the highest amplitude, a , in the first 5%
- 1658 of the histogram
- 1659 b. Check if the highest amplitude is $\geq 1/10$ of the maximum of all
- 1660 Gaussian amplitudes
- 1661 c. Check if the width, c , of the Gaussian with the highest amplitude is \leq
- 1662 4 bins
- 1663 d. If these three conditions are met, save the $[a,b,c]$ values as $[a_0,b_0,c_0]$.
- 1664 e. If the three conditions are not met, search again within the first 10%.
- 1665 Repeat the process, incrementing the percentage of histogram

1666 searched by 5% up to 30%. As soon as the conditions are met, save
1667 the $[a_0, b_0, c_0]$ values and break out of the percentage histogram search
1668 loop.

1669 13. If a narrow noise peak was found, sort the remaining Gaussians from largest
1670 to smallest area, estimated by $a \cdot c$, then append $[a_0, b_0, c_0]$ to the beginning of
1671 the sorted $[a, b, c]$ arrays. If a narrow noise peak was not found, sort all
1672 Gaussians by largest to smallest area.

1673 a. If a narrow noise peak was not found, check in sorted order if one of
1674 the Gaussians are in the first 10% of the histogram. If so, it becomes
1675 the first Gaussian.

1676 b. Reject any Gaussians that are fully contained within another.

1677 c. Reject Gaussians whose centers are within 3 standard deviations of
1678 another, unless only two Gaussians remain

1679 14. If there are two or more Gaussians remaining, they are referred to as
1680 Gaussian 1 and Gaussian 2, assumed to be the noise and signal Gaussians.

1681 15. Determine the threshold value that will define the cutoff between noise and
1682 signal.

1683 a. If the absolute difference of the two Gaussians becomes near zero,
1684 defined as $< 1e-8$, set the first bin index where that occurs, past the
1685 first Gaussian peak location, as the threshold. This would typically be
1686 set if the two Gaussians are far away from each other.

1687 b. Else, the threshold value is the intersection of the two Gaussians,
1688 which can be estimated as the first bin index past the first Gaussian
1689 peak location where there is a minimum absolute difference between
1690 the two Gaussians.

1691 c. If there is only one Gaussian, it is assumed to be the noise Gaussian,
1692 and the threshold is set to $b + c$.

1693 16. Label all photons having a neighbor count above the threshold as signal.

1694 17. Label all photons having a neighbor count below the threshold as noise.

18. Reject noise photons.
19. Retain signal photons for feeding into next step of processing.
20. Use Logical OR to combine DRAGANN signal photons with ATL03 medium-high confidence signal photons (flags 3-4) as ATL08 signal photons.
21. Calculate a signal to noise ratio (SNR) for the L -km segment by dividing the number of ATL08 signal photons by the number of noise (i.e., all – signal) photons.

4.3.1 Preprocessing to dynamically determine a DRAGANN parameter

While a default value of $P=20$ was found to work well when testing with MABEL flight data, further testing with simulated data showed that $P=20$ is not sufficient in cases of very low or very high noise. Additional testing with real ATL03 data have shown the ground signal to be much stronger, and the canopy signal to be much weaker, than originally anticipated. Therefore, a preprocessing step for dynamically calculating P and running the core DRAGANN function is described in this subsection. This assumes L -km to be 10 km (with additional L -km buffering).

1. Define a DRAGANN processing window of 170 segments (~ 3.4 km), and a buffer of 10 segments (~ 200 m).
2. The buffer is applied to both sides of each DRAGANN processing window to create buffered DRAGANN processing windows (referenced as “buffered window” for the rest of this section) that will overlap the DRAGANN processing windows next to them.
3. For each buffered window within the L -km segment, calculate a histogram of points with 1 m elevation bins.
4. For each buffered window histogram, calculate the median counts.
5. Bins with counts below the buffered window median count value are estimated to be noise. Calculate the mean count of noise bins.
6. Bins with counts above the buffered window median count value are estimated to be signal. Calculate the mean count of signal bins.

- 1723 7. Determine the time elapsed over the buffered window.
- 1724 8. Calculate estimated noise and signal rates for each buffered window
- 1725 by multiplying each window's mean counts of noise bins and signal
- 1726 bins, determined from steps 5 and 6 above, by 1/(elapsed time) to
- 1727 return the rates in terms of points/meter[elevation]/second[across].
- 1728 9. Calculate a noise ratio for each window by dividing the noise rate by
- 1729 the signal rate.
- 1730 10. If, for all the buffered windows in the *L-km* segment, the noise rate is
- 1731 less than 20 and the noise ratio is less than 0.15; OR any noise rate is
- 1732 0; OR any signal rate is greater than 1000: re-calculate steps 3-9
- 1733 using the entire *L-km* segment. Continue with the following steps
- 1734 using results from the one *L-km* window (instead of multiple buffered
- 1735 windows).
- 1736 11. Now, determine the DRAGANN parameter, P, for each buffered
- 1737 window based on the following conditionals:
- 1738 a. If the signal rate is NaN (i.e., an invalid value), set the signal
- 1739 index array to empty and move on to the next buffered
- 1740 window.
- 1741 b. If noise rate < 20 || noise ratio < 0.15:
- 1742 P = signal rate
- 1743 If signal rate is < 5, P = 5; if signal rate > 20, P = 20
- 1744 c. Else P = 20.
- 1745 12. Run DRAGANN on the buffered window points using the calculated P.
- 1746 13. If DRAGANN fails to find a signal (i.e., only one Gaussian found), run
- 1747 DRAGANN again with P = 10.
- 1748 14. If DRAGANN still fails to find a signal, try to determine P a second time
- 1749 using the following conditionals:
- 1750 a. If (noise rate >= 20) ...
- 1751 && (signal rate > 100) ...

```
1752         && (signal rate < 250),
1753         P = (signal rate)/2
1754     b. Else if signal rate >= 250,
1755         if noise rate >= 250,
1756             P = (noise rate)*1.1
1757         else,
1758             P = 250
1759     c. Else, P = mean(noise rate, signal rate)
1760 15. Run DRAGANN on the buffered window points using the newly
1761     calculated P.
1762     a. If still no signal points are found, set a dragannError flag.
1763 16. If signal points were found by DRAGANN, for each buffered window
1764     calculate a signal check by dividing the number of signal points found
1765     via DRAGANN by the number of total points in the buffered window.
1766 17. If dragannError has been set, or there are suspect signal statistics, the
1767     following snippet of pseudocode will check those conditionals and try
1768     to iteratively find a better P value to run DRAGANN with:
1769
1770     try_count = 0
1771
1772     While dragannError ...
1773     || ( (noise rate >= 30) ...
1774         && (signal check > noise ratio) ...
1775         && (noise ratio >= 0.15) ) ...
1776     || (signal check < 0.001):
1777
1778         if P < 3,
1779             break
1780         else,
1781             P = P*0.75
1782         end
1783
1784     if try_count < 2
1785         Clear out signal index results from previous DRAGANN run
1786         Re-run DRAGANN with new P value
1787         Recalculate the signal check
```



```
1788         end
1789
1790         if no signal index results are returned
1791             P = P*0.75
1792         end
1793
1794         try_count = try_count + 1
1795
1796     end
1797
1798     18. If no signal photons are found by DRAGANN because only one
1799         Gaussian was found, set the threshold as  $b+c$  (i.e., one standard
1800         deviation away from the Gaussian peak location) for a final DRAGANN
1801         run. Otherwise, set the signal index array to empty and move on to the
1802         next buffered window.
1803
1804     19. Assign the signal values found from DRAGANN for each buffered
1805         window to the original DRAGANN processing window range of points.
1806
1807     20. Combine signal points from each DRAGANN processing window back
1808         into one  $L$ -km array of signal points for further processing.
```

1807

1808 **4.3.2 Iterative DRAGANN processing**

1809 It is possible in processing segments with high noise rates that DRAGANN will
1810 incorrectly identify clusters of noise as signal. One way to reduce these false positive
1811 noise clusters is to run the alternative DRAGANN process (Sec 1.1.1) again with the
1812 input being the signal output photons from the first run through alternative
1813 DRAGANN. Note that this methodology is still being tested, so by default this option
1814 should not be set.

- 1815 1. If $SNR < 1$ (TBD) from alternative DRAGANN run, run alternative DRAGANN
1816 process again using the output signal photons from first DRAGANN run as the
1817 input to the second DRAGANN run.
- 1818 2. Recalculate SNR based on output of second DRAGANN run.

1819

1820 **4.4 Is Canopy Present**

- 1821 1. If L -km segment is within an ATL08 region encompassing Antarctica (regions
1822 7, 8, 9, 10) or Greenland (region 11), assume no canopy is present: canopy
1823 flag = 0. Else:
1824 2. Determine the center Latitude/Longitude position for the L -km segment.
1825 3. Determine the corresponding tile from the Landsat continuous cover
1826 product.
1827 4. For each unique XY position in the ATLAS segment, extract the canopy cover
1828 value from the Landsat CC product
1829 5. Compute the average canopy cover value for the L -km segment (based on the
1830 Landsat values).
1831 6. If canopy cover > 5%, set canopy flag = 1 (assumes canopy is present)
1832 7. If canopy cover <= 5%, set canopy flag = 0 (assumes no canopy is present)

1833

1834 **4.5 Compute Filtering Window**

- 1835 1. Next step is to run a surface filter with a variable window size (variable in
1836 that it will change from L -km segment to L -km segment). The window-size is
1837 denoted as Window.
1838 2. $Window = \text{ceil}[5 + 46 * (1 - e^{-a*length})]$, where $length$ is the number of
1839 photons in the segment.
1840 3. $a = \frac{\log(1 - \frac{21}{51-5})}{-28114} \approx 21 \times 10^{-6}$, where a is the shape parameter for the window
1841 span.
1842

4.6 De-trend Data

1. The input data are the signal photons identified by DRAGANN and the ATL03 classification (signal_conf_ph) values of 3-4.
2. Generate a rough surface by connecting all unique (time) photons to each other. Let's call this surface interp_A.
3. Run a median filter through interp_A using the window size set by the software. Output = Asmooth.
4. Define a reference DEM limit (ref_dem_limit) as 120 m (TBD).
5. Remove any Asmooth values further than the ref_dem_limit threshold from the reference DEM, and interpolate the Asmooth surface based on the remaining Asmooth values. The interpolation method to use is the shape preserving piecewise cubic Hermite interpolating polynomial – hereafter labeled as “pchip” (Fritsch & Carlson, 1980).
6. Compute the approximate relief of the L -km segment using the 95th - 5th percentile heights of the signal photons. We are going to filter Asmooth again and the smoothing is a function of the relief.
7. Define the SmoothSize using the conditional statements below. The SmoothSize will be used to detrend the data as well as to create an interpolated ground surface later.

SmoothSize = 2 * Window
 - If relief ≥ 900, SmoothSize = round(SmoothSize/4)
 - If relief ≥ 400 && ≤ 900, SmoothSize = round(SmoothSize/3)
 - If relief ≥ 200 && ≤ 400, SmoothSize = round(SmoothSize/2)
8. Greatly smooth Asmooth by first running Asmooth 10 times through a median filter then a smoothing filter with a moving average method on the result. Both the median filter and the smoothing filter use a window size of SmoothSize.

1870

1871 **4.7 Filter outlier noise from signal**

- 1872 1. If there are any signal data that are 150 meters above Asmooth, remove them
1873 from the signal data set.
- 1874 2. If the standard deviation of the detrended signal is greater than 10 meters,
1875 remove any signal value from the signal data set that is 2 times the standard
1876 deviation of the detrended signal below Asmooth.
- 1877 3. Calculate a new Asmooth surface by interpolating (pchip method) a surface
1878 from the remaining signal photons and median filtering using the Window
1879 size, then median filter and smooth (moving average method) 10 times again
1880 using the SmoothSize.
- 1881 4. Detrend the signal photons by subtracting the signal height values from the
1882 Asmooth surface height values. Use the detrended heights for surface finding.

1883

1884 **4.8 Finding the initial ground estimate**

- 1885 1. At this point, the initial signal photons have been noise filtered and de-
1886 trended and should have the following format: X, Y, detrended Z, T (T=time).
1887 From this, the input data into the ground finding will be the ATD (along track
1888 distance) metric (such as time) and the detrended Z height values.
- 1889 2. Define a medianSpan as Window*2/3.
- 1890 3. Identifying the ground surface is an iterative process. Start by assuming that
1891 all the input signal height photons are the ground. The first goal is the cut
1892 out the lower height excess photons in order to find a lower bound for
1893 potential ground photons. This process is done 5 times and an offset of 4
1894 meters is subtracted from the resulting lower bound. The smoothing filter
1895 uses a moving average again:

1896 for j=1:5

```
1897         cutOff = median filter (ground, medianSpan)
1898         cutOff = smooth filter (cutOff, Window)
1899         ground = ground( (cutOff – ground) > -1 )
1900     end
1901     lowerbound = median filter (ground, medianSpan*3)
1902     middlebound = smooth filter (lowerbound, Window)
1903     lowerbound = smooth filter (lowerbound, Window) – 4
1904 end;
1905 4. Create a linearly interpolated surface along the lower bound points and only
1906    keep input photons above that line as potential ground points:
1907
1908         top = input( input > interp(lowerbound) )
1909
1910 5. The next goal is to cut out excess higher elevation photons in order to find an
1911    upper bound to the ground photons. This process is done 3 times and an
1912    offset of 1 meter is added to the resulting upper bound. The smoothing filter
1913    uses a moving average:
1914
1915         for j = 1:3
1916             cutOff = median filter (top, medianSpan)
1917             cutOff = smooth filter (cutOff, Window)
1918             top = top( (cutOff – top) > -1 )
1919         end
1920         upperbound = median filter (top, medianSpan)
1921         upperbound = smooth filter (upperbound, Window) + 1
1922
1923 6. Create a linearly interpolated surface along the upper bound points and
1924    extract the points between the upper and lower bounds as potential ground
1925    points:
1926
1927         ground = input( ( input > interp(lowerbound) ) & ...
1928             ( input < interp(upperbound) ) )
```

1924 7. Refine the extracted ground points to cut out more canopy, again using the
1925 moving average smoothing:

1926 For j = 1:2
1927 cutOff = median filter (ground, medianSpan)
1928 cutOff = smooth filter (cutOff, Window)
1929 ground = ground((cutOff – ground) > -1)
1930 end

1931 8. Run the ground output once more through a median filter using window side
1932 medianSpan and a smoothing filter using window size Window, but this time
1933 with the Savitzky-Golay method.

1934 9. Finally, linearly interpolate a surface from the ground points.

1935 10. The first estimate of canopy points are those indices of points that are
1936 between 2 and 150 meters above the estimated ground surface. Save these
1937 indices for the next section on finding the top of canopy.

1938 11. The output from the final iteration of ground points is temp_interpA – an
1939 interpolated ground estimate.

1940 12. Find ground indices that lie within +/- 0.5 m of temp_interpA.

1941 13. Apply the ground indices to the original heights (i.e., not the de-trended data)
1942 to label ground photons.

1943 14. Interpolate a ground surface using the pchip method based on the ground
1944 photons. Output is interp_Aground.

1945

1946 **4.9 Find the top of the canopy (if canopy_flag = 1)**

1947 1. The input are the ATD metric (i.e., time), and the de-trended Z values indexed
1948 by the canopy indices extracted from step 4.8(10).
1949 2. Flip this data over so that we can find a canopy “surface” by multiplying the
1950 de-trended canopy heights by -1.0 and adding the mean(heights).

3. Finding the top of canopy is also an iterative process. Follow the same steps described in 4.8(2) – 4.8(9), but use the canopy indexed and flipped Z values in place of the ground input.
4. Final retained photons are considered top of canopy photons. Use the indices of these photons to define top of canopy photons in the original (not de-trended) Z values.
5. Build a kd-tree on canopy indices.
6. If there are less than three canopy indices within a 15m radius, reassign these photons to noise photons.

4.10 Compute statistics on de-trended data

1. The input data have been noise filtered and de-trended and should have the following input format: X, Y, detrended Z, T.
2. The input data will contain signal photons as well as a few noise photons near the surface.
3. Compute statistics of heights in the along-track direction using a sliding window. Using the window size (window), compute height statistics for all photons that fall within each window. These include max height, median height, mean height, min height, and standard deviation of all photon heights. Additionally, in each window compute the median height and standard deviation of just the initially classified top of canopy photons, and the standard deviation of just the initially classified ground photon heights. Currently only the median top of canopy, and all STD variables are being utilized, but it's possible that other statistics may be incorporated as changes/improvements are made to the code.
4. Slide the window $\frac{1}{4}$ of the window span and recompute statistics along the entire *L-km* segment. This results in one value for each statistic for each window.

- 1979 5. Determine canopy index categories for each window based upon the total
1980 distribution of STD values for all signal photons along the *L-km* segment
1981 based on STD quartiles.
1982 6. Open canopy have STD values falling within the 1st quartile.
1983 7. Canopy Level 1 has STD values falling from 1st quartile to median STD value.
1984 8. Canopy Level 2 has STD values falling from median STD value to 3rd quartile.
1985 9. Canopy Level 3 has STD values falling from 3rd quartile to max STD.
1986 10. Linearly interpolate the window STD values (both for all photons and
1987 ground-only photons) back to the native along-track resolution and calculate
1988 the interpolated all-photon STD quartiles to create an interpolated canopy
1989 level index. This will be used later for interpolating a ground surface.
1990

1991 **4.11 Refine Ground Estimates**

- 1992 1. Smooth the interpolated ground surface 10 times. All further ground surface
1993 smoothing use the moving average method:

1994 For j= 1:10

1995 AgroundSmooth = median filter (interp_Aground, SmoothSize*5)
1996 AgroundSmooth = smooth filter (AgroundSmooth, SmoothSize)
1997 End
1998
1999 2. This output (AgroundSmooth) from the filtering/smoothing function is an
2000 intermediate ground solution and it will be used to estimate the final
2001 solution.
2002 3. If there are **no canopy indices** identified along the entire segment (OR
2003 canopy_flag = 0) AND relief >400 m
2004 FINALGROUND = median filter (Asmooth, SmoothSize)
2005 FINALGROUND = smooth filter (FINALGROUND, SmoothSize)


```
2006         Else
2007             FINALGROUND = AgroundSmooth
2008         end
2009     4. If there are canopy indices identified along the segment:
2010         If there is a canopy photon identified at a location along-track above the
2011         ground surface, then at that location along-track
2012             FINALGROUND = AgroundSmooth
2013         else if there is a location along-track where the interpolated ground STD has
2014         an interpolated canopy level>=3
2015             FINALGROUND = Interp_Aground*1/3 + AgroundSmooth*2/3
2016         else
2017             FINALGROUND = Interp_Aground*1/2 + Asmooth*1/2
2018         end
2019     5. Smooth the resulting interpolated ground surface (FINALGROUND) once
2020         using a median filter with window size of SmoothSize, then a smoothing filter
2021         twice with window size of SmoothSize. Select ground photons that lie within
2022         the point spread function (PSF) of FINALGROUND.
2023     6. PSF is determined by sigma_atlas_land (Eq. 1.2) calculated at the photon
2024         resolution and thresholded between 0.5 to 1 m.
2025         a. Estimate the terrain slope by taking the gradient of
2026             FINALGROUND.Gradient is reported at the center of
2027             ((finalground(n+1)-finalground(n-1))/(dist_x(n+1)-dist_x(n-1)))/2
2028         b. Linearly interpolate the sigma_h values to the photon resolution.
2029         c. Calculate sigma_topo (Eq. 1.3) at the photon resolution.
2030         d. Calculate sigma_atlas_land at the photon resolution using the sigma_h
2031             and sigma_topo values at the photon resolution.
2032         e. Set PSF equal to sigma_atlas_land.
```

- 2033 i. Any PSF < 0.5 m is set to 0.5 m as the minimum PSF.
- 2034 ii. Any PSF > 1 m is set to 1 m as the maximum PSF. Set psf_flag to
- 2035 true.

2036

2037 **4.12 Canopy Photon Filtering**

- 2038 1. The first canopy filter will remove photons classified as top of canopy that
- 2039 are significantly above a smoothed median top of canopy surface. To
- 2040 calculate the smoothed median top of canopy surface:
- 2041 a. Linearly interpolate the median and standard deviation canopy
- 2042 window statistics, calculated from 4.10 (3), to the top of canopy
- 2043 photon resolution. Output variables: interpMedianC, interpStdC.
- 2044 b. Calculate a canopy window size using Eq. 3.4, where *length* = number
- 2045 of top of canopy photons. Output variable: winC.
- 2046 c. Create the median filtered and smoothed top of canopy surface,
- 2047 smoothedC, using a locally weighted linear regression smoothing
- 2048 method, “lowess” (Cleveland, 1979):

2049 smoothedC = median filter (interpMedianC, winC)

2050

2051 if SNR > 1, canopySmoothSpan = winC*2;

2052 else, canopySmoothSpan = smoothSpan;

2053

2054 smoothedC = smooth filter (smoothedC, canopySmoothSpan)

- 2055 d. Add the detrended heights back into the smoothedC surface:

2056 smoothedC = smoothedC + Asmooth

- 2057 2. Set canopy height thresholds based on the interpolated top of canopy STD:

2058 If SNR > 1, canopySTDthresh = 3; else, canopySTDthresh = 2;
2059 canopy_height_thresh = canopySTDthresh*interpStdC

2060 high_cStd = canopy_height_thresh > 10

2061 low_cStd = canopy_height_thresh < 3

2062 canopy_height_thresh(high_cStd) =
2063 canopy_height_thresh(high_cStd)/2

2064 canopy_height_thresh(low_cStd) = 3

2065 3. Relabel as noise any top of canopy photons that are higher than smoothedC +
2066 canopy_height_thresh.
2067 4. Next, interpolate a top of canopy surface using the remaining top of canopy
2068 photons (here we are trying to create an upper bound on canopy points). The
2069 interpolation method used is pchip. This output is named interp_Acanopy.
2070 5. Photons falling below interp_Acanopy and above FINALGROUND+PSF are
2071 labeled as canopy points.
2072 6. For 500 signal photon segments, if number of all canopy photons (i.e., canopy
2073 and top of canopy) is:
2074 < 5% of the total (when SNR > 1), OR
2075 < 10% of the total (when SNR <= 1),
2076 relabel the canopy photons as noise.
2077 7. Interpolate, using the pchip method, a new top of canopy surface from the
2078 filtered top of canopy photons. This output is again named interp_Acanopy.
2079 8. Again, label photons that lie between interp_Acanopy and
2080 FINALGROUND+PSF as canopy photons.
2081 9. Since the canopy points have been relabeled, we need to do a final
2082 refinement of the ground surface:

2083 If canopy is present at any location along-track

2084 FINALGROUND = AgroundSmooth (at that location)

2085 Else if canopy is not present at a location along-track

2086 FINALGROUND = interp_Aground

2087 Smooth the resulting interpolated ground surface (FINALGROUND) once

2088 using a median filter with window size of SmoothSize, then a moving average

2089 smoothing filter twice with window size of SmoothSize.

2090 10. Relabel ground photons based on this new (and last) FINALGROUND solution

2091 +/- a recalculated PSF (via steps in 4.11 (6)). Points falling below the buffer

2092 are labeled as noise.

2093 11. Using Interp_Acanopy and this last FINALGROUND solution + PSF buffer,

2094 label all photons that lie between the two as canopy photons.

2095 12. Repeat the canopy cover filtering: For 500 signal photon segments, if

2096 number of all canopy photons (i.e., canopy and top of canopy) is:

2097 < 5% of the total (when SNR > 1), OR

2098 < 10% of the total (when SNR <= 1),

2099 relabel the canopy photons as noise. This is the last canopy labeling step.

2100

2101 **4.13 Compute individual Canopy Heights**

2102 1. At this point, each photon will have its final label assigned in

2103 **classed_pc_flag**: 0 = noise, 1 = ground, 2 = canopy, 3 = top of canopy.

2104 2. For each individual photon labeled as canopy or top of canopy, subtract the Z

2105 height value from the interpolated terrain surface, FINALGROUND, at that

2106 particular position in the along-track direction.

2107 3. The relative height for each individual canopy or top of canopy photon will

2108 be used to calculate canopy products described in Section 4.16. Additional

2109 canopy products will be calculated using the absolute heights, as described in

2110 Section 4.16.1.

2111

2112 **4.14 Final photon classification QA check**

- 2113 1. Find any ground, canopy, or top of canopy photons that have elevations
2114 further than the ref_dem_limit from the reference DEM elevation value.
2115 Convert these to the noise classification.
- 2116 2. Find any relative heights of canopy or top of canopy photons that are greater
2117 than 150 m above the interpolated ground surface, FINALGROUND. Convert
2118 these to the noise classification.
- 2119 3. Find any FINALGROUND elevations that are further than the ref_dem_limit
2120 from the reference DEM elevation value. Convert those FINALGROUND
2121 elevations to an invalid value, and convert any classified photons at the same
2122 indices to noise.
- 2123 4. If more than 50% of photons are removed in a segment, set ph_removal_flag
2124 to true.

2125

2126 **4.15 Compute segment parameters for the Land Products**

- 2127 1. For each 100 m segment, determine the classed photons (photons classified
2128 as ground, canopy, or top of canopy).
- 2129 a. If there are fewer than 50 classed photons in a 100 m segment, do not
2130 calculate land or canopy products.
- 2131 b. If there are 50 or more classed photons in a 100 m segment, extract
2132 the ground photons to create the land products.
- 2133 2. If the number of ground photons > 5% of the total number of classed photons
2134 within the segment (this control value of 5% can be modified once on orbit):
- 2135 a. Compute statistics on the ground photons: mean, median, min, max,
2136 standard deviation, mode, and skew. These heights will be reported

2137 on the product as **h_te_mean**, **h_te_median**, **h_te_min**, **h_te_max**,
 2138 **h_te_mode**, and **h_te_skew** respectively described in Table 2.1.

2139 b. Compute the standard deviation of the ground photons about the
 2140 interpolated terrain surface, FINALGROUND. This value is reported as
 2141 **h_te_std** in Table 2.1.

2142 c. Compute the residuals of the ground photon Z heights about the
 2143 interpolated terrain surface, FINALGROUND. The product is the root
 2144 sum of squares of the ground photon residuals combined with the
 2145 **sigma_atlas_land** term in Table 2.5 as described in Equation 1.4. This
 2146 parameter reported as **h_te_uncertainty** in Table 2.1.

2147 d. Compute a linear fit on the ground photons and report the slope. This
 2148 parameter is **terrain_slope** in Table 2.1.

2149 e. Calculate a best fit terrain elevation at the mid-point location of the
 2150 100 m segment:

2151 i. Calculate each terrain photon's distance along-track into the
 2152 100 m segment using the corresponding ATL03 20 m products
 2153 segment_length and dist_ph_along, and determine the mid-
 2154 segment distance (expected to be 50 m \pm 0.5 m).

2155 1. Use the mid-segment distance to linearly interpolate a
 2156 mid-segment time (**delta_time** in Table 2.4). Use the
 2157 mid-segment time to linearly interpolate other mid-
 2158 segment parameters: interpolated terrain surface,
 2159 FINALGROUND, as **h_te_interp** (Table 2.1); **latitude**
 2160 and **longitude** (Table 2.4).

2161 ii. Calculate a linear fit, as well as 3rd and 4th order polynomial fits
 2162 to the terrain photons in the segment.

2163 iii. Create a slope-adjusted and weighted mid-segment variable,
 2164 weightedZ, from the linear fit: Use terrain_slope to apply a
 2165 slope correction to each terrain photon by subtracting the

2166 terrain photon heights from the linear fit. Determine the mid-
2167 segment location of the linear fit, and add that height to the
2168 slope corrected terrain photons. Apply a linear weighting to
2169 each photon based on its distance to the mid-segment location:
2170 $1 / \sqrt{(\text{photon distance along} - \text{mid-segment distance})^2}$.
2171 Calculate the weighted mid-segment terrain height, weightedZ:
2172 $\text{sum}(\text{each adjusted terrain height} * \text{its weight}) / \text{sum}(\text{all}$
2173 $\text{weights})$.

2174 iv. Determine which of the three fits is best by calculating the
2175 mean and standard deviation of the fit errors. If one of the fits
2176 has both the smallest mean and standard deviations, use that
2177 fit. Else, use the fit with the smallest standard deviation. If
2178 more than one fit has the same smallest mean and/or standard
2179 deviation, use the fit with the higher polynomial.

2180 v. Use the best fit to define the mid-segment elevation. This
2181 parameter is **h_te_best_fit** in Table 2.1.

2182 1. If h_te_best_fit is farther than 3 m from h_te_interp (best
2183 fit diff threshold), check if: there are terrain photons on
2184 both sides of the mid-segment location; or the elevation
2185 difference between weightedZ and h_te_interp is
2186 greater than the best fit diff threshold; or the number of
2187 ground photons in the segment is $\leq 5\%$ of total
2188 number of classified photons per segment. If any of
2189 those cases are present, use h_te_interp as the corrected
2190 h_te_best_fit. Otherwise use weightedZ as the corrected
2191 h_te_best_fit.

2192 f. Compute the difference of the median ground height from the
2193 reference DTM height. This parameter is **h_dif_ref** in Table 2.4.
2194

3. If the number of ground photons in the segment $\leq 5\%$ of total number of classified photons per segment,
 - a. Report an invalid value for terrain products: **h_te_mean**, **h_te_median**, **h_te_min**, **h_te_max**, **h_te_mode**, **h_te_skew**, **h_te_std**, and **h_te_uncertainty** respectively as described in Table 2.1.
 - b. If the number of ground photons in the segment is $\leq 5\%$ of total number of classified photons in the segment, compute **terrain_slope** via a linear fit of the interpolated ground surface, FINALGROUND, instead of the ground photons.
 - c. Report the mid-segment interpolated terrain surface, FinalGround, as **h_te_interp** as described in Table 2.1, and report **h_te_best_fit** as the h_te_interp value.

4.16 Compute segment parameters for the Canopy Products

1. For each 100 m segment, determine the classed photons (photons classified as ground, canopy, or top of canopy).
 - a) If there are fewer than 50 classed photons in a 100 m segment, do not calculate land or canopy products.
 - b) If there are 50 or more classed photons in a 100 m segment, extract all canopy photons (i.e., canopy and top of canopy; henceforth referred to as “canopy” unless otherwise noted) to create the canopy products.
2. Only compute canopy height products if the number of canopy photons is $> 5\%$ of the total number of classed photons within the segment (this control value of 5% can be modified once on orbit).
 - a) If the number of ground photons is also $> 5\%$ of the total number of classed photons within the segment, set **canopy_rh_conf** to 2.
 - b) If the number of ground photons is $< 5\%$ of the total number of classed photons within the segment, continue with the relative canopy height calculations, but set canopy_rh_conf to 1.

c) If the number of canopy photons is < 5% of the total number of classed photons within the segment, regardless of ground percentage, set canopy_rh_conf to 0 and report an invalid value for each canopy height variable.

3. Again, the relative heights (height above the interpolated ground surface, FINALGROUND) have been computed already. All parameters derived in the section are based on relative heights.

4. Sort the heights and compute a cumulative distribution of the heights. Select the height associated with the 98% maximum height. This value is **h_canopy** listed in Table 2.2.

5. Compute statistics on the relative canopy heights. Min, Mean, Median, Max and standard deviation. These values are reported on the product as **h_min_canopy**, **h_mean_canopy**, **h_max_canopy**, and **canopy_openness** respectively in Table 2.2.

6. Using the cumulative distribution of relative canopy heights, select the heights associated with the **canopy_h_metrics** percentile distributions (25, 50, 60, 70, 75, 80, 85, 90, 95), and report as listed in Table 2.2.

7. Compute the difference between h_canopy and canopy_h_metrics(50). This parameter is **h_dif_canopy** reported in Table 2.2 and represents an amount of canopy depth.

8. Compute the standard deviation of all photons that were labeled as Top of Canopy (flag 3) in the photon labeling portion. This value is reported on the data product as **toc_roughness** listed in Table 2.2.

9. The quadratic mean height, **h_canopy_quad** is computed by

$$qmh = \sqrt{\frac{\sum_{i=1}^{N_{ca}} h_i^2}{N_{ca}}}$$

where N_{ca} is the number of canopy photons in the segment and h_i are the individual canopy heights.

2251

2252 **4.16.1 Canopy Products calculated with absolute heights**

- 2253 1. The absolute canopy height products are calculated if the number of canopy
2254 photons is > 5% of the total number of classed photons within the segment.
2255 No number of ground photons threshold is applied for these.
- 2256 2. The **centroid_height** parameter in Table 2.2 is represented by all the classed
2257 photons for the segment (canopy & ground). To determine the centroid
2258 height, compute a cumulative distribution of all absolute classified heights
2259 and select the median height.
- 2260 3. Calculate **h_canopy_abs**, the 98th percentile of the absolute canopy heights.
- 2261 4. Compute statistics on the absolute canopy heights: Min, Mean, Median, and
2262 Max. These values are reported on the product as **h_min_canopy_abs**,
2263 **h_mean_canopy_abs**, and **h_max_canopy_abs**, respectively, as described in
2264 Table 2.2.
- 2265 5. Again, using the cumulative distribution of absolute canopy heights, select
2266 the heights associated with the **canopy_h_metrics_abs** percentile
2267 distributions (25, 50, 60, 70, 75, 80, 85, 90, 95), and report as listed in Table
2268 2.2.

2269 **4.17 Record final product without buffer**

- 2270 1. Now that all products have be determined via processing of the *L-km*
2271 segment with the buffer included, remove the products that lie within the
2272 buffer zone on each end of the *L-km* segment.
- 2273 2. Record the final *L-km* products and move on to process the next *L-km*
2274 segment.

2275

2276

5 DATA PRODUCT VALIDATION STRATEGY

Although there are no Level-1 requirements related to the accuracy and precision of the ATL08 data products, we are presenting a methodology for validating terrain height, canopy height, and canopy cover once ATL08 data products are created. Parameters for the terrain and canopy will be provided at a fixed size of 100 m along the ground track referred to as a segment. Validation of the data parameters should occur at the 100 m segment scale and residuals of uncertainties are quantified (i.e. averaged) at the 5-km scale. This 5-km length scale will allow for quantification of errors and uncertainties at a local scale which should reflect uncertainties as a function of surface type and topography.

5.1 Validation Data

Swath mapping airborne lidar is the preferred source of validation data for the ICESat-2 mission due to the fact that it is widely available and the errors associated with most small-footprint, discrete return data sets are well understood and quantified. Profiling airborne lidar systems (such as MABEL) are more challenging to use for validation due to the low probability of exact overlap of flightlines between two profiling systems (e.g. ICESat-2 and MABEL). In order for the ICESat-2 validation exercise to be statistically relevant, the airborne data should meet the requirements listed in Table 5.1. Validation data sets should preferably have a minimum average point density of 5 pts/m². In some instances, however, validation data sets with a lower point density that still meet the requirements in Table 5.1 may be utilized for validation to provide sufficient spatial coverage.

Table 5.1. Airborne lidar data vertical height (Z accuracy) requirements for validation data.

| ICESat-2 ATL08 Parameter | Airborne lidar (rms) |
|--------------------------|---|
| Terrain height | <0.3 m over open ground (vertical) <0.5 m (horizontal) |

| | |
|---------------|--|
| Canopy height | <2 m temperate forest, < 3 m tropical forest |
| Canopy cover | n/a |

2301

2302 Terrain and canopy heights will be validated by computing the residuals between the
2303 ATL08 terrain and canopy height value, respectively, for a given 100 m segment and
2304 the terrain height (or canopy height) of the validation data for that same
2305 representative distance. Canopy cover on the ATL08 data product shall be validated
2306 by computing the relative canopy cover ($cc = \text{canopy returns} / \text{total returns}$) for the
2307 same representative distance in the airborne lidar data.

2308 It is recommended that the validation process include the use of ancillary data sets
2309 (i.e. Landsat-derived annual forest change maps) to ensure that the validation results
2310 are not errantly biased due to non-equivalent content between the data sets.

2311 Using a synergistic approach, we present two options for acquiring the required
2312 validation airborne lidar data sets.

2313

2314 **Option 1:**

2315 We will identify and utilize freely available, open source airborne lidar data as the
2316 validation data. Potential repositories of this data include OpenTopo (a NSF
2317 repository or airborne lidar data), NEON (a NSF repository of ecological monitoring
2318 in the United States), and NASA GSFC (repository of G-LiHT data). In addition to
2319 small-footprint lidar data sets, NASA Mission data (i.e. ICESat and GEDI) can also be
2320 used in a validation effort for large scale calculations.

2321

2322 **Option 2:**

Option 2 will include Option 1 as well as the acquisition of additional airborne lidar data that will benefit multiple NASA efforts.

GEDI: With the launch of the Global Ecosystems Dynamic Investigation (GEDI) mission in 2018, there are tremendous synergistic activities for data validation between both the ICESat-2 and GEDI missions. Since the GEDI mission, housed on the International Space Station, has a maximum latitude of 51.6 degrees, much of the Boreal zone will not be mapped by GEDI. The density of GEDI data will increase as latitude increases north to 51.6 degrees. Since the data density for GEDI would be at its highest near 51.6 degrees, we would propose to acquire airborne lidar data in a “GEDI overlap zone” that would ample opportunity to have sufficient coverage of benefit to both ICESat-2 and GEDI for calibration and validation.

We recommend the acquisition of new airborne lidar collections that will meet our requirements to best validate ICESat-2 as well as be beneficial for the GEDI mission. In particular, we would like to obtain data over the following two areas:

- 1) Boreal forest (as this forest type will NOT be mapped with GEDI)
- 2) GEDI high density zone (between 50 to 51.6 degrees N). Airborne lidar data in the GEDI/ICESat-2 overlap zone will ensure cross-calibration between these two critical datasets which will allow for the creation of a global, seamless terrain, canopy height, and canopy cover product for the ecosystem community.

In both cases, we would fly data with the following scenario:

Small-footprint, full-waveform, dual wavelength (green and NIR), high point density (>20 pts/m²) and, over low and high relief locations. In addition, the newly acquired lidar data must meet the error accuracies listed in Table 5.1.

Potential candidate acquisition areas include: Southern Canadian Rocky Mountains (near Banff), Pacific Northwest mountains (Olympic National Park, Mt. Baker-Snoqualmie National Forest), and Sweden/Norway. It is recommended that the airborne lidar acquisitions occur during the summer months to avoid snow cover in either 2016 or 2017 prior to launch of ICESat-2.

5.2 Internal QC Monitoring

In addition to the data product validation, internal monitoring of data parameters and variables is required to ensure that the final ATL08 data quality output is trustworthy. Table 5.2 lists a few of the computed parameters that should provide insight into the performance of the surface finding algorithm within the ATL08 processing chain.

Table 5.2. ATL08 parameter monitoring.

| Group | Description | Source | Monitor | Validate in Field |
|--|--|----------|--|--|
| h_te_median | Median terrain height for segment | computed | | Yes against airborne lidar data. The airborne lidar data should have an absolute accuracy of <30 cm rms. |
| n_te_photons n_ca_photons n_toc_photons | Number of classed (sum of terrain, canopy, and top of canopy) photons in a 100 m segment | computed | Yes. Build an internal counter for the number of segments in a row | |

**ICESat-2 Algorithm Theoretical Basis Document for Land-Vegetation
Along-Track Products (ATL08)
Release 002**

| | | | |
|--------------------|--|----------|---|
| | | | where there aren't enough photons (currently a minimum of 50 photons per 100 m segment is used) |
| h_te_interp | Interpolated terrain surface height, FINALGROUND | computed | Difference h_te_interp and h_te_median and determine if the value is > a specified threshold. 2 m is suggested as the threshold value. This is an internal check to evaluate whether the median elevation for a segment is roughly the same as the interpolated surface height. |
| h_dif_ref | Difference between h_te_median and ref_dem | computed | This value will be computed and flagged if the difference is > 25 m. The |

**ICESat-2 Algorithm Theoretical Basis Document for Land-Vegetation
Along-Track Products (ATL08)
Release 002**

| | | | | |
|------------------------|--|----------|---|--|
| | | | reference DEM is the onboard DEM. | |
| h_canopy | 95% height of individual canopy heights for segment | computed | Yes, > a specified threshold (e.g. 60 m) | Yes against airborne lidar data. The canopy heights derived from airborne lidar data should have a relative accuracy <2 m in temperate forest, <3 m in tropical forest |
| h_dif_canopy | Difference between h_canopy and canopy_h_metrics(50) | computed | Yes, this is an internal check to make sure the calculations on canopy height are not suspect | |
| psf_flag | Flag is set if computed PSF exceeds 1m | computed | Yes, this is an internal check to make sure the calculations are not suspect | |
| ph_removal_flag | Flag is set if more than 50% of classified photons in a segment is removed during final QA check | computed | | |

***ICESat-2 Algorithm Theoretical Basis Document for Land-Vegetation
Along-Track Products (ATL08)
Release 002***

| | | | |
|-------------------------|---|----------|---|
| dem_removal_flag | Flag is set if more than 20% of classified photons in a segment is removed due to a large distance from the reference DEM | computed | Yes, this will check if bad results are due to bad DEM values or because too much noise was labeled as signal |
|-------------------------|---|----------|---|

2362

In addition to the monitoring parameters listed in Table 5.2, a plot such as what is shown in Figure 5.1 would be helpful for internal monitoring and quality assessment of the ATL08 data product. Figure 5.1 illustrates in graphical form what the input point cloud look like in the along-track direction, the classifications of each photon, and the estimated ground surface (FINALGROUND).

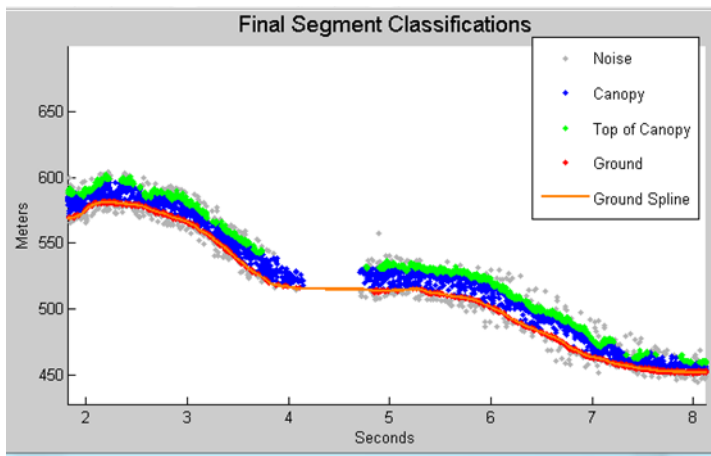


Figure 5.1. Example of L -km segment classifications and interpolated ground surface.

**ICESat-2 Algorithm Theoretical Basis Document for Land-Vegetation
Along-Track Products (ATL08)
Release 002**

2371 The following parameters are to be calculated and placed in the QA/QC group on the
2372 HDF5 data file, based on Table 5.2 of the ATL08 ATBD. Statistics shall be computed
2373 on a per-granule basis and reported on the data product. If any parameter meets the
2374 QA trigger conditional, an alert will be sent to the ATL08 ATBD team for product
2375 review.

2376 Table 5.3. QA/QC trending and triggers.

| QA/QC trending description | QA trigger conditional |
|--|------------------------|
| Percentage of segments with > 50 classed photons | None |
| Max, median, and mean of the number of contiguous segments with < 50 classed photons | None |
| Number and percentage of segments with difference in h_te_interp – h_te_median is greater than a specified threshold (2 m TBD) | > 50 segments in a row |
| Max, median, and mean of h_diff_ref over all segments | None |
| Percentage of segments where h_diff_ref > 25 m | Percentage > 75% |
| Percentage of segments where the h_canopy is > 60m | None |
| Max, median, and mean of h_diff | None |
| Number and percentage of Landsat continuous tree cover pixels per processing (L-km) segment with values > 100 | None |
| Percentage of segments where psf_flag is set | Percentage > 75% |

| | |
|--|---|
| Percentage of classified photons removed in a segment during final photon QA check | Percentage > 50% (i.e., ph_removal_flag is set to true) |
| Percentage of classified photons removed in a segment during the reference DEM threshold removal process | Percentage > 20% (i.e., dem_removal_flag is set to true) |

2377

2378

6 REFERENCES

- Carroll, M. L., Townshend, J. R., DiMiceli, C. M., Noojipady, P., & Sohlberg, R. A. (2009). A new global raster water mask at 250 m resolution. *International Journal of Digital Earth*, 2(4), 291–308. <http://doi.org/10.1080/17538940902951401>
- Channan, S., K. Collins, and W. R. Emanuel (2014). Global mosaics of the standard MODIS land cover type data. University of Maryland and the Pacific Northwest National Laboratory, College Park, Maryland, USA.
- Chauve, Adrien, et al. (2008). Processing full-waveform lidar data: modelling raw signals. *International archives of photogrammetry, remote sensing and spatial information sciences 2007*, 102-107.
- Cleveland, W. S. (1979). Robust Locally Weighted Regression and Smoothing Scatterplots. *Journal of the American Statistical Association*, 74(368), 829–836. <http://doi.org/10.2307/2286407>
- Friedl, M.A., D. Sulla-Menashe, B. Tan, A. Schneider, N. Ramankutty, A. Sibley and X. Huang (2010). MODIS Collection 5 global land cover: Algorithm refinements and characterization of new datasets, 2001-2012, Collection 5.1 IGBP Land Cover, Boston University, Boston, MA, USA.
- Fritsch, F.N., and Carlson, R.E. (1980). Monotone Piecewise Cubic Interpolation. *SIAM Journal on Numerical Analysis*, 17(2), 238–246. <http://doi.org/10.1137/0717021>
- Goshtasby, A., and O'Neill, W.D. (1994). Curve fitting by a Sum of Gaussians. *Graphical Models and Image Processing*, 56(4), 281-288.

**ICESat-2 Algorithm Theoretical Basis Document for Land-Vegetation
Along-Track Products (ATL08)
Release 002**

- 2402 Goetz and Dubayah (2011). Advances in remote sensing technology and
2403 implications for measuring and monitoring forest carbon stocks and change. *Carbon*
2404 *Management*, 2(3), 231-244. doi:10.4155/cmt.11.18
- 2405 Hall, F.G., Bergen, K., Blair, J.B., Dubayah, R., Houghton, R., Hurtt, G., Kelndorfer, J.,
2406 Lefsky, M., Ranson, J., Saatchi, S., Shugart, H., Wickland, D. (2011). Characterizing 3D
2407 vegetation structure from space: Mission requirements. *Remote sensing of*
2408 *environment*, 115(11), 2753-2775
- 2409 Harding, D.J., (2009). Pulsed laser altimeter ranging techniques and implications for
2410 terrain mapping, in Topographic Laser Ranging and Scanning: Principles and
2411 Processing, Jie Shan and Charles Toth, eds., CRC Press, Taylor & Francis Group, 173-
2412 194.
- 2413 Neuenschwander, A.L. and Magruder, L.A. (2016). The potential impact of vertical
2414 sampling uncertainty on ICESat-2/ATLAS terrain and canopy height retrievals for
2415 multiple ecosystems. *Remote Sensing*, 8, 1039; doi:10.3390/rs8121039
- 2416 Neuenschwander, A.L. and Pitts, K. (2019). The ATL08 Land and Vegetation Product
2417 for the ICESat-2 Mission. *Remote Sensing of Environment*, 221, 247-259.
2418 <https://doi.org/10.1016/j.rse.2018.11.005>
- 2419 Neumann, T., Brenner, A., Hancock, D., Robbins, J., Saba, J., Harbeck, K. (2018). ICE,
2420 CLOUD, and Land Elevation Satellite – 2 (ICESat-2) Project Algorithm Theoretical
2421 Basis Document (ATBD) for Global Geolocated Photons (ATL03).
- 2422 Olson, D. M., Dinerstein, E., Wikramanayake, E. D., Burgess, N. D., Powell, G. V. N.,
2423 Underwood, E. C., D'Amico, J. A., Itoua, I., Strand, H. E., Morrison, J. C., Loucks, C. J.,
2424 Allnutt, T. F., Ricketts, T. H., Kura, Y., Lamoreux, J. F., Wettengel, W. W., Hedao, P.,
2425 Kassem, K. R. (2001). Terrestrial ecoregions of the world: a new map of life on Earth.
2426 *Bioscience*, 51(11), 933-938.

***ICESat-2 Algorithm Theoretical Basis Document for Land-Vegetation
Along-Track Products (ATL08)
Release 002***

2427 Sexton, J.O., Song, X.-P., Feng, M. Noojipady, P., Anand, A., Huang, C., Kim, D.-H.,
2428 Collins, K.M., Channan, S., DiMiceli, C., Townshend, J.R.G. (2013). Global, 30-m
2429 resolution continuous fields of tree cover: Landsat-based rescaling of MODIS
2430 Vegetation Continuous Fields with lidar-based estimations of error. *International*
2431 *Journal of Digital Earth*, 130321031236007. doi:10.1080/17538947.2013.786146.

2432

Appendix A

DRAGANN Gaussian Deconstruction

John Robbins

20151021

Updates made by Katherine Pitts:

20170808

20181218

Introduction

This document provides a verbal description of how the DRAGANN (Differential, Regressive, and Gaussian Adaptive Nearest Neighbor) filtering system deconstructs a histogram into Gaussian components, which can also be called *iteratively fitting a sum of Gaussian Curves*. The purpose is to provide enough detail for ASAS to create operational ICESat-2 code required for the production of the ATL08, Land and Vegetation product. This document covers the following Matlab functions within DRAGANN:

- mainGaussian_dragann
- findpeaks_dragann
- peakWidth_dragann
- checkFit_dragann

Components of the k-d tree nearest-neighbor search processing and histogram creation were covered in the document, *DRAGANN k-d Tree Investigations*, and have been determined to function consistently with UTexas DRAGANN Matlab software.

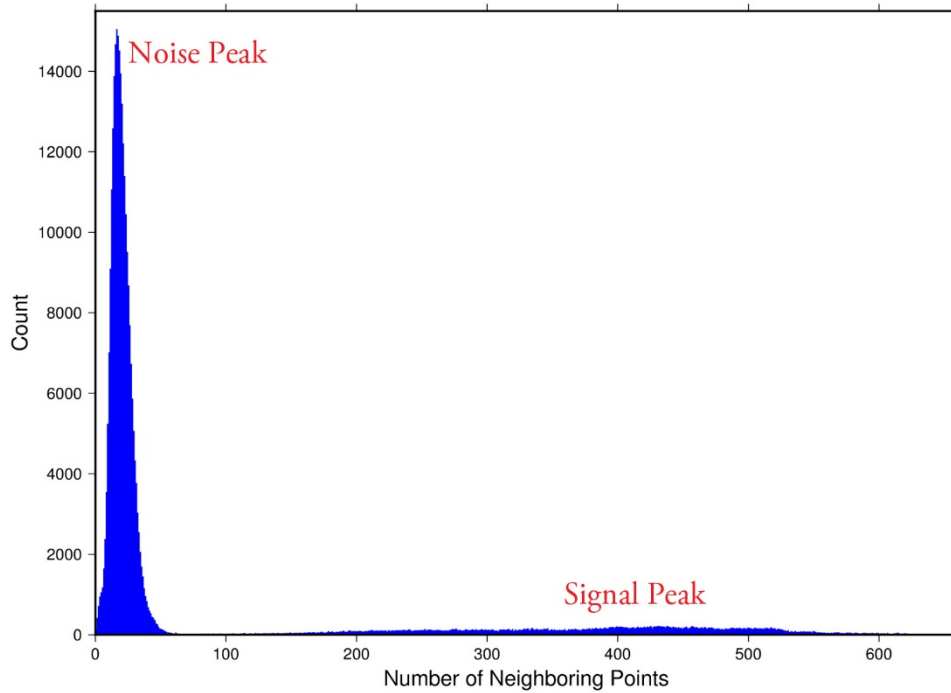
Histogram Creation

Steps to produce a histogram of nearest-neighbor counts from a normalized photon cloud segment have been completed and confirmed. Figure A.1 provides an example of such a histogram. The development, below, is specific to the two-dimensional case and is provided as a review.

The histogram represents the frequency (count) of the number of nearby photons within a specified radius, as ascertained for each point within the photon cloud. The radius, R , is established by first normalizing the photon cloud in time (x-axis) and in height (y-axis), i.e., both sets of coordinates (time & height) run from 0 to 1; then an

2468 average radius for finding 20 points is determined based on forming the ratio of 20
2469 to the total number of the photons in the cloud (N_{total}): $20/N_{total}$.

2470



2471

2472 **Figure A.1.** Histogram for Mabel data, channel 43 from SE-AK flight on July 30, 2014
2473 at 20:16.

2474 Given that the total area of the normalized photon cloud is, by definition, 1, then this
2475 ratio gives the average area, A , in which to find 20 points. A corresponding radius is
2476 found by the square root of A/π . A single equation describing the radius, as a
2477 function of the total number of photons in the cloud (remembering that this is done
2478 in the cloud normalized, two-dimensional space), is given by

2479
$$R = \sqrt{\frac{20/N_{total}}{\pi}} \quad (A.1)$$

2480 For the example in Figure A.1, R was found to be 0.00447122. The number of
2481 photons falling into this radius, at each point in the photon cloud, is given along the
2482 x-axis; a count of their number (or frequency) is given along the y-axis.

2483

2484 **Gaussian Peak Removal**

2485

2486 At this point, the function, mainGaussian_dragann, is called, which passes the
2487 histogram and the number of peaks to detect (typically set to 10).

2488 This function essentially estimates (i.e., fits) a sequence of Gaussian curves, from
2489 larger to smaller. It determines a Gaussian fit for the highest histogram peak, then
2490 removes it before determining the fit for the next highest peak, etc. In concept, the
2491 process is an iterative sequential-removal of the ten largest Gaussian components
2492 within the histogram.

2493 In the process of *sequential least-squares*, parameters are re-estimated when input
2494 data is incrementally increased and/or improved. The present problem operates in
2495 a slightly reverse way: the data set is fixed (i.e., the histogram), but components
2496 within the histogram (independent Gaussian curve fits) are removed sequentially
2497 from the histogram. The paper by Goshtasby & O'Neill (1994) outlines the concepts.

2498 Recall that a Gaussian curve is typically written as

2499
$$y = a \cdot \exp(-(x - b)^2 / 2c^2) \quad (\text{A.2})$$

2500 where a = the height of the peak; b = position of the peak; and c = width of the bell
2501 curve.

2502 The function, mainGaussian_dragann, computes the $[a, b, c]$ values for the ten
2503 highest peaks found in the histogram. At initialization, these $[a, b, c]$ values are set to
2504 zero. The process begins by locating histogram peaks via the function,
2505 findpeaks_dragann.

2506

2507 **Peak Finding**

2508 As input arguments, the findpeaks_dragann function receives the histogram and a
2509 minimum peak size for consideration (typically set to zero, which means all peaks
2510 will be found). An array of index numbers (i.e., the “number of neighboring points”,
2511 values along x-axis of Figure A.1) for all peaks is returned and placed into the
2512 variable peaks.

2513 The methodology for locating each peak goes like this: The function first computes
2514 the derivatives of the histogram. In Matlab there is an intrinsic function, called diff,
2515 which creates an array of the derivatives. Diff essentially computes the differences
2516 along sequential, neighboring values. “ $Y = \text{diff}(X)$ calculates differences between
2517 adjacent elements of X .” [from Matlab Reference Guide] Once the derivatives are
2518 computed, then findpeaks_dragann enters a loop that looks for changes in the sign
2519 of the derivative (positive to negative). It skips any derivatives that equal zero.

2520 For the k th derivative, the “next” derivative is set to $k+1$. A test is made whereby if
2521 the $k+1$ derivative equals zero and $k+1$ is less than the total number of histogram

2522 values, then increment “*next*” to $k+2$ (i.e., find the next negative derivative). The test
2523 is iterated until the start of the “down side” of the peak is found (i.e., these iterations
2524 handle cases when the peak has a flat top to it).

2525 When a sign change (positive to negative) is found, the function then computes an
2526 approximate index location (variable *maximum*) of the peak via

$$2527 \qquad \qquad \qquad \textit{maximum} = \textit{round}\left(\frac{\textit{next}-k}{2}\right) + k \qquad \qquad \qquad (\text{A.3})$$

2528 These values of *maximum* are retained in the peaks array (which can be *grown* in
2529 Matlab) and returned to the function mainGaussian_dragann.

2530 Next, back within mainGaussian_dragann, there are two tests to determine whether
2531 the first or last elements of the histogram are peaks. This is done since the
2532 findpeaks_dragann function will not detect peaks at the first or last elements, based
2533 solely on derivatives. The tests are:

2534 If (histogram(1) > histogram(2) && max(histogram)/histogram(1) < 20) then
2535 insert a value of 1 to the very first element of the peaks array (again, Matlab can
2536 easily “grow” arrays). Here, max(histogram) is the highest peak value across the
2537 whole histogram.

2538 For the case of the last histogram value (say there are N-bins), we have

2539 If (histogram(N) > histogram(N-1) && max(histogram)/histogram(N) < 4) then
2540 insert a value of N to the very last element of the peaks array.

2541 One more test is made to determine whether there any peaks were actually found
2542 for the whole histogram. If none were found, then the function,
2543 mainGaussian_dragann, merely exits.

2544

2545 **Identifying and Processing upon the Ten Highest Peaks**

2546 The function, mainGaussian_dragann, now begins a loop to analyze the ten highest
2547 peaks. It begins the n^{th} loop (where n goes from 1 to 10) by searching for the largest
2548 peak among all remaining peaks. The index number, as well as the magnitude of the
2549 peak, are retained in a variable, called maximum, with dimension 2.

2550 In each pass in the loop, the $[a,b,c]$ values (see eq. 2) are retained as output of the
2551 function. The values of a and b are set equal to the index number and peak
2552 magnitude saved in maximum(1) and maximum(2), respectively. The c -value is
2553 determined by calling the function, peakWidth_dragann.

2554 *Determination of Gaussian Curve Width*

2555 The function, peakWidth_dragann, receives the whole histogram and the index
2556 number (maximum(1)) of the peak for which the value c is needed, as arguments.
2557 For a specific peak, the function essentially searches for the point on the histogram
2558 that is about $\frac{1}{2}$ the size of the peak and that is furthest away from the peak being
2559 investigated (left and right of the peak). If the two sides (left and right) are
2560 equidistant from the peak, then the side with the smallest value is chosen ($> \frac{1}{2}$
2561 peak).

2562 Upon entry, it first initializes c to zero. Then it initializes the index values left, xL and
2563 right, xR as index-1 and index+1, respectively (these will be used in a loop,
2564 described below). It next checks whether the n^{th} peak is the first or last value in the
2565 histogram and treats it as a special case.

2566 At initialization, first and last histogram values are treated as follows:

2567 If first bin of histogram (peak = 1), set left = 1 and xL = 1.

2568 If last bin of histogram, set right = m and xR = m , where m is the final index of the
2569 histogram.

2570 Next, a search is made to the left of the peak for a nearby value that is smaller than
2571 the peak value, but larger than half of the peak value. A while-loop does this, with
2572 the following conditions: (a) left > 0, (b) histogram value at left is \geq half of histo
2573 value at peak and (c) histo value at left is \leq histo value at peak. When these
2574 conditions are all true, then xL is set to left and left is decremented by 1, so that the
2575 test can be made again. When the conditions are no longer met (i.e., we've moved to
2576 a bin in the histogram where the value drops below half of the peak value), then the
2577 program breaks out of the while loop.

2578 This is followed by a similar search made upon values to the right of the peak. When
2579 these two while-loops are complete, we then have the index numbers from the
2580 histogram representing bins that are above half the peak value. This is shown in
2581 Figure A.2.

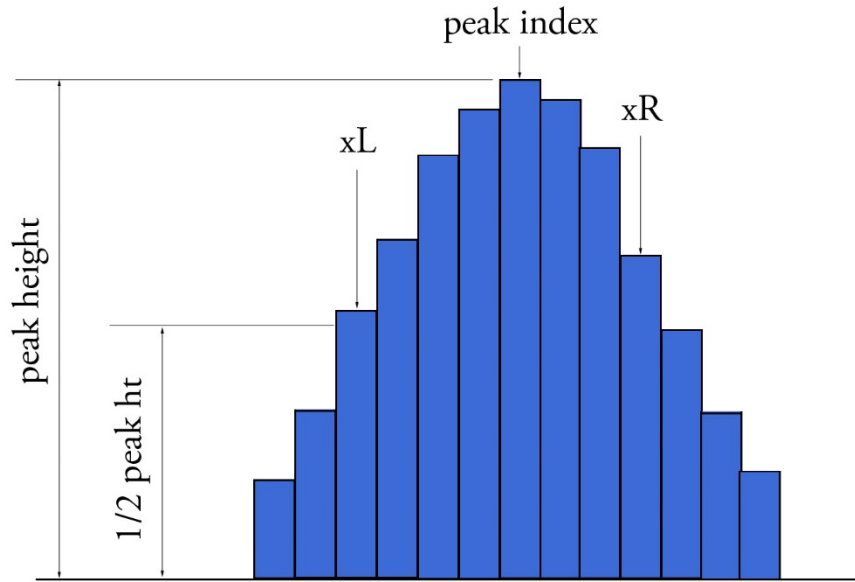


Figure A.2. Schematic representation of a histogram showing xL and xR parameters determined by the function `peakWidth_dragann`.

A test is made to determine which of these is furthest from the middle of the peak. In Figure A.2, xL is furthest away and the variable x is set to equal xL . The histogram “height” at x , which we call V_x , is used (as well as x) in an inversion of Equation A.2 to solve for c :

$$c = \sqrt{\frac{-(x-b)^2}{2 \ln \left(\frac{V_x}{a} \right)}} \quad (\text{A.4})$$

The function, `peakWidth_dragann`, now returns the value of c and control returns to the function, `mainGaussian_dragann`.

The `mainGaussian_dragann` function then picks-up with a test on whether the returned value of c is zero. If so, then use a value of 4, which is based on an *a priori* understanding that c usually falls between 4 and 6. If the value of c is not zero, then add 0.5 to c .

At this point, we have the $[a,b,c]$ values of the Gaussian for the n^{th} peak. Based on these values, the Gaussian curve is computed (via Equation A.2) and it is removed (subtracted) from the current histogram (and put into a new variable called `newWave`).

After a Gaussian curve is removed from the current histogram, the following peak width calculations could potentially have a V_x value less than 1 from a . This would

2602 cause the width, c , to be calculated as unrealistically large. Therefore, a check is put
2603 in place to determine if $a - V_x < 1$. If so, V_x is set to a value of $a - 1$.

2604 *Numeric Optimization Steps*

2605 The first of the optimization steps utilizes a Full Width Half Max (*FWHM*) approach,
2606 computed via

2607
$$FWHM = 2c\sqrt{2\ln 2} \quad (A.5)$$

2608 A left range, L_r , is computed by $L_r = \text{round}(b - FWHM/2)$. This tested to make sure it
2609 doesn't go off the left edge of the histogram. If so, then it is set to 1.

2610 Similarly, a right range, R_r , is computed by $R_r = \text{round}(b + FWHM/2)$. This is also tested
2611 to be sure that it doesn't go off the right edge of the histogram. If so, then it is set to
2612 the index value for the right-most edge of the histogram.

2613 Using these new range values, create a temporary segment (between L_r and R_r) of
2614 the newWave histogram, this is called errorWave. Also, set three delta parameters
2615 for further optimization:

2616 DeltaC = 0.05; DeltaB = 0.02; DeltaA = 1

2617 The temporary segment, errorWave is passed to the function checkFit_dragann,
2618 along with a set of zero values having the same number of elements as errorWave,
2619 the result, at this point, is saved into a variable called oldError. The function,
2620 checkFit_dragann, computes the sum of the squares of the difference between two
2621 histogram segments (in this case, errorWave and zeros with the same number of
2622 elements as errorWave). Hence, the result, oldError, is the sum of the squares of the
2623 values of errorWave. This function is applied in optimization loops, to refine the
2624 values of b and c , described below.

2625 *Optimization of the b-parameter.* The do-loop operates at a maximum of 1000 times.
2626 It's purpose is to refine the value of b , in 0.02 increments. It increments the value of
2627 b by DeltaB, to the right, and computes a new Gaussian curve based on $b + \Delta b$, which
2628 is then removed from the histogram with the result going into the variable
2629 newWave. As before, checkFit_dragann is called by passing the range-limited part of
2630 newWave (errorWave) and returning a new estimate of the error (newError) which
2631 is then checked against oldError to determine which is smaller. If newError is \geq
2632 oldError, then the value of b that produced oldError is retained, and the testing loop
2633 is exited.

2634 *Optimization of the c-parameter.* Now the value of c is optimized, first to the left,
2635 then to the right. It is performed independently of, but similarly, to the b -parameter,
2636 using do-loops with a maximum of 1000 passes. These loops increment (to right) or
2637 decrement (to left) by a value of 0.05 (DeltaC) and use checkFit_dragann to, again,

2638 check the quality of the fit. The loops (right and left) kick-out when the fit is found to
2639 be smallest.

2640 The final, optimized Gaussian curve is now removed (subtracted) from the
2641 histogram. After removal, a statement “corrects” any histogram values that may
2642 drop below zero, by setting them to zero. This could happen due to any mis-fit of the
2643 Gaussian.

2644 The n^{th} loop is concluded by examining the peaks remaining in the histogram
2645 without the peak just processed by sending the n^{th} -residual histogram back into the
2646 function findpeaks_dragann. If the return of peak index numbers from
2647 findpeaks_dragann reveals more than 1 peak remaining, then the index numbers for
2648 peaks that meet these three criteria are retained in an array variable called these:

- 2649 1. The peak must be located above $b(n)-2*c(n)$, and
 - 2650 2. The peak must be located below $b(n)+2*c(n)$, and
 - 2651 3. The height of the peak must be $< a(n)/5$.
- 2652

2653 The peaks meeting all three of these criteria are to be eliminated from further
2654 consideration. What this accomplishes is eliminate the nearby peaks that have a size
2655 lower than the peak just previously analyzed; thus, after their elimination, only
2656 leaving peaks that are further away from the peak just processed and are
2657 presumably “real” peaks. The n^{th} iteration ends here, and processing begins with the
2658 revised histogram (after having removed the peak just analyzed).

2659

2660 **Gaussian Rejection**

2661 The function mainGaussian_dragann returns the $[a,b,c]$ parameters for the ten
2662 highest peaks from the original histogram. The remaining code in dragann examines
2663 each of the ten Gaussian peaks and eliminates the ones that fail to meet a variety of
2664 conditions. This section details how this is accomplished.

2665 First, an approximate area, $\text{area1}=a*c$, is computed for each found peak and b , for all
2666 ten peaks, being the index of the peaks, are converted to an actual value via
2667 $b+\text{min}(\text{numptsinrad})-1$ (call this allb).

2668 Next, a rejection is made for all peaks that have any component of $[a,b,c]$ that are
2669 imaginary (Matlab isreal function is used to confirm that all three components are
2670 real, in which case it passes).

2671 To check for a narrow noise peak at the beginning of the histogram in cases of low
2672 noise rates, such as during nighttime passes, a check is made to first determine if the
2673 highest Gaussian amplitude, a , within the first 5% of the histogram is $\geq 1/10 * \text{the}$

2674 maximum amplitude of all Gaussians. If so, that peak's Gaussian width, c , is checked
2675 to determine if it is ≤ 4 bins. If neither of those conditions are met in the first 5%,
2676 the conditions are rechecked for the first 10% of the histogram. This process is
2677 repeated up to 30% of the histogram, in 5% intervals. Once a narrow noise peak is
2678 found, the process breaks out of the incremental 5% histogram checks, and the
2679 noise peak values are returned as $[a0, b0, c0]$.

2680 If a narrow noise peak was found, the remaining peak area values, $area1$ ($a*c$), then
2681 pass through a descending sort; if no narrow noise peak was found, all peak areas go
2682 through the descending sort. So now, the $[a,allb,c]$ -values are sorted from largest
2683 "area" to smallest, these are placed in arrays $[a1, b1, c1]$. If a narrow noise peak was
2684 found, it is then appended to the beginning of the $[a1, b1, c1]$ arrays, such that $a1 =$
2685 $[a0\ a1]$, $b1 = [b0\ b1]$, $c1 = [c0\ c1]$.

2686 In the case that a narrow noise peak was not found, a test is made to check that at
2687 least one of the peaks is within the first 10% of the whole histogram. It is done
2688 inside a loop that works from peak 1 to the number of peaks left at this point. This
2689 loop first tests whether the first (sorted) peak is within the first 10% of the
2690 histogram; if so, then it simply kicks out of the loop. If not, then it places the loop's
2691 current peak into a holder ($ihold$) variable, increments the loop to the next peak and
2692 runs the same test on the second peak, etc. Here's a Matlab code snippet:

```
2693     inds = 1:length(a1);  
2694     for i = 1:length(b1)  
2695         if b1(i) <= min(numptsinrad) + 1/10*max(numptsinrad)  
2696             if i==1  
2697                 break;  
2698             end  
2699             ihold = inds(i);  
2700             for j = i:-1:2  
2701                 inds(j) = inds(j-1);  
2702             end  
2703             inds(1) = ihold;  
2704             break  
2705         end  
2706     end
```

2707

2708 The j -loop expression gives the $init_val:step_val:final_val$. The semi-colon at the end
2709 of statements causes Matlab to execute the expression without printout to the user's
2710 screen. When this loop is complete, then the indexes ($inds$) are re-ordered and
2711 placed back into the $[a1,b1,c1]$ and $area1$ arrays.

2712 Next, are tests to reject any Gaussian peak that is entirely encompassed by another
2713 peak. A Matlab code snippet helps to describe the processing.

```
2714     % reject any gaussian if it is fully contained within another  
2715     isR = true(1,length(a1));  
2716     for i = 1:length(a1)  
2717         ai = a1(i);
```



```
2718     bi = b1(i);
2719     ci = c1(i);
2720     aset = (1-(c1/ci).^2);
2721     bset = ((c1/ci).^2*2*bi - 2*b1);
2722     cset = -(2*c1.^2.*log(a1/ai)-b1.^2+(c1/ci).^2*bi^2);
2723     realset = (bset.^2 - 4*aset.*cset >= 0) | (a1 > ai);
2724     isR = isR & realset;
2725 end
2726 a2 = a1(isR);
2727 b2 = b1(isR);
2728 c2 = c1(isR);
```

2729

2730 The logical array isR is initialized to all be true. The i-do-loop will run through all
2731 peaks. The computations are done in array form with the variables aset,bset,cset all
2732 being arrays of length(a1). At the bottom of the loop, isR remains “true” when
2733 either of the conditions in the expression for realset is met (the single “|” is a logical
2734 “or”). Also, the nomenclature, “.*” and “.^”, denote element-by-element array
2735 operations (not matrix operations). Upon exiting the i-loop, the array variables
2736 [a2,b2,c2] are set to the [a1,b1,c1] that remain as “true.” [At this point, in our test
2737 case from channel 43 of East-AK Mable flight on 20140730 @ 20:16, six peaks are
2738 still retained: 18, 433, 252, 33, 44.4 and 54.]

2739 Next, reject Gaussian peaks whose centers lay within 3σ of another peak, unless only
2740 two peaks remain. The code snippet looks like this:

```
2741     isR = true(1, length(a2));
2742     for i = 1:length(a2)
2743         ai = a2(i);
2744         bi = b2(i);
2745         ci = c2(i);
2746         realset = (b2 > bi+3*ci | b2 < bi-3*ci | b2 == bi);
2747         realset = realset | a2 > ai;
2748         isR = isR & realset;
2749     end
2750     if length(a2) == 2
2751         isR = true(1, 2);
2752     end
2753     a3 = a2(isR);
2754     b3 = b2(isR);
2755     c3 = c2(isR);
```

2756

2757 Once again, the isR array is initially set to “true.” Now, the array, realset, is tested
2758 twice. In the first line, one of three conditions must be true. In the second line, if
2759 realset is true or $a2 > ai$, then it remains true. At this point, we’ve pared down, from
2760 ten Gaussian peaks, to two Gaussian peaks; one represents the noise part of the
2761 histogram; the other represents the signal part.

2762 If there are less than two peaks left, a thresholding/histogram error message is
2763 printed out. If the lastTryFlag is not set, DRAGANN ends its processing and an empty
2764 IDX value is returned. The lastTryFlag is set in the preprocessing function which

2765 calls DRAGANN, as multiple DRAGANN runs may be tried until sufficient signal is
2766 found.

2767 If there are two peaks left, then set the array [a,b,c] to those two peaks. [At this
2768 point, in our test case from channel 43 of East-AK Mable flight on 20140730 @
2769 20:16, the two peaks are: 18 and 433.]

2770

2771 **Gaussian Thresholding**

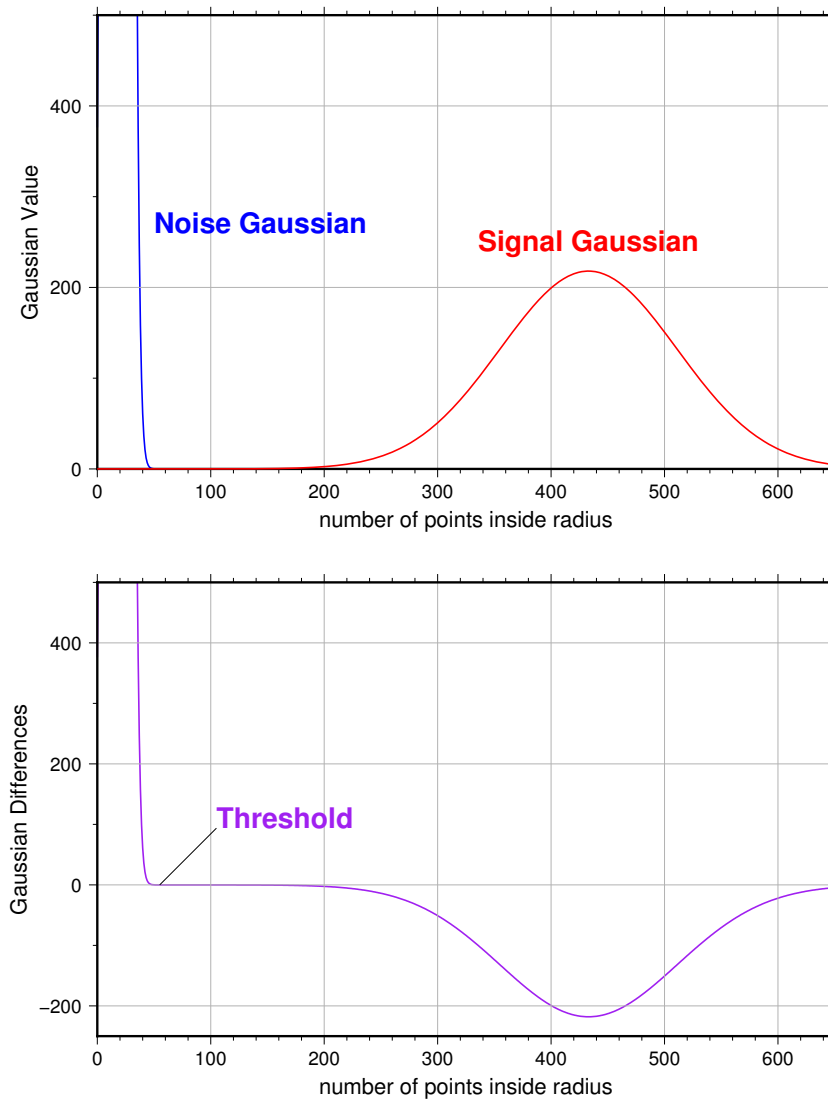
2772 With the two Gaussian peaks identified as noise and signal, all that is left is to
2773 compute the threshold value between the Gaussians.

2774 An array of xvals is established running from min(numptsinrad) to
2775 max(numptsinrad). In our example, xvals has indices between 0 and 653. For each
2776 of these xvals, Gaussian curves (allGauss) are computed for the two Gaussian peaks
2777 [a,b,c] determined at the end of the previous section. This computation is performed
2778 via a function called gaussmaker which receives, as input, the xvals array and the
2779 [a,b,c] parameters for the two Gaussian curves. An array of heights of the Gaussian
2780 curves is returned by the function, computed with Equation A.2. In Matlab, the
2781 allGauss array has dimension 2x654. An array, noiseGauss is set to be equal to the
2782 1st column of allGauss.

2783 An if-statement checks whether the b array has more than 1 element (i.e., consisting
2784 of two peaks), if so, then nextGauss is set to the 2nd column of allGauss, and a
2785 difference, noiseGauss-nextGauss, is computed.

2786 The following steps are restricted to be between the two main peaks. First, the first
2787 index of the absolute value of the difference that is near-zero (defined as 1e-8) is
2788 found, if it exists, and put into the variable diffNearZero. This is expected to be found
2789 if the two Gaussians are far away from each other in the histogram.

2790 Second, the point (i.e., index) is found of the minimum of the absolute value of the
2791 difference; this index is put into variable, signchanges. This point is where the sign
2792 changes from positive to negative as one moves left-to-right, up the Gaussian curve
2793 differences (noise minus next will be positive under the peak of the noise curve, and
2794 negative under the next (signal) curve). Figure A.3 (top) shows the two Gaussian
2795 curves. The bottom plot shows their differences.



2796

2797 **Figure A.3.** Top: two remaining Gaussian curves representing the noise (blue) and
 2798 signal (red) portions of the histogram in F1gure A.1. Bottom: difference noise –
 2799 signal of the two Gaussian curves. The threshold is defined as the point where the
 2800 sign of the differences change.

2801 If there is any value stored in diffNearZero, that value is now saved into the variable
 2802 threshNN. Else, the value of the threshold in signchanges is saved into threshNN,
 2803 concluding the if-statement for b having more than 1 element.

2804 An else clause ($b \neq 1$), merely sets threshNN to $b+c$, i.e., 1-standard deviation away
2805 from mean of the (presumably) noise peak.

2806 The final step is mask the signal part of the histogram where all indices above the
2807 threshNN index are set to logical 1 (true). This is applied to the numptsinrad array,
2808 which represents the photon cloud. After application, dragann returns the cloud
2809 with points in the cloud identified as “signal” points.

2810 The Matlab code has a few debug statements that follow, along with about 40 lines
2811 for plotting.

2812

2813 **References**

2814 Goshtasby, A & W. D. O'Neill, Curve Fitting by a Sum of Gaussians, *CVGIP: Graphical*
2815 *Models and Image Processing*, V. 56, No. 4, 281-288, 1994.